NOTICE

The quality of this microform is heavily dependent upon the quality of the original thesis submitted for microfilming. Every effort has been made to ensure the highest quality of reproduction possible.

If pages are missing, contact the university which granted the degree.

Some pages may have indistinct print especially if the original pages were typed with a poor typewriter ribbon or if the university sent us an inferior photocopy.

Reproduction in full or in part of this microform is governed by the Canadian Copyright Act, R.S.C. 1970, c. C-30, and subsequent amendments.

AVIS

La qualité de cette microforme dépend grandement de la qualité de la thèse soumise au microfilmage. Nous avons tout fait pour assurer une qualité supérieure de reproduction.

S'il manque des pages, veuillez communiquer avec l'université qui a conféré le grade.

La qualité d'impression de certaines pages peut laisser à désirer, surtout si les pages originales ont été dactylographiées à l'aide d'un ruban usé ou si l'université nous a fait parvenir une photocopie de qualité inférieure.

La reproduction, même partielle, de cette microforme est soumise à la Loi canadienne sur le droit d'auteur, SRC 1970, c. C-30, et ses amendements subséquents.

Canada

Chl *a* FLUORESCENCE AND HCO_3^- TRANSPORT IN THE CYANOBACTERIUM SYNECHOCOCCUS UTEX 625

Christopher M. Crotty

A Thesis

in

The Department

of

Biology

Presented in Partial Fulfillment of the Requirements

for the Degree of Master of Science at

Concordia University

Montreal, Quebec, Canada

June 1992

ISBN 0-315-97641-1

ABSTRACT

Chl a FLUORESCENCE AND HCO_3^- TRANSPORT IN THE CYANOBACTERIUM Synechococcus leopoliensis UTEX 625

Christopher M. Crotty

Chl a fluorescence was quenched under conditions where active transport of HCO_3^- was occuring in air grown cells of the cyanobacterium Synechococcus UTEX 625. Quenching of chl a fluorescence was observed to occur under conditions where CO_2 fixation and O_2 evolution was prevented by the Calvin cycle inhibitor, glycolaldehyde. The HCO_3^- transport capacity of the cells was not diminished by this inhibitor, indicating that chl a fluorescence quenching was not specifically dependent on electron flow to CO_2, but rather more indicative of the size of the internal pool of DIC (CO_2 + HCO_3^- + $CO_3^=$). The requirement of air grown cells for mM levels of Na^+ for HCO_3^- transport was characterized using both chl a fluorescence as an indirect monitor for DIC transport and the more direct silicone fluid centrifugation method. Measurements using either method revealed that increasing the extracellular pH in the range between 8.0 - 9.5 resulted in an decrease in the $K_{1/2}$ for Na^+ from 8.3 to 1.2 mM Na^+ with 20 μM DIC present. Similarly, the $K_{1/2}$ for Na^+ for photosynthesis decreased from 5.5 to 1.3 mM as extracellular pH was increased from 8.0 to 9.5 with 20 μM DIC present. The relation between the initial rate of fluorescence quenching and the initial rate of HCO_3^- transport was examined by linear regression analysis and found to be highly significant ($r = 0.785$, $n = 43$,

$p < 0.005$) by the students t-test.

An inhibitor of carbonic anhydrase, ethoxyzolamide (EZA), was used to characterize DIC transport in cyanobacteria grown under three different growth DIC concentrations. Both 30 $\mu L.L^{-1}$ CO_2 grown and standing culture cells possessed a HCO_3^- transport mechanism which was Na^+ independent and sensitive to low levels of EZA ($K_i = 58\ \mu M$) whereas air grown cells were Na^+ dependent and EZA insensitive ($K_i > 200\ \mu M$). Both 30 $\mu L.L^{-1}$ CO_2 and standing culture cells possessed residual Na^+ stimulated HCO_3^- transport capability which enabled these cells a measure of relief from EZA inhibition when 25 mM Na^+ was present. Measurements of photosynthesis, DIC transport, and chl a fluorescence quenching were consistent in establishing the effects of Na^+ and EZA on DIC transport in the three different cell types, indicating the usefulness of chl a fluorescence as an indirect monitor for DIC transport.

The results favour a model of DIC transport where at least two, and possibly three separate and distinct pathways for DIC transport occur in Synechococcus UTEX 625.

ACKNOWLEDGMENTS

I have been fortunate enough to have received the assistance and encouragement of many people throughout the course of my M.Sc. studies. I would like to express my sincere thanks to my Supervisor, Dr. George Espie for generous financial support. In many ways, Dr. Espie fulfilled the role of the ideal Supervisor by both encouraging independence of thought and by providing guidance and assistance when it was required.

Thanks to the members of the research group; Ramani Kandasamy, Pascal Tyrrell, Lori Seguin, and Rob Skleryk, for providing a convival (and animated!) environment in which to work. Thanks also to Dr. Scott Hinch and Heather Wilson for their help in making my stay in Mississauga both enjoyable and productive.

I would like to thank my Supervisory Committee members; Dr. R. Storms, Dr. N. Kapoor, and Dr. A. Miller, for taking the time to read the thesis. I would like to express my sincere thanks also to Dr. C. Cupples for allowing me the use of her lab space and computer facilities. Thanks to the secretarial staff in the Biology Department at Concordia, including Wendy Lee Legare, for their help.

Invariably, there are difficult periods in research. The love and support of Manon Briere helped to make those moments less dramatic and made the successful and productive periods all the more satisfying. I am grateful to my mother, Ruth, for her constant love and encouragement throughout the course of my studies and I would also like to thank her husband, Raymond, for his help and his interest.

TABLE OF CONTENTS

LIST OF FIGURES

LIST OF TABLES

ABBREVIATIONS

DIC, Dissolved inorganic carbon (CO_2 + HCO_3^- + $CO_3^=$); BTP, 1,3 - bis(tris[hydroxymethyl] methylamine - propane; CA, carbonic anhydrase; EZA, ethoxyzolamide; F_m^*, maximum fluorescence yield; F_v^*, variable fluorescence

F_o, minimum fluorescence; chl a , chlorophyll a; Rubisco, ribulose bisphosphate carboxylase/oxygenase; DCMU, 3- (3,4 - dichlorophenyl) -1 dimethyl urea; DMSO, dimethylsulfoxide

INTRODUCTION

REQUIREMENT FOR A DIC CONCENTRATING MECHANISM

Cyanobacteria are aquatic phototrophic prokaryotes which fix CO_2 by the Calvin cycle of reductive photosynthesis. The ability of cyanobacteria to utilize inorganic carbon efficiently for photosynthesis is limited by the poor catalytic efficiency of the primary CO_2 fixing enzyme in the cycle, ribulose-1,5-bisphosphate carboxylase/oxygenase (RUBISCO, EC 4.1.1.39). RUBISCO isolated from cyanobacteria possesses a $K_m(CO_2)$ of 200-300 μM (Kaplan et al., 1980, Andrews and Abel,1981) which is 10-30 fold higher than that found in C-3 or C-4 terrestrial plants. The effect of O_2 as a competitive and alternative substrate for RUBISCO is to further reduce the apparent affinity of RUBISCO for CO_2 under natural conditions. Further deleterious effects of O_2 are associated with carbon and energy losses incurred through the metabolism of phosphoglycolate, a product of RuBP oxygenation (Lorimer, 1981). In this regard, Shelp and Canvin (1984) calculated that, based on a CO_2/O_2 substrate specificity factor of 36, and with 10 μM CO_2 and 250 μM O_2 (air-equilibrium, 25°C) in solution, the ratio of carboxylase to oxygenase activity (v_c/v_o) would be about 1.7, leading to substantial rates of photo-respiration in comparison to photosynthesis. By way of contrast, C3 plants typically have specificity factors of around 80 (Ogren,1984) and at ambient CO_2 and O_2 levels, the v_c/v_o is about 2.5 (Canvin,1990). Similar considerations apply to an efficient C3 - C4 intermediate plant with a specificity factor of around 90, leading to v_c/v_o of around 4.3.

The photosynthetic properties of cyanobacteria are in direct contrast with the decidedly sub-optimal catalytic efficiency of RUBISCO. Most notably, cyanobacteria

grown at low concentrations of dissolved inorganic carbon (< 500 μM DIC, DIC = Σ $[CO_2]$ + $[HCO_3^-]$ + $[CO_3^=]$) possess very high rates of photosynthesis, low CO_2 compensation points (Birmingham and Colman,1979), low levels of phosphoglycolate production (Ingle and Colman,1976) and high photosynthetic affinity for CO_2 (Kaplan et al.,1980; Miller and Colman,1980; Badger and Andrews,1982; Miller et al.,1984a).

It has become increasingly clear that cyanobacteria can photosynthesize and grow at very low ambient CO_2 concentrations, which are subsaturating for RUBISCO because of their ability to transport DIC, thus elevating the level of CO_2 around RUBISCO. Intracellular DIC concentrations of as high as 100 mM, and accumulation ratios ($[DIC]_i/[DIC]_o$) on the order of 2000 fold have been measured (Badger and Andrews,1982; Badger et al., 1985; Espie and Kandasamy,1992). Furthermore, active CO_2 transport has been shown to occur against a concentration gradient of approximately 18000 fold ($[CO_2]_i/[CO_2]_o$) (Miller et al.,1988b). The CO_2 concentration at equilibrium with other DIC species at an intracellular pH of 7.5 (Coleman and Colman,1981) will be approximately 6 % of the total DIC. It can be calculated that intracellular DIC concentrations of as low as 5 mM will provide intracellular CO_2 levels which approach the K_m of cyanobacterial RUBISCO. At a pH_o of 8.0, where cyanobacteria photosynthesize and grow quite readily, the measured pH_i of 7.5 and membrane potential of -120 mV (Miller et al.,1984b) precludes the possibility of passive equilibration of either CO_2 or HCO_3^- being responsible for such large accumulation ratios. The intracellular accumulation of DIC thus requires the input of metabolic energy.

CARBONIC ANHYDRASE AND DIC SPECIES IN SOLUTION

The interconversion of DIC species in solution will proceed according to the following reactions;

(A) $CO_2 + H_2O \rightleftharpoons^1 H_2CO_3 \rightleftharpoons^2 HCO_3^- + H^+ \rightleftharpoons^3 CO_3^= + H^+$

(B) $CO_2 + OH^- \rightleftharpoons HCO_3^-$

For the hydration of CO_2 to form HCO_3^- and H^+ by way of H_2CO_3 formation, the rate limiting step is known to be (A)1 ($t_{1/2}$ = 7 sec. at 30°C, Badger,1987; Miller,1990 and references therein). Reactions (A)2 and (A)3 are essentially instantaneous and can thus be considered to be at equilibrium at all times (Miller and Colman, 1980). Reaction (B) becomes important at pH 8.0 and predominant at around pH 10.0.

The utilization of CO_2 by RUBISCO acts as a drawdown on the intracellular DIC pool. The rate of CO_2 supply by uncatalyzed HCO_3^- dehydration can thus potentially limit the rate of photosynthesis. If it is assumed that HCO_3^- is the DIC species arriving in the cytosol following transport, it can be calculated that a $[DIC]_i$ of 2 M would be required to support CO_2 saturated rates of photosynthesis in the absence of rapid (ie. catalyzed) interconversion of DIC species (Badger et al.,1985). Regardless of which species arrives internally, there is evidence for very rapid hydration-dehydration cycles of HCO_3^- and CO_2 occurring inside the cell, based on measurements of ^{18}O exchange between ^{18}O labelled HCO_3^- and CO_2 in whole cells (Badger et al.,1985; Tu et al.,1987; Miller et al.,1990). Further evidence of catalyzed interconversion of intracellular DIC has been provided by electrometric studies of cell-free extracts of cyanobacteria (Yagawa et al.,1984; Lanaras et al.,1985). It has now been well established that this intracellular

conversion of DIC in cyanobacteria is catalyzed by carbonic anhydrase, an ubiquitous enzyme found in, among other locations, mammalian red blood cells, spinach chloroplasts, and the periplasmic space of Chlamydomonas reinhardtii, an eukaryotic green algae (Silverman,1991). In the model proposed by Badger et al. (1985), the presence of low amounts of intracellular carbonic anhydrase activity allows for maximal rates of photosynthesis at intracellular [DIC] (30 - 60 mM) similar to what has been observed experimentally. The flow of DIC in cyanobacteria has been shown to be from the external medium, to the intracellular DIC pool, to carbon fixation products. Furthermore, the rate of carbon fixation has been shown to be dose dependent on the magnitude of the intracellular DIC (Kaplan et al.,1980; Shelp and Canvin,1984; Espie and Kandasamy,1992). Thus the function of internal carbonic anhydrase in cyanobacteria is to equilibrate the CO_2 and HCO_3^- concentrations in the immediate environment of RUBISCO, providing a supply of CO_2 which is proportional to the intracellular DIC concentration.

Early evidence for HCO_3^- transport in cyanobacteria was based on a consideration of the theoretical supply rate of CO_2 from uncatalyzed dehydration of HCO_3^- present in the medium and the comparison of this rate to the measured rate of photosynthesis (Miller and Colman,1980). Measured rates of photosynthesis in excess of the theoretical rate of HCO_3^- dehydration were suggestive of an active HCO_3^- transport mechanism. Calculations of the dehydration rate assumed the absence of extracellular carbonic anhydrase which, in the absence of HCO_3^- transport, would allow for DIC uptake rates in excess of the theoretical supply rate of CO_2 through either active or passive CO_2

influx. The possibility of extracellular carbonic anhydrase in cyanobacteria has been investigated exhaustively using a variety of techniques including; mass spectrometry (Badger and Andrews,1982; Miller et al,1988b), isotopic disequilibrium (Badger and Andrews,1982; Espie and Canvin,1987; Miller and Canvin,1987) and electrometric assay (Yagawa et al,1984). No evidence of extracellular carbonic anhydrase in cyanobacteria has been reported to date.

In air equilibrated solutions or in most natural aquatic environments, the relative amounts of each of the three most stable DIC species, CO_2, HCO_3^-, and $CO_3^=$ will vary with pH. The concentration of dissolved CO_2 in air-equilibrated solution is generally 10-12 μM, however at pH 8.0 and at 30°C this amount is 1.6 % of the total DIC species (Miller, 1990; and references therein). The percentage of CO_2 in solution decreases sharply as pH increases above pH 7.5. Since the solubility of CO_2 in solution is pH independent, the end result is that the total DIC in solution increases roughly 10-fold for each pH unit increase (Badger,1987; Miller,1990). As alkalophiles, cyanobacteria can be expected to encounter much less CO_2 in solution than either HCO_3^- or $CO_3^=$. For this reason, and in view of the absence of extracellular carbonic anhydrase, the nature of the inorganic carbon species utilized by the DIC transport mechanism(s) has important consequences for cyanobacterial photosynthesis.

CO_2 TRANSPORT

The active transport of CO_2 was first demonstrated conclusively by Badger and Andrews (1982).Using mass spectrometry to monitor extracellular CO_2, these investigators showed that the illumination of a cell suspension of cyanobacteria resulted

in the rapid depletion of $[CO_2]_o$ to levels approaching zero. Similar evidence for CO_2 transport in cyanobacteria was presented by Miller et al.(1988b). That the drop in $[CO_2]_o$ following illumination was due to the selective removal of CO_2 by the cells was indicated by the the restoration of pre-illumination levels of CO_2 by the addition of carbonic anhydrase (Miller et al.,1988b) The conditions used by Miller et al (1988b) for these experiments ensured that CO_2 was the only DIC species being transported. The fact that $[CO_2]_o$ was close to zero in the experiments of Badger and Andrews (1982) and Miller et al (1988b) indicated that the HCO_3^- dehydration rate was limiting with respect to CO_2 transport. The addition of carbonic anhydrase to cell suspensions relieves this kinetic limitation to the CO_2 supply rate, ensuring maintenance of the equilibrium between HCO_3^- and CO_2. With CA present, the rate limiting step in DIC uptake is at the level of the active CO_2 transport mechanism in cells without active HCO_3^- transport capacity (Miller et al.,1988b).

Cyanobacteria have been shown to transport CO_2 against a concentration gradient on the order of 18000:1 ($[CO_2]_i$:$[CO_2]_o$) (Miller et al.,1988b). The maintenance of chemical disequilibrium between CO_2 and HCO_3^- outside the cell, and the magnitude of the accumulation ratio of CO_2 require the expenditure of metabolic energy. The source of this energy is not known with any certainty, however CO_2 transport is known to be blocked by DCMU, CCCP, by the ATPase inhibitor DES, and by darkness (Badger and Andrews,1982; Miller et al.,1988b).

The active transport of CO_2 is not strictly dependent on extracellular Na^+. However it has been shown that 100 μM Na^+ will stimulate CO_2 transport approximately

2-fold at pH 8.0 (Espie et al.,1988b; Miller et al.,1988b). This effect of Na^+ is specific since neither Cl^- nor K^+ were effective at stimulating CO_2 transport.

Growth at low [DIC] ($<500\ \mu M$) produced cells possessing high transport affinity for CO_2 (0.2 μM at pH 8.0) (Espie et al.,1991) This high affinity CO_2 transport mechanism is responsible in large part for the high photosynthetic affinity for CO_2 of these cells.

HCO_3^- TRANSPORT

The active transport of HCO_3^- in cyanobacteria was first demonstrated by Miller and Colman (1980). These investigators showed that measured rates of photosynthesis were much faster than those which could have been supported by CO_2 formation from dehydration of HCO_3^- Direct measurements of HCO_3^- transport, using the silicone fluid centrifugation technique were subsequently reported (Kaplan et al.,1980) and provided confirmation of the results of Miller and Colman (1980). A Na^+ requirement for HCO_3^- dependent photosynthesis (Miller et al,1984b; Espie et al.,1988b) and HCO_3^- transport (Reinhold et al.,1984; Espie et al.,1988b) has been demonstrated for air-grown cyanobacteria. The dose dependence of photosynthesis and transport with respect to mM levels of Na^+ exhibits a hyperbolic relation typical of Michaelis-Menten kinetics. It has been shown that there exists a complex interaction between pH_o, $[Na^+]_o$, and $[DIC]_o$ for photosynthesis in Synechococcus UTEX 625 (Espie et al.,1988b). Reinhold et al.(1984) had previously argued that the effect of Na^+ was to increase the affinity of the transport mechanism for HCO_3^-. It is known that high concentrations of DIC (>1 mM) can overcome the requirement for Na^+ in air-grown cells (Miller et al.,1984b; Espie and

Canvin,1987; Espie et al.,1988b). At these high concentrations of DIC both the absolute amount and the rate of formation of CO_2 (from dehydration of HCO_3^-) are substantial enough to allow CO_2 transport rates which are sufficient to supply RUBISCO with saturating levels of CO_2. At pH 8.0, the DIC required for half saturation of photosynthesis ($K_{1/2}^{DIC}$) in air - grown cells has been shown to be 30 μM and 600 μM, in the presence and absence of 20 mM Na^+, respectively (Canvin et al.,1990). This effect of Na^+ on the affinity for DIC can be explained solely by consideration of CO_2 formation from dehydration of HCO_3^-. Similarly, for measurements of photosynthesis, the Na^+ concentration required for half-saturation at a given DIC concentration decreased with increasing DIC (Espie et al.,1988b). The decrease in the Na^+ requirement at higher DIC is thought to reflect the increasing contribution of CO_2 transport to DIC uptake at DIC concentrations higher than 100 μM (Espie et al.,1988b).

The effect of Na^+ has been shown to be specific, Cl^-, and K^+ are ineffective and Li^+ acts as a competitive inhibitor (Reinhold et al.,1984; Miller et al.,1984b; Espie et al.,1988b).

POSSIBLE EFFECT(S) OF Na^+ ON HCO_3^- TRANSPORT

The mechanism of action of Na^+ on HCO_3^- transport in air-grown cells of Synechococcus UTEX 625 is unknown. Four possible roles for Na^+ can be identified:

(1)HCO_3^- transport occurs in these cells via a Na^+/HCO_3^- symport. This is thermodynamically plausible in view of the calculated Na^+ motive force (Ritchie,1992). However, HCO_3^- stimulated Na^+ uptake has not been shown for air-grown cells. A recent study of Na^+ fluxes in high CO_2 grown cells of Synechococcus PCC 7942 indicates that

Na^+ is actively extruded from the cell, thus forming a Na^+ gradient capable of driving solute uptake (Ritchie,1992). The details of this process remain speculative. No evidence has yet been presented which would eliminate Na^+/HCO_3^- symport as a mechanism for DIC uptake. In support of the symport hypothesis, it has been shown that 50 μM monensin, which collapses the Na^+ gradient by exchanging Na^+ for H^+, will inhibit Na^+ dependent but not Na^+ independent HCO_3^- uptake (R.Kandasamy, M.Sc. thesis,1991).

(2) Na^+ binds to the transport protein and alters the kinetic parameters without itself being transported. This possibility has not been discounted by any evidence arguing against it, however it should be stated that there is no evidence for an allosteric effect of Na^+ on HCO_3^- transport. Furthermore, the progressive increase in the transport affinity for HCO_3^- with increasing Na^+ (Reinhold et al.,1984) can be explained by the relative contributions of HCO_3^- and CO_2 transport at varying DIC concentrations (Espie et al.,1988b; Canvin et al.,1990; Miller,1990) without necessarily invoking that the affinity for HCO_3^- of the Na^+ dependent HCO_3^- transporter varies as a function of the external Na^+.

(3) Na^+ acts by assisting in pH_i regulation through Na^+/H^+ antiport activity. This possibility does not affect directly HCO_3^- transport per se. Na^+/H^+ antiport activity has been shown in salt stressed cyanobacteria (Blumwald et al,1984) and in high CO_2 grown cells capable only of CO_2 transport (Kaplan et al.,1989). The physiological significance of Na^+/H^+ antiporter activity in cyanobacteria remains unclear. A study by Ritchie (1992) indicates that the proton motive force cannot support Na^+ efflux at alkaline pH in Synechococcus PCC 7942 grown on 5% CO_2. On the other hand, H^+ efflux driven

by Na^+ influx down its electrochemical gradient would exacerbate the problem encountered by the cell during steady state photosynthesis when OH^- ions are generated stoichiometrically with carbon fixation.

(4) The passive influx of Na^+ acts as a counter-ion flux to balance the primary electrogenic influx of HCO_3^-. It has been calculated that influx of HCO_3^- through a primary electrogenic pump mechanism would hyperpolarize the cell by 9 mV/msec (Miller, 1990). Thus a charge balancing ion flux would appear to be necessary to prevent excessive hyperpolarization.

Na^+ INDEPENDENT HCO_3^- TRANSPORT

The Na^+ requirement for HCO_3^- transport in cyanobacteria is not absolute. Slowly growing cells maintained in culture without bubbling of CO_2 (standing culture cells) possess the ability to transport HCO_3^- in the absence of mM levels of Na^+ (Espie and Canvin,1987; Espie and Kandasamy,1992). The Na^+ independent HCO_3^- transport mechanism has also been shown to be independent of K^+, Cl^-, or Li^+ concentration (Espie and Canvin,1987). In fact, Li^+ acts as a competitive inhibitor with respect to Na^+, of HCO_3^- dependent photosynthesis in air-grown cells (Espie et al.,1988b) and has been shown to have no effect on transport and photosynthesis in standing culture cells (Espie et al.,1987; R.Kandasamy, M.Sc. thesis,1991). The Na^+ independent mechanism also appears to be unaffected by monensin, which inhibits Na^+ stimulated HCO_3^- uptake in air-grown cells (R.Kandasamy, M.Sc. thesis,1991).

MODELS OF HCO_3^- AND CO_2 UPTAKE

Four characteristic modes of DIC transport can be resolved based on; (1) affinity

for substrate (CO_2 or HCO_3^-) (2) Na^+ dependence or independence (Price and Badger,1989b; Badger and Gallagher,1987; Espie et al.,1991). The differential effect of Na^+ on HCO_3^- transport in Synechococcus UTEX 625 grown under different growth DIC (Espie and Kandasamy,1992) as well as the differential effect of specific inhibitors of Na^+ dependent HCO_3^- uptake, argue in favour of separate and distinct HCO_3^- transport mechanisms, one Na^+ dependent and the other not. As well, high and low affinity CO_2 transporters can be resolved on the basis of measurements of transport and photosynthesis (Badger and Gallagher,1987; Miller and Canvin,1987; Price and Badger,1989a;b; Espie et al.,1991). The low affinity CO_2 pump is evident in cyanobacteria grown under high DIC (>1mM) ($K_{1/2}$ CO_2 = 5-15 μM, Price and Badger,1989b; Mayo et al., 1989) whereas the high affinity CO_2 pump is evident in cells grown at low DIC (<200 uM) ($K_{1/2}$ CO_2 = 0.2 μM, Espie et al.,1991).

The possibility that CO_2 and HCO_3^- transport share a common trans-membrane pathway has been proposed, based on the finding that CO_2 and HCO_3^- transport appear to be equally inhibited by ethoxyzolamide (EZA), an inhibitor of carbonic anhydrase (Price and Badger,1989a). In their version of the transport process, Price and Badger (1989a) speculate that the transport of HCO_3^- proceeds through a "front-end" mechanism which converts HCO_3^- to CO_2 at a site close to the active site of the CO_2 transporter (see Fig 1a). Both CO_2 and HCO_3^- transport would proceed by the translocation of CO_2. Based on evidence consistent with the hypothesis that HCO_3^- is the DIC species entering the cytosol, regardless of the DIC species supplied externally, Price and Badger proposed that the translocation of DIC requires a "carbonic anhydrase like moiety" to hydrate CO_2,

converting it to HCO_3^- as it enters the cytosol. Thus the transport of HCO_3^- requires a dehydration and then a rehydration reaction before entering the cytosol, while CO_2 transport requires a hydration reaction (Fig.1a). The hydration reaction is thus the common step in the transport of both CO_2 and HCO_3^- according to Price and Badger. It is supposed that this is the basis for the equal levels of inhibition of CO_2 and HCO_3^- transport by EZA.

If CO_2 and HCO_3^- transport share a common pathway, then there should be some interaction between simultaneous CO_2 and HCO_3^- transport such that high rates of transport of one substrate would interfere with the transport of the other substrate. Although no information is available for competition experiments between CO_2 transport and Na^+ independent HCO_3^- transport, it has been shown, based on CO_2 uptake measurements in the presence of varying levels of HCO_3^-, that the Na^+ dependent HCO_3^- transport mechanism is not likely to contribute to CO_2 transport via a "front-end" mechanism (Espie et al., 1991). The distinction between CO_2 transport and Na^+ dependent HCO_3^- transport can also be made on the basis of studies using inhibitors of carbonic anhydrase such as COS and H_2S, which inhibited high-affinity CO_2 transport but which did not greatly affect Na^+ dependent HCO_3^- transport (Miller et al.,1989, Espie et al.,1989). In experiments using the CO_2 transport inhibitor H_2S, it was shown that this inhibitor had no effect on the Na^+ independent HCO_3^- transport mechanism (Espie and Kandasamy,1992). In the absence of HCO_3^- competition experiments where the Na^+ independent mechanism is the primary means of HCO_3^- uptake, and CO_2 transport is monitored, the possibility that the Na^+ independent HCO_3^- transport mechanism shares

FIGURE 1

Models of DIC transport in cyanobacteria: (A) shows the model of Price and Badger (1989a) postulating a common translocatory step for CO_2 and HCO_3^- transport (B) shows the model of Espie et al (1989) indicating separate uptake mechanisms for CO_2 and HCO_3^- transport.

A

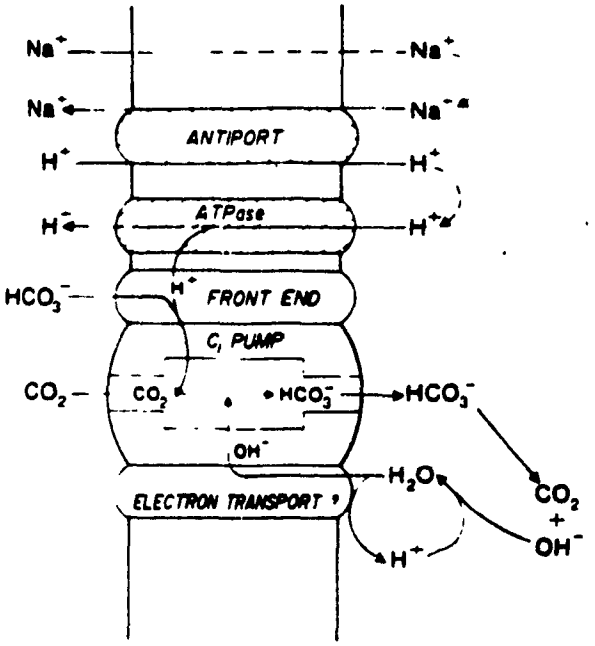
Na+
Na+
Na+
Na+
ANTIPORT
H+
H+
H+
H+
ATPase
HCO3-
H+
FRONT END
Ci PUMP
CO2
CO2
HCO3-
HCO3-
OH-
H2O
CO2
+
OH-
ELECTRON TRANSPORT
H+

B

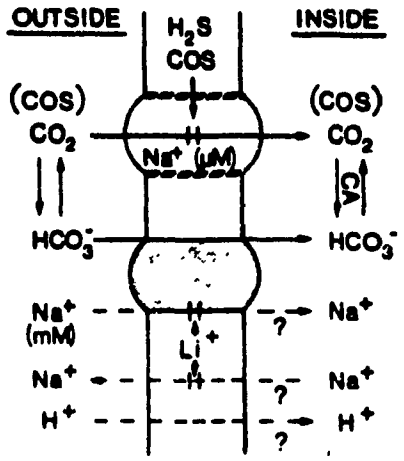
OUTSIDE
H2S
COS
INSIDE
(COS)
(COS)
CO2
CO2
Na+ (μM)
CA
HCO3-
HCO3-
Na+
(mM)
Na+
Li+
Na+
Na+
H+
H+
?
?
?

a common pathway with CO_2 transport cannot be completely excluded. Thus, two major models have evolved for DIC transport in cyanobacteria as indicated in Fig 1. The "common pathway" model of Price and Badger (1989a) is shown in Fig 1a, and a model which depicts CO_2 and HCO_3^- transport as being separate and distinct processes (Espie et al.,1989) is shown in Fig 1b.

EFFECT OF GROWTH DIC

Previous results have shown that there exists a complex interaction between photosynthesic affinity for DIC ($K_{1/2}^{DIC}$), growth rate (μ) and the exogenous DIC experienced by the cells during growth (Turpin et al.,1985). With respect to photosynthetic affinity for DIC, chemostat cultures of cyanobacteria exist in either a fully induced state (low $K_{1/2}^{DIC}$ at low μ) or a repressed state (high $K_{1/2}^{DIC}$ at high μ) and the transition between these two states occurs abruptly at around $\mu = 1.7$ day^{-1} (Miller et al.,1984a). For chemostat culture cells with fully induced high-affinity for DIC ($\mu < 1.7$ day^{-1}) the $K_{1/2}^{DIC}$ was found to be independent of growth rate (Turpin et al.,1985). The growth rate, however, varied with exogenous DIC according to the Monod relation for growth rate as a function of a nutrient present in growth limiting quantities, in this case DIC (Turpin et al.,1985). Studies with batch culture grown cells of Synechococcus UTEX 625 have revealed that cyanobacteria can vary their photosynthetic affinity for DIC in response to the exogenous DIC (Mayo et al.,1986; Badger and Gallagher,1987). This process of photosynthetic adaptation manifests itself across a wide range of exogenous DIC concentrations (10 μM - 2 mM) independently of the CO_2 concentration present in the growth medium (Mayo et al.,1986). The variation in photosynthetic affinity

has been shown to be due to variation in the transport kinetics in response to exogenous DIC experienced during growth (Mayo et al.,1989).

The exogenous DIC experienced during growth also has an influence on the quantity, size, and distribution of intracellular polyhedral bodies within Synechococcus UTEX 625 called carboxysomes (McKay et al.,in press). Carboxysomes contain most if not all of the functional RUBISCO in cyanobacteria (Shively,1988). The electron microscopy study by McKay et al (in press) has revealed that growth at low DIC (30 μM DIC) resulted in a large number of small carboxysomes positioned at the interface between the centroplasm and the thylakoid membranes whereas growth at high DIC resulted in a smaller number of large carboxysomes per cell. The carboxysomes of cells grown on high DIC were observed to be more random and irregular in their morphology and distribution. The functional significance of the size and distribution of carboxysomes bears on the possibility that carboxysomes act as a barrier preventing the diffusion of recently transported CO_2 back into the extracellular medium (Reinhold et al.,1991).

Growth of Synechococcus UTEX 625 at high DIC has been shown to increase the active site density of RUBISCO by about 3 fold (Mayo et al.,1989). Consequently, cells grown at low DIC (<30 μM) exhibit low values of P_{max} (150 - 300 μmol $O_2.mg^{-1}$ chl.h^{-1}) while high DIC grown cells (1-2 mM DIC) exhibit higher P_{max} values (500 - 600 μmol $O_2.mg^{-1}$ chl.h^{-1}) (Mayo et al., 1989). Combining the results of Mayo et al (1989) and McKay et al (in press) indicates that low DIC grown cells possesss an increased number of carboxysomes, each containing 1/3 less RUBISCO.

CHL a FLUORESCENCE QUENCHING AND DIC TRANSPORT

Studies conducted with Synechococcus UTEX 625 have shown that the transport and accumulation of DIC causes quenching of chl a fluorescence (Miller and Canvin,1987b; Miller et al,1988a;1988c;1991; Espie et al.,1991). The addition of glycolaldehyde or iodoacetamide, both of which block CO_2 fixation, does not prevent chl a fluorescence quenching (Miller and Canvin,1989; Miller et al, 1991). This result indicates that chl a fluorescence quenching is not strictly dependent on events associated with CO_2 fixation (ie. electron transport resulting in $NADP^+$ reduction). The addition of 3-(3,4-dichlorophenyl)-1,1-dimethylurea (DCMU) results in a rapid and monophasic recovery of fluorescence yield, indicating that chl a fluorescence quenching responds to changes in the red-ox status of Q_A, the primary electron acceptor of PSII (Miller and Canvin,1987b).

Both CO_2 (via $NADP^+$) and O_2 can act as electron acceptors, providing a means for the re-oxidation of Q_A (Miller et al.,1991) The reduction of O_2 has been proposed to occur via a Mehler type reaction (Miller et al.,1988c; Miller et al.,1991). The photoreduction of O_2 is stimulated by DIC transport and explains how Q_A can be re-oxidized (and thus chl a fluorescence quenched) in the absence of electron flow to CO_2 (ie. when Calvin cycle inhibitors are present) (Miller et al.,1991).

Measurements of CO_2 transport rate have been shown to be linearly related to measurements of initial rates of chl a fluorescence quenching over a wide range of CO_2 transport rates (Espie et al.,1991; Miller et al.,1991). Similarly, calculated intracellular DIC concentrations were correlated with the extent of chl a fluorescence quenching

(Miller et al.,1988a; Miller et al., 1991; Espie and Kandasamy,1992). The mechanistic basis underlying these empirical correlations is not known at present. One possibility which has been advanced relates to the "HCO_3^- effect" on electron flow as discussed by Blubaugh and Govindjee (1988). In support of this proposal, the re-oxidation of Q_A^-, as well as O_2 evolution, have both been shown, in HCO_3^- depleted thylakoids of Synechocystis 6803, to be stimulated by the addition of mM levels of HCO_3^- (Cao and Govindjee,1988). The molecular mechanism of this HCO_3^- effect on electron transport is proposed to be; (A) as a proton donor to plastoquinone, (B) as a ligand to the non-heme iron in Q_A-Fe-Q_B (Blubaugh and Govindjee,1988). A requirement for HCO_3^- in electron transport localized to the oxidizing side of plastoquinone in Synechococcus UTEX 625 is consistent with the following observations. First, in the absence of internal HCO_3^- (ie. at the CO_2 compensation point), Miller et al (1988c) observed that O_2 photoreduction did not occur. Only when DIC was accumulated internally as a result of active transport did fluorescence quenching (indicating electron transport) and O_2 photoreduction occur. Second, the chl a fluorescence yield in Synechococcus UTEX 625 did not decrease at the CO_2 compensation point (Miller et al,1991;). A state - 2 transition, resulting from the reduction of PQ (Mullineaux and Allen, 1989) would be expected to result in a decrease in the chl a fluorescence yield if the flow of electrons to PQ were not interrupted by the absence of intracellular HCO_3^- at the CO_2 compensation point (Miller et al.,1991). Thus, the requirement for HCO_3^- in electron transport in cyanobacteria, as well as the observations described above, are the basis for the possibility that chl a fluorescence quenching is related to DIC transport by an association

- dissociation reaction between intracellular HCO_3^- and the Q_A binding site (Miller et al., 1991).

In the present investigation, I have first described the relationship between chl a fluorescence quenching, HCO_3^- transport, and photosynthesis in air - grown cells of the cyanobacterium Synechococcus UTEX 625. Studies of the interaction between these three phenomena, as well as previous studies relating the initial rate of chl a fluorescence quenching to the initial rate of CO_2 transport (Espie et al., 1991), provided a rationale for the use of chl a fluorescence quenching as an indirect monitor for DIC transport under conditions where HCO_3^- is the DIC species being transported. The effects of Na^+_o and pH_o on photosynthesis, chl a fluorescence quenching and HCO_3^- transport are described in terms of a possible model for Na^+ dependent HCO_3^- transport. Finally, studies with an inhibitor of carbonic anhydrase, ethoxyzolamide (EZA), on DIC transport in cells grown under three different conditions allowed an accurate assesment of the specificity of this inhibitor with regard to CO_2 and HCO_3^- uptake mechanisms.

MATERIALS AND METHODS

ORGANISM

The unicellular cyanobacterium Synechococcus leopoliensis UTEX 625 (University of Texas Culture Collection, Austin, Texas) was maintained at 30°C on 1.4 % (v/v) agar plates made with unbuffered Allen's medium (Allen, 1968). Illumination was provided at 25 μmol photons.$m^{-2}.s^{-1}$(PAR).

GROWTH CONDITIONS

Synechococcus UTEX 625 was grown autotrophically under three different conditions for experimental purposes. (1) Standing cultures were initiated by aseptically introducing 3-4 transfer loops of cells from agar plate colonies, into 50 mL of unbuffered Allen's medium contained in a foam-stoppered 125 mL erlenmeyer flask. These cells, initially at 0.3 - 0.6 μg.chl a $.mL^{-1}$, were grown at 30° C and illuminated at 25 μmol photons.$m^{-2}.s^{-1}$ (PAR). Diffusion of CO_2 from the atmosphere through the foam stopper was the only source of CO_2 for growth. Under these conditions, the cells attained 4 - 6 μg. chl a $.mL^{-1}$ after 4 - 7 days, at which time they were harvested for experiments. At harvest, the pH of the growth medium was about 10. The exogenous DIC in the medium was about 20 μM. (2) Air - grown cells were started by adding a volume of mid-log phase standing culture cells to 50 mL. of unbuffered Allen's medium in a 20 x 2.5 cm. (i.d.) cylindrical glass culture tube. The initial chl a concentration was typically 0.2 - 0.4 $\mu g.mL^{-1}$. The cells were illuminated with 50 μmol photons.$m^{-2}.s^{-1}$ (PAR) and maintained at 30°C. CO_2 was supplied by bubbling the cultures with air (0.03% CO_2 v/v) which was delivered through a sterile glass tube (3.0 mm i.d.) at a rate of 70 $mL.min^{-1}$.

Under these conditions the cells reached a chl a concentration of 4 - 6 $\mu g.mL^{-1}$ after 36 - 48 hours during which time the cells were harvested for experiments. The pH of the medium at this time was 10.0 to 10.5 and the exogenous DIC was between 60 and 200 μM. (3) Finally, 30 $\mu L.L^{-1}$ CO_2 grown cells were grown by adding approximately 10 to 20 μg chl a of standing culture cells to 50 mL of Allen's medium buffered with 25 mM BTP/HCl at either pH 8.0 or 9.5. The media was contained in a 20 x 2.5 cm (i.d.) cylindrical glass culture tube. These cells were maintained at 30°C and illuminated at 50 $\mu mol\ photons.m^{-2}.s^{-1}$. CO_2 was supplied by bubbling the cells with 30 $\mu L.L^{-1}$ (0.003 % v/v) CO_2 in air at a flow rate of 270 $mL.min^{-1}$. The gas was passed through a sterile glass tube (7 mm i.d.) with a sintered glass tip that allowed for an even and diffuse distribution of gas bubbles throughout the solution. Under these conditions the cells were at 4 - 6 μg chl a mL^{-1} after 60 - 72 hours. The exogenous DIC at this time was about 3 μM. The gas flow through both air-grown and 30 $\mu L.L^{-1}.L$ CO_2 grown cells was regulated by a flow-meter (Cole-Parmer). Illumination in all cases was provided by a combination of Sylvania Gro-Lux and cool white fluorescent lamps. Photosynthetically active light radiation (PAR, 400 - 700 nm) was measured with a Li - Cor (Lincoln, Nebraska) Li - 185B quantum sensor and meter and is expressed as $\mu mol\ photons.m^{-2}.s^{-1}$.

PREPARATION OF LOW DIC BUFFER

Low DIC buffer was prepared by first adding a predetermined amount of 2N HCl to 100 mL of distilled H_20. The solution was then bubbled with N_2 for 20 minutes to dissipate dissolved CO_2 and thus remove DIC. Solid bis-tris-propane (BTP) (0.706

g/100mL) was subsequently added to the solution and the flask was quickly closed with an air tight stopper. This procedure enabled preparation of a 25 mM BTP solution of appropriate pH which contained approximately 10-20 μM DIC and less than 8 μM Na^+. The level of contaminant DIC in the buffer was measured by allowing standing culture cells to consume the DIC photosynthetically in an O_2 electrode cuvette. The amount of DIC present was assumed to be stoichiometrically equal to the amount of O_2 evolved. Alternatively, the DIC concentration in the buffer or in the cell - free growth medium at harvest was determined by gas chromatography as described by Birmingham and Colman (1979).

EXPERIMENTAL CONDITIONS

Cells were removed from the growth medium and centrifuged for 1 min. at 12000 x g in a Beckman microfuge E. The supernatant was discarded and the cell pellet was resuspended in low DIC, BTP/HCl buffer. This procedure was repeated three times in order to remove Na^+ and DIC from the cell suspension. Cells prepared in this way were used in subsequent experiments.

The chl a concentration of cell suspensions was determined as described by Mackinney (1941). Cells were pelleted by centrifugation, the supernatant discarded and chl a was extracted with 1.4 mL of methanol. The methanol extraction was carried out at -10°C in the dark for at least 30 minutes. The methanol extract was separated from cell debris by centrifugation for 1 min. at 12000 x g. The [chl a] was determined spectrophotometrically at 665 nm. For a 1 mL suspension of cells the equation is:

$$\text{chl a } (\mu g.mL^{-1}) = 13.42 \times A_{665} \times 1.4$$

O_2 EVOLUTION

O_2 evolution was measured using a thermostatted (30°C) Clark type oxygen electrode (Hansatech,Norfolk,U.K.). Washed cells (1.5 mL, 7 - 15 μg chl *a*.mL^{-1}) were placed in the electrode chamber and purged with N_2. The chamber was then closed to the atmosphere and the cells were allowed to consume the residual DIC present (approx. 20 μM) in the medium. The medium was stirred using a magnetic stirrer. Additions to the medium were made using a Hamilton syringe inserted into a capillary inlet in the plunger used to seal the chamber. The calibration of the electrode was carried out by adjusting the electrode signal under conditions where the O_2 concentration was known to be zero (vigorous gassing with N_2 for 5 mins.) and 230 μM O_2 (gassing with 20.8% O_2 for 5 mins.). At 30°C, 20.8% O_2 yields 230 μM O_2 in aqueous solution at equilibrium (Truesdale and Downing,1956). The range of signal output, measured on a chart recorder, thus corresponded to a defined range of O_2 concentration.

Actinic light to drive photosynthesis was provided by a quartz halogen projector lamp. The light intensity at the surface of the cuvette was 125 μmol photons.m^{-2}.s^{-1} (PAR).

FLUOROMETRY

Changes in chl *a* fluorescence yield were measured using a pulse amplitude modulation fluorometer (PAM 101 H.Walz,Effeltrich, FRG) developed by Schreiber (Schreiber *et al.*, 1986). A weak (2 - 5 μmol photons.m^{-2}.s^{-1}) , pulse - modulated (1 μsec flashes at 100 kHz) red light beam (λ = 650 nm) generated by a light emitting diode (LED) was used to repetitively excite chlorophyll *a* in PSII. The pulsed light beam

was passed through a short pass filter (λ <680 nm) to eliminate long wavelength radiation. Fluorescence emitted from chl a in PSII was received by a photo-diode detector shielded by a long pass (λ >700 nm) filter. The pulsed fluorescence signal was amplified in two steps by a pulse amplifier and a "selective window amplifier" and further processed to give a continuous output signal that was directed to a strip chart recorder. Only the pulse modulated fluorescence signal (@ 100 kHz) was amplified by the system. Continuous (non-modulated) fluorescence caused by the actinic light used to drive photosynthesis was not amplified and not recorded. Consequently, the signal directly reflects chl a fluorescence yield, which may vary between a minimum value, F_o and a maximum value F_m^*, depending on the oxidation-reduction status of Q_A (Schreiber et al., 1986). The weak, pulse modulated light is insufficient to cause any significant change in the red - ox status of Q_A (Schreiber et al., 1986).

Generally, fluorescence transients were recorded from cells in the O_2 electrode chamber in order to facilitate simultaneous measurements of fluorescence yield and photosynthesis. The cell suspension was optically connected to the emitter and detector by a fiber optic bundle which passed light in both directions.

The F_o was determined by illuminating dark adapted cells (5 mins.) with the pulse modulated light beam alone (Fig 2). Under these circumstances, Q_A, the primary quinone electron acceptor in PSII is mostly oxidized in the absence of significant electron flow through PSII (Miller et al., 1991). When these cells are then exposed to actinic light (125 μmol photons.m^{-2}.s^{-1}) and provided they are at the CO_2 compensation point, the fluorescence yield gradually, over a period of 60 - 90 seconds, increases to a level near

FIGURE 2

The chl a fluorescence of Synechococcus UTEX 625 was measured as described in the text. Cells were dark - adapted for 5 minutes in the O_2 electrode chamber in 25 mM BTP/HCl buffer (pH 8.0 - 9.5) at 30°C. The F_o or minimal fluorescence yield was obtained after illumination of the cells with a weak pulse modulated light (PLIGHT, 2 - 5 μmol photons.$m^{-2}.s^{-1}$). With the pulse light on, and while the cells were still in the dark, a brief (1s) flash of high intensity light (FLASH, 1600 μmol photons.$m^{-2}.s^{-1}$) was insufficient to obtain the highest fluorescence yield (F_m^*). The cells were subsequently exposed to actinic light (ALIGHT, 100 μmol photons.$m^{-2}.s^{-1}$) resulting in a gradual increase in fluorescence yield which plateaued after 1 - 2 minutes. The maximum fluorescence yield (F_m^*) was then obtained by providing the cells with a brief flash (FLASH) of saturating light intensity (1600 μmol photons.$m^{-2}.s^{-1}$). The addition of DIC (100 μM) caused a rapid decrease in the fluorescence yield ("quenching"). The decrease in fluorescence yield subsequently reversed, eventually plateauing at a level close to F_m^*. In all subsequent experiments, the addition of DIC to cell suspensions was done while the cells were at the CO_2 compensation point (ie. fluorescence yield was at a steady - state near F_m^*).

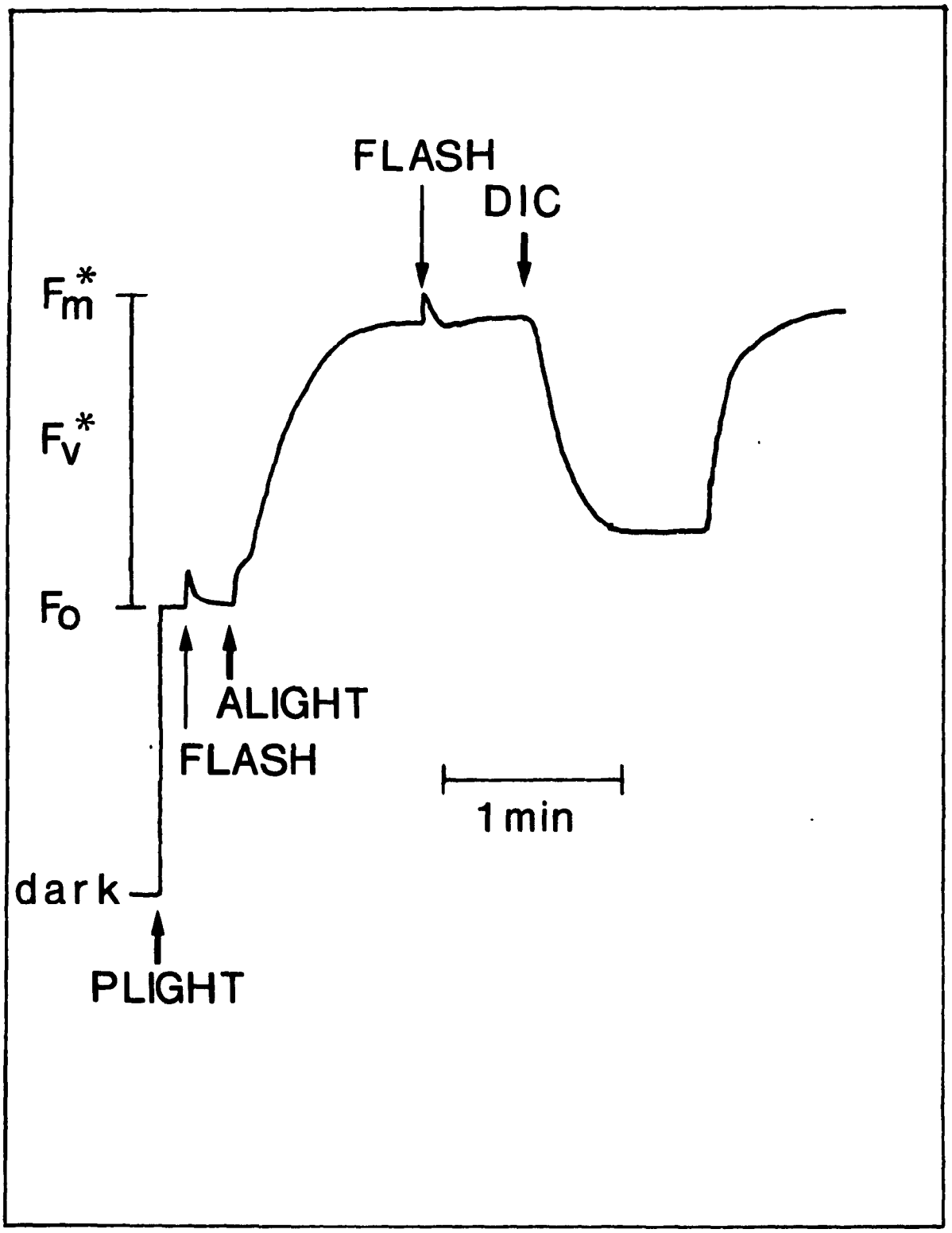
FLASH
DIC
F_m^*
F_v^*
F_o
ALIGHT
FLASH
1 min
dark
PLIGHT

maximum (Fig 2). The maximum fluorescence yield (F_m^*) is obtained by providing a brief (1 sec.) flash of saturating white light (1600 μmol photons.m^{-2}.s^{-1}) which has the effect of fully reducing Q_A. The F_m^* can alternately be measured by adding 20 μM 3-(3,4-dichlorophyl)-1,1-dimethyl urea (DCMU), which has the effect of blocking electron flow out of Q_A. F_m^* is found therefore under conditions where Q_A is fully reduced, either by a saturating pulse of light or by adding DCMU. The difference between F_m^* and F_o is the variable fluorescence, F_v^* (Fig 2).

The intracellular accumulation of inorganic carbon in certain cyanobacteria causes quenching of chl a fluorescence (Miller et al., 1991; Espie et al., 1991, see also Fig 2). Estimates of the initial rate of fluorescence quenching were obtained over 10 - 15 second time intervals after the addition of inorganic carbon to cell suspensions at the CO_2 compensation point, by determining the slope of a tangent drawn to chart recorder traces of fluorescence transients.

SILICONE FLUID CENTRIFUGATION

The direct measurement of DIC transport, intracellular DIC accumulation and carbon fixation was carried out using the silicone fluid centrifugation technique. The experiments were carried out in 400 μL microcentrifuge tubes containing 100 μL of terminating solution (2N KOH in 10 % v/v methanol) over which was layered a less dense silicone fluid mixture (AR 20 : AR 200, 1.75:1 (v/v), Wacker-Chemie, FGR). The top layer consisted of 80 or 90 μL of cell suspension (app. 10 μg chl a.mL^{-1}) at the CO_2 compensation point. The tubes were capped and placed in a microcentrifuge. Illumination was provided at 300 μmol photons.m^{-2}.s^{-1} (PAR) and the temperature was maintained at

30°C. ^{14}C labelled DIC (10 - 20 μL) was introduced into the cell suspension using a Hamilton syringe to give a final volume of 100 μL. Trial runs using coloured dye solutions indicated that rapid and uniform distribution of the ^{14}C could be obtained when a 10 μL volume was injected into the cell suspension. At timed intervals following the addition of ^{14}C the cells were separated from the reaction medium by centrifugation (12000 x g) for 60 seconds. Recovery of the cells at the bottom of the tube by this method was 95 %. Following centrifugation the tubes and contents were frozen in liquid N_2 and stored at -10°C until processed.

The frozen tubes were cut at the silicone fluid/KOH-MeOH interface and the KOH-MeOH as well as the cell pellet were removed and collected. The tube tip was washed with 100 μL of 10 mM KOH and this was added to the KOH-MeOH-pellet mixture. Of this 200 μL of solution, 50 μL was added to 5 mL of scintillation fluid (Universol, ICN), mixed, and stored in the dark for at least 3 hours. The radioactivity of the sample was determined by scintillation counting (Beckman LS 7500). Of the remaining 150 μL of KOH-MeOH-pellet mixture, a 50 μL aliquot was removed and placed in a 5 mL scintillation vial. Acetic acid (300 μL) was added to the 50 μL aliquot and the mixture was incubated at 92°C for three hours, during which time the unfixed inorganic carbon was evaporated as $^{14}CO_2$. Once the acetic acid was evaporated, the dry residue containing acid stable ^{14}C photosynthetic products was dissolved in 200 μL of distilled H_2O. To this was added 5 mL scintillation fluid. The radioactivity of the sample was determined by scintillation counting. Total ^{14}C present in the cell pellet was obtained from the first treatment (50 μL MeOH-KOH-pellet). Knowing the specific activity of the

added ^{14}C, the measured radioactivity in dpms was converted to μmol C_i.mg chl^{-1} using the equation:

$$\mu\text{mol } C_i\text{.mgchl } \underline{a} = (4.2\text{dpm} - \alpha\text{dpm})(\text{S.A.x mgchl } \underline{a} \text{ x } 2.22 \text{ x} 10^6)^{-1}$$

Alpha (α) in this equation refers to the proportion of the total incubation volume which remains with the cells in passing through the silicone fluid layer. Since this is a source of radioactivity which is external to the cell volume, this fraction of the activity was subtracted in order to determine the radioactivity present in the cells. The dpm's are multiplied by 4.2 as a consequence of the fractional recovery (95 %) and the fact that 1/4 of the total ^{14}C label recovered was counted (4/0.95 = 4.2). Acid stable counts were converted to μmoles C_i.mg chl^{-1} using a variation of equation (2), without the alpha correction factor since extracellular ^{14}C is removed prior to counting. Pool formation (mM DIC_i) was calculated by subtracting acid stable counts from total C counts and dividing by the intracellular volume. The intracellular volumes for air-grown, standing culture, and 30 μL.L^{-1} CO_2 grown cells were taken as 48.5, 62.0, and 62.9 μL.mg chl $\underline{a}^{-1}$, respectively (Kandasamy, R.A.,M.Sc.Thesis, 1991; Price and Badger, 1989a). The alpha values for air-grown and standing culture cells were taken as 0.00212 and 0.00266, respectively (Kandasamy, R.A.,M.Sc.Thesis, 1991). The alpha value for 30 μL.L^{-1} CO_2 grown cells was not determined but was assumed to be 0.00266.

The preparation of stock solutions of ^{14}C labelled HCO_3^- of defined concentration and specific activity for $DI^{14}C$ uptake experiments required measuring the level of contaminant DIC in the stock buffer. This was done by measuring the amount of O_2 evolved as is described under "PREPARATION OF LOW DIC BUFFER". The level of

contamination was generally 10 - 20 μM DIC. Experimental stock solutions of 50, 200, and 500 μM DIC were prepared by adding a defined volume of ^{14}C-labelled HCO_3^- from a manufacturer's stock solution (56 μCuries.μmol^{-1}, 33 mM DIC, Amersham, Toronto) to the stock buffer (pH 8.75, 5 mM BTP/HCl) in a stoppered, 1 mL glass vial. Additions through the rubber stopper were made with a Hamilton syringe. The specific activity of the experimental stock solutions was determined by counting 10 uL aliquots of each stock in a liquid scintillation counter, and dividing by the total DIC (including contaminant).

Experiments to determine the uptake of $^{14}CO_2$ involved essentially the same experimental set up as for $H^{14}CO_3^-$ uptake. The experimental stock solution of $^{14}CO_2$ required a low pH buffer (10 mM phthallic acid, pH 4.0) to maintain the added ^{14}C label as $^{14}CO_2$. The succesive removal of aliquots of $^{14}CO_2$ from the stoppered vial resulted in succesively increasing the head space. Loss of $^{14}CO_2$ into the head space was measured by removing, periodically, 10 uL aliquots to be counted in a liquid scintillation counter. The loss of $^{14}CO_2$ into the head space could be compensated for by succesively increasing the volume of the $^{14}CO_2$ solution to be added to the cells to obtain a consistent, desired concentration of $^{14}CO_2$. When the concentration of $^{14}CO_2$ declined by 50%, the stock was discarded and a new stock was made up.

INHIBITORS

Glycolaldehyde was prepared as a 3M stock in distilled H_2O. Ethoxyzolamide was prepared in dimethylsulfoxide at concentrations up to 200 mM. The addition of 1% dimethylsulfoxide had no effect on either photosynthetic O_2 evolution or chl a fluorescence.

CHEMICALS

Glycolaldehyde, ethoxyzolamide, and BTP (Bis-Tris-Propane) and phthallic acid were obtained from Sigma Chemical Co. (St.Louis, Mi). Compressed gas (0.003% v/v CO2, 20.8% v/v O_2 in N_2, O_2 in N_2) was obtained from Union Carbide (Montreal) and Linde (Toronto).

RESULTS

RELATIONSHIP BETWEEN PHOTOSYNTHESIS, DIC POOL FORMATION, AND FLUORESCENCE QUENCHING

Cyanobacteria grown with air-bubbling are strictly and specifically dependent on mM levels of extracellular Na^+ for photosynthesis at low DIC ($<100\ \mu M$) and alkaline pH (>pH 7.0) (Miller et al,1984; Espie et al, 1988b; Reinhold et al,1984). The results depicted in Fig. 3 indicate that, for air-grown cells provided with 20 μM DIC at pH 9.1, both the initial rate of intracellular DIC accumulation and the maximum pool size attained were dependent on the levels of added Na^+ in the range from 1-25 mM Na^+, as measured using the silicon fluid centrifugation technique. With 25 mM extracellular NaCl, the maximum pool size (25 mM DIC) was attained approximately 20 to 40 seconds after DIC addition. After 40 seconds, the calculated [DIC] remaining in the medium was 8.9 μM. The accumulation ratio ($[DIC]_i/[DIC]_o$) at 20 seconds was thus 2810. Taking a membrane potential of -120 mV (Miller et al, 1984b), the free energy difference ($\Delta G°$) for HCO_3^- at 20 seconds was calculated to be +7.08 kcal·mol^{-1}. Thus, DIC transport was proceeding against a very large electrochemical gradient indicating active transport. Active CO_2 transport is also known to occur in air-grown cells even in the absence of mM levels of Na^+ (Miller et al,1988b). However in the absence of extracellular CA, the rate of CO_2 supply is limited by the rate of spontaneous dehydration of HCO_3^-. For the experiment shown in Fig. 3, the total C_i uptake measured over the first ten seconds, with 1 mM extracellular Na^+ present, exceeded the rate of CO_2 supply by 45 fold. Thus, in the presence of mM levels of Na^+, the primary pathway for DIC

FIGURE 3

Time course of intracellular DIC accumulation in air grown cells provided with (○) 1 mM, (●) 2 mM, (▽) 5 mM, (▼) 10 mM, and (□) 25 mM NaCl. Data represent the average of duplicate or triplicate measurements. Experiments were conducted at pH 9.08, 30°C, and light was supplied at 300 μmol photons.m^{-2}.s^{-1}. The [chl] ranged from 6.8 to 8.2 μg.mL^{-1}. The initial [DIC] was 20 μM with a specific activity of 48.7 μCi.$\mu$$mol^{-1}$.

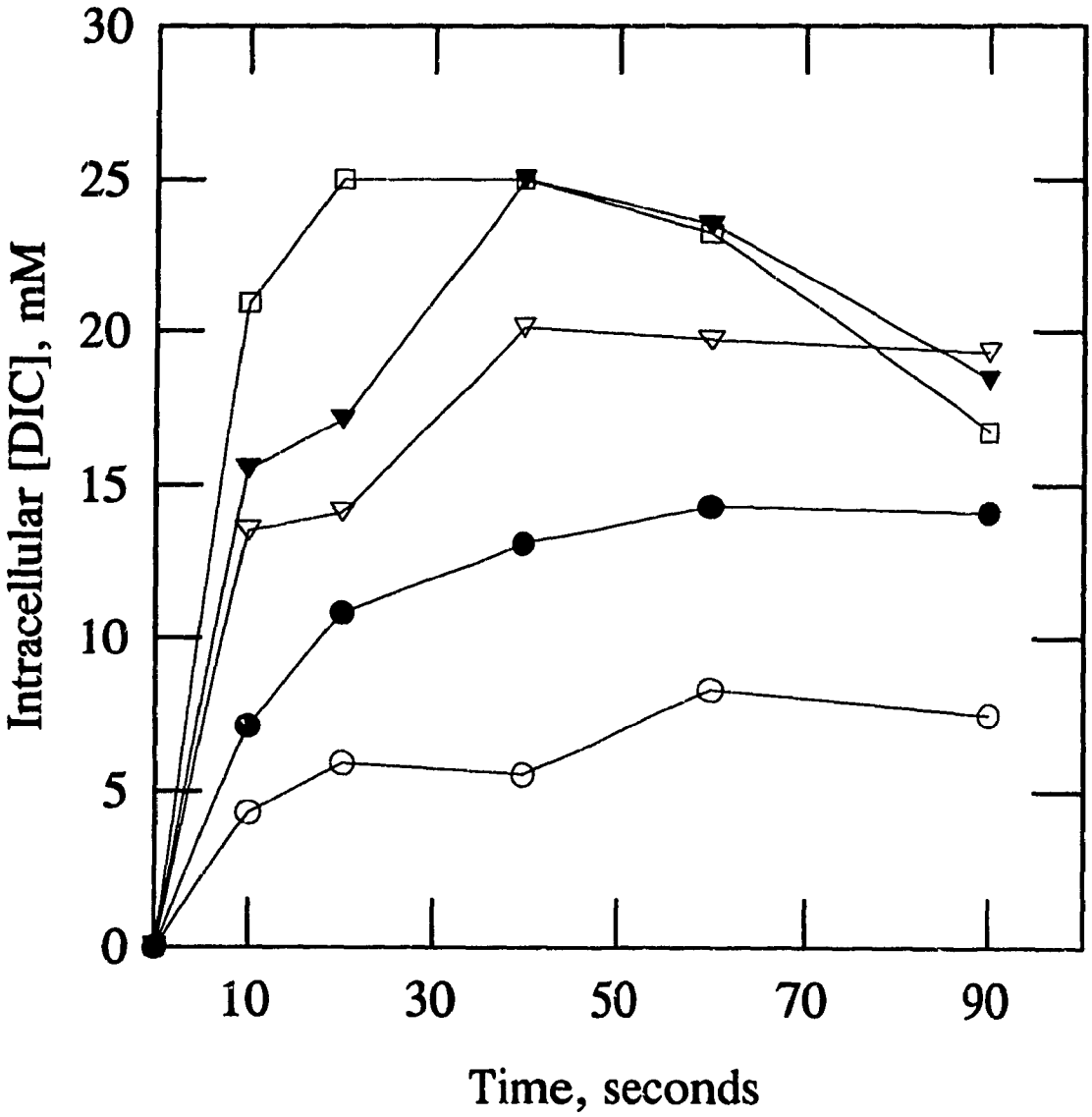
30
25
20
15
10
5
0
Intracellular [DIC], mM
10
30
50
70
90
Time, seconds

entry into air-grown cells was the Na^+ dependent HCO_3^- transport mechanism.

When a low [DIC] (20 μM) was added to air-grown cells at the CO_2 compensation point in the absence of mM levels of Na^+, very little change in the yield of chl a fluorescence was observed (Espie and Kandasamy, 1992). There was only a small DIC pool formed under these circumstances and the rate of photosynthesis was attributable entirely to CO_2 transport supported by HCO_3^- dehydration in the medium (Espie et al, 1988b; Espie and Kandasamy, 1992). The addition of mM levels of Na^+ resulted in a rapid quenching of chl a fluorescence (Espie and Kandasamy, 1992; Fig. 4). Figure 4 illustrates that both the initial rate of chl a fluorescence quenching and the extent of quenching were responsive to increasing levels of Na^+ in the range 1 - 25 mM.

The relationship between the extent of fluorescence quenching (expressed as $\%F'_v$) and the maximum intracellular DIC concentration attained by air-grown cells at 20 μM DIC and varying Na^+_o is depicted in Fig. 5. The data shown in Fig. 5 were obtained from Figs. 3 and 4. Analysis of the two sets of data indicated that they were highly correlated ($r = .987$) by linear regression ($y = 1.5 x - 3.36$). Statistical analysis (Students -t) revealed that the probability of obtaining an r - value this high by chance alone is less than 0.2 % ($P < 0.002$). No data was obtained at intracellular DIC concentrations lower than 7.5 mM, however extrapolation of the linear regression (and the 95 % confidence intervals) predicted that fluorescence quenching would be absent in the absence of an intracellular DIC pool. In fact, at the CO_2 compensation point where the intracellular DIC pool was small, chl a fluorescence was always near its maximum and little quenching was observed (Espie and Kandasamy, 1992).

FIGURE 4

Effect of 1 - 25 mM Na^+ on the time course of chl a fluorescence quenching in air - grown cells. Experiments were conducted at pH 9.08, 30°C, and light was supplied at 100 μmol photons.m^{-2}.s^{-1}. The initial DIC was 20 μM (added at time indicated by arrow) and the chl concentration was 5.8 μg.ml^{-1}. Individual time courses have been overlaid to facilitate comparison.

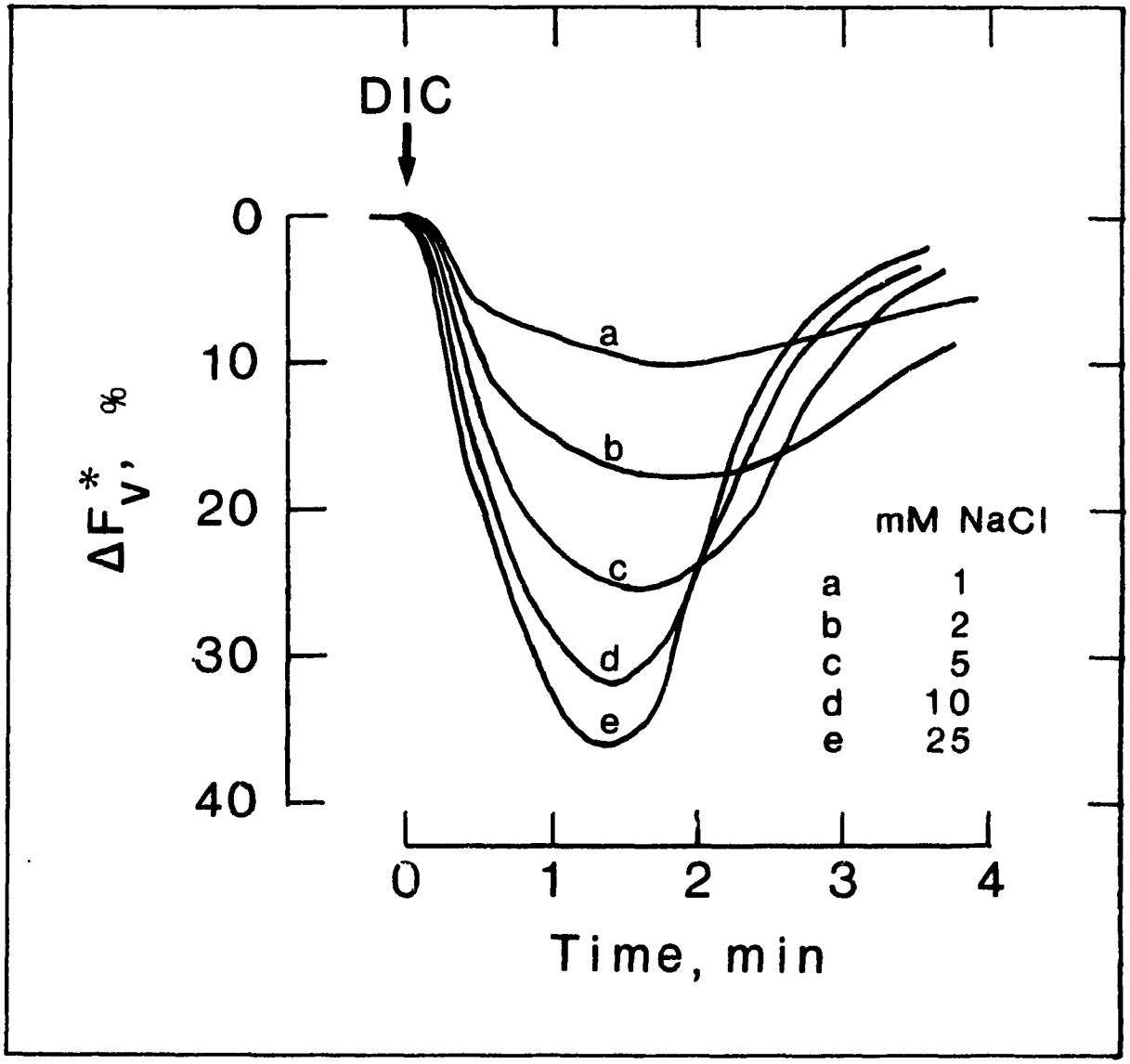
DIC
0
10
20
30
40
ΔF_v^*, %
a
b
c
d
e
mM NaCl
a 1
b 2
c 5
d 10
e 25
0
1
2
3
4
Time, min

FIGURE 5

Correlation between the extent of chl a fluorescence quenching (% F^{*}_{v}, obtained from Fig 4 and the maximum intracellular DIC accumulated (mM DIC, obtained from Fig 3) in air-grown cells. Increases in both quenching and maximum pool size were obtained by varying extracellular Na^{+} from 1 - 25 mM while holding [DIC] constant at 20 μM. At pH 9.1 and 20 μM DIC, Na^{+} dependent HCO_3^- transport is the predominant mechanism of DIC acquisition. The data were correlated (r = .987) by linear regression (y = 1.5x - 3.36). Shown is the linear regression and 95 % confidence intervals.

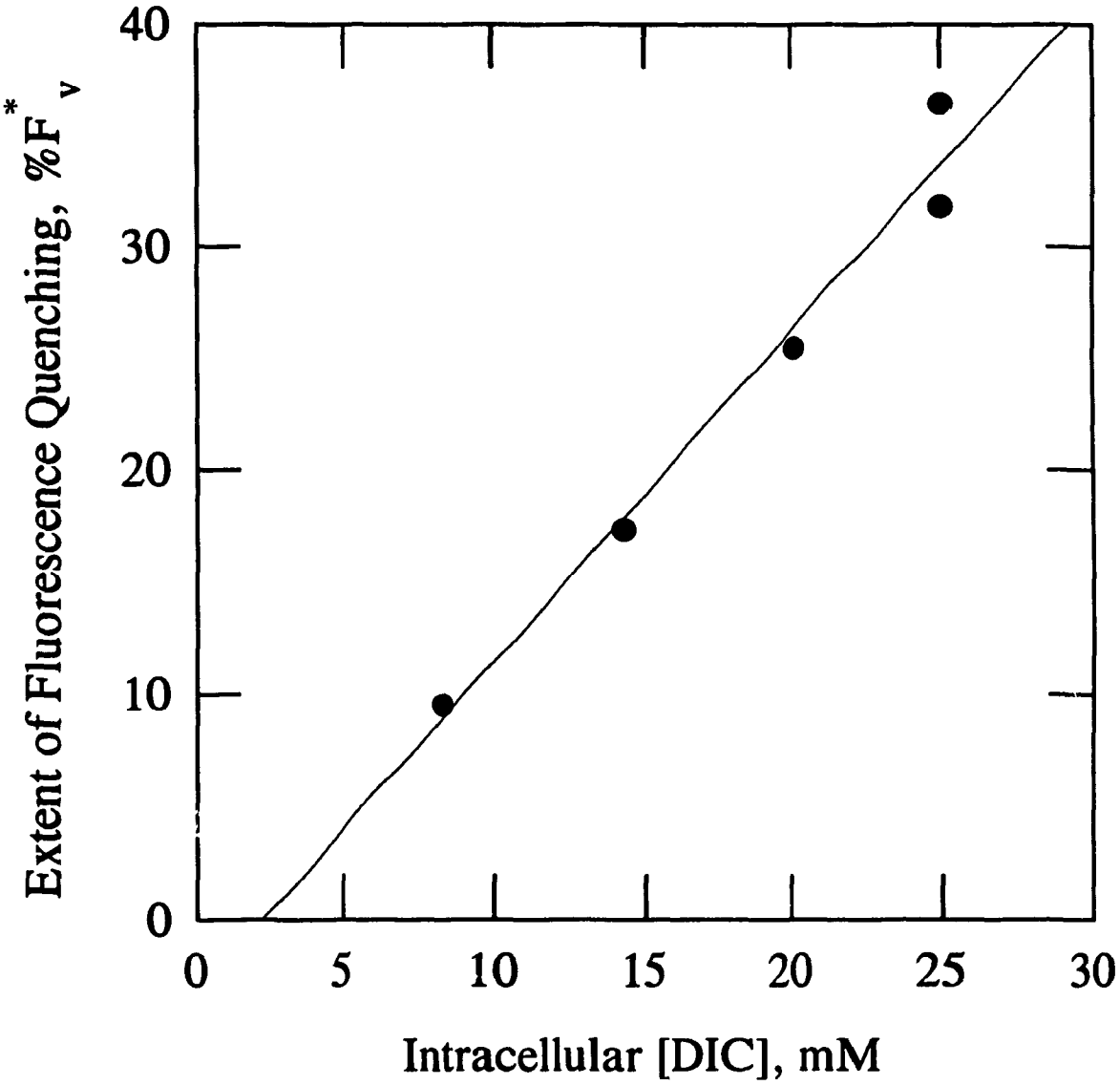
Extent of Fluorescence Quenching, %F*v
40
30
20
10
0
0
5
10
15
20
25
30
Intracellular [DIC], mM

The data shown in Figs.3,4,& 5 were obtained under conditions where HCO_3^- was the main [DIC] species being transported. A similar correlation, obtained under conditions where CO_2 transport was the main route for DIC acquisition from the extracellular medium has recently been presented (Miller et al,1991; Espie and Kandasamy, 1992). It can be concluded that; (1) fluorescence quenching provided a quantitative and accurate indicator of the size of the internal DIC pool, regardless of the DIC species being transported (2) the absence of fluorescence quenching can be taken to indicate that little or no DIC pool formation occured.

The flow of DIC in cyanobacterial photosynthesis has been shown to proceed from the external environment to the internal pool and then to carbon fixation products of photosynthesis (Kaplan et al,1980; Shelp and Canvin, 1984; Espie and Kandasamy, 1992). It has also been shown that the rate of carbon dioxide fixation is proportional to the size of the internal DIC pool (Kaplan et al. 1980; Shelp and Canvin, 1984; Espie and Kandasamy, 1992). If the extent of fluorescence quenching is an indication of the size of the pool, then there should be a relation between the extent of fluorescence quenching ($\%F'_v$) and the rate of photosynthesis. The data presented in Fig. 6 indicate that the rate of photosynthesis was linearly related to the extent of fluorescence quenching. The data provide further evidence that the fluorescence quenching technique monitored the size of the intracellular [DIC] pool under conditions where HCO_3^- was the main [DIC] species being transported.

The fluorescence quenching technique has been shown to monitor the accumulation of intracellular DIC, even when CO_2 fixation is blocked by Calvin cycle

FIGURE 6

Correlation between the extent of fluorescence quenching ($\%F'_v$) and photosynthesis (μmol O_2.mg^{-1} chl.h^{-1}) in air-grown cells. Photosynthesis and fluorescence quenching were measured simultaneously at 30°C. Illumination was provided at 100 μmol photons.m^{-2}.s^{-1}. Both parameters were varied by varying the initial extracellular [DIC] (4 - 100 μM), the extracellular pH (8.0 - 9.5), and the extracellular Na^+ (1 - 25 mM). Results shown are from six separate experiments using four separate batches of cells.

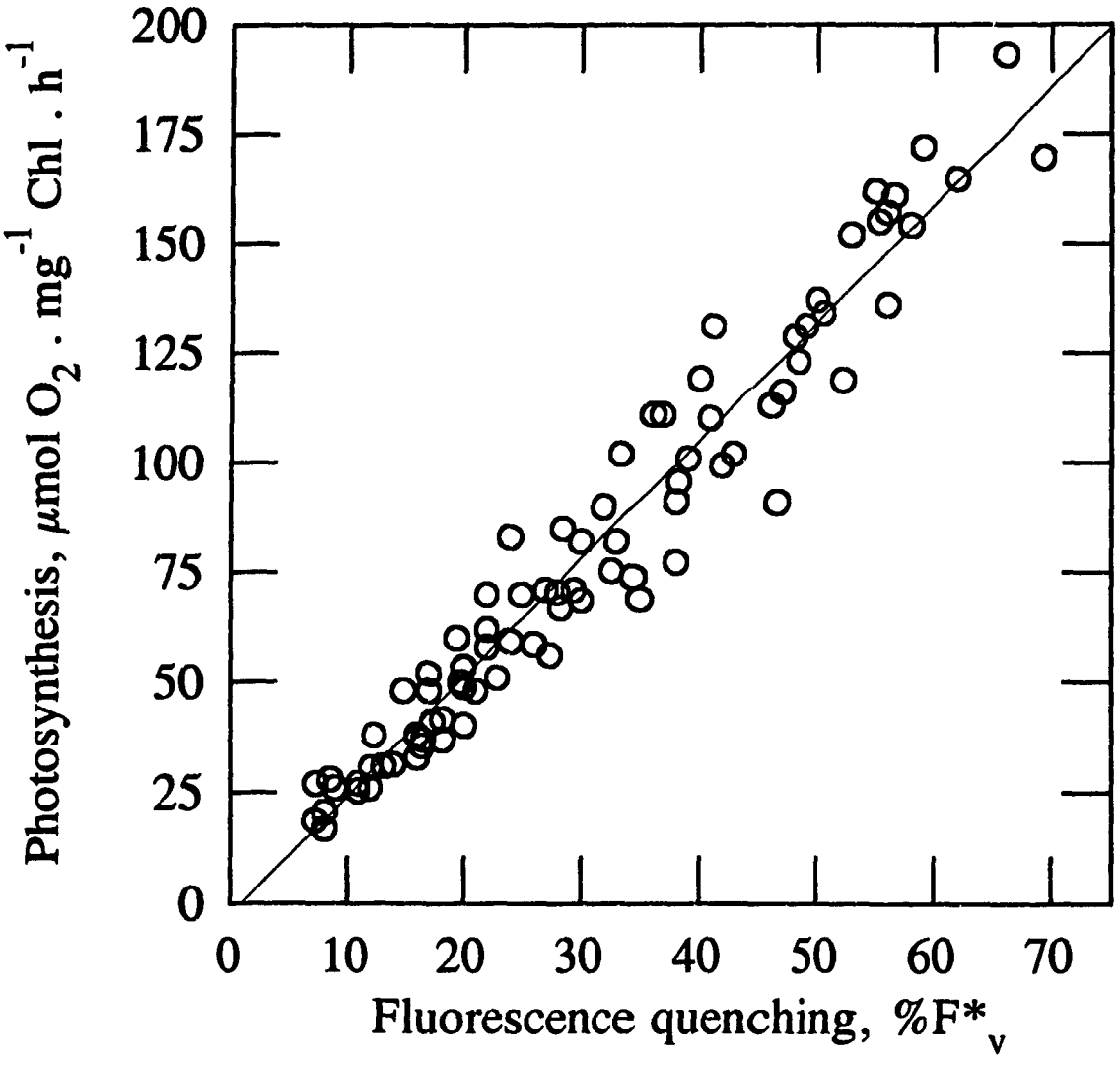
Photosynthesis, μmol O_2 . mg^{-1} Chl . h^{-1}
200
175
150
125
100
75
50
25
0
0
10
20
30
40
50
60
70
Fluorescence quenching, $\%F^*_v$

inhibitors such as glycolaldehyde (Miller and Canvin,1989; Fig. 7) or iodoacetimide (Miller et al,1988c). Figure 7 shows that the initial rate of chl a fluorescence quenching was reduced by about 50 % by 15 mM glycolaldehyde, however the maximal extent of quenching was little affected. The effect of glycolaldehyde on chl a fluorescence quenching is variable since, in some instances the initial rate of quenching is unaffected (Espie, unpublished observation). The variability is likely due to varying levels of O_2 in the medium (see below).

Saturating flashes of high intensity light (1600 μmol photons$\cdot m^{-2}\cdot s^{-1}$) resulted in the recovery of about 70 % of $F^{\bullet}_v$ without glycolaldehyde, and about 60 % of $F^{\bullet}_v$ with glycolaldehyde present. Without glycolaldehyde present, the dissipation of the pool through CO_2 fixation resulted in a rapid recovery of fluorescence yield after approximately 90 seconds. With glycolaldehyde the inhibition of CO_2 fixation prevented the dissipation of the pool and the fluorescence remained quenched. In Fig. 7 the maximum extent of quenching was not affected by glycolaldehyde however in some experiments the addition of glycolaldehyde reduced the maximum extent of quenching by up to 40 % (Miller and Canvin, 1989). It is known that DIC transport will stimulate electron flow to O_2 (Miller et al, 1988c), and in the absence of electron flow to CO_2, the quenching of chl a fluorescence will vary with the O_2 concentration in the medium (Miller et al,1991). The results of Fig. 7 indicate that a substantial portion of the chl a fluorescence quenching induced by DIC transport was independent of the events associated with CO_2 fixation. The presence of 15 mM glycolaldehyde did not affect total DIC uptake (Fig. 8). The inhibition of carbon dioxide fixation by glycolaldehyde (Fig.

FIGURE 7

Effect of 15 mM glycolaldehyde on chl a fluorescence quenching initiated by the addition of 20 μM DIC in air-grown cells. Experiment was conducted at pH 8.1, 30° C, with 25 mM NaCl, and light was supplied at 100 μmol photons.m^{-2}.s^{-1}. A saturating, 1 second flash of high intensity white light (1600 μmol photons.m^{-2}.s^{-1}) was provided to the cells periodically in order to fully reduce Q_A, and to estimate F'_m.

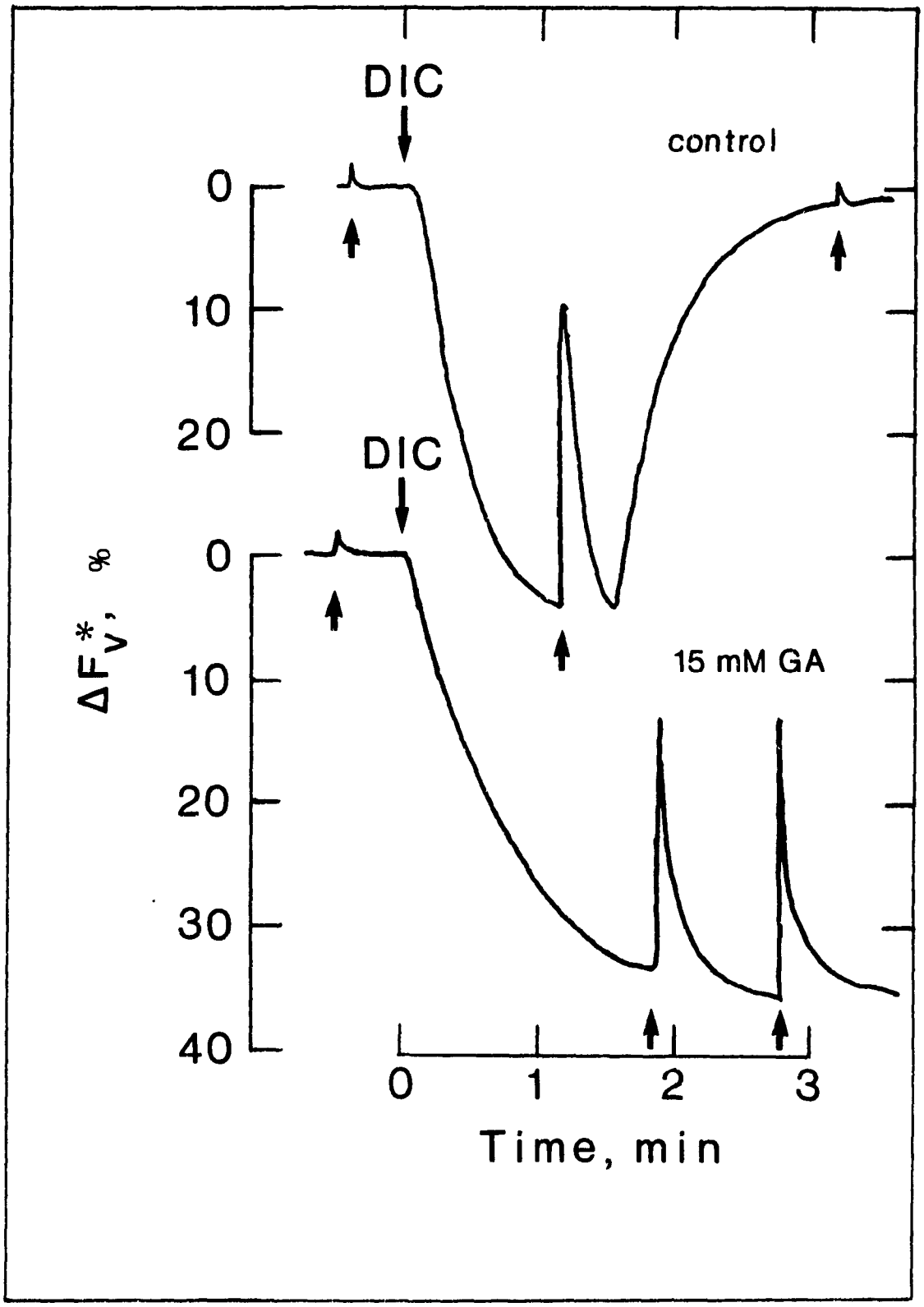
DIC
control
0
10
20
DIC
0
10
20
30
40
ΔF_v^*, %
15 mM GA
0
1
2
3
Time, min

FIGURE 8

Time course of (A) intracellular DIC accumulation and (B) carbon dioxide fixation in air grown cells in the (●) presence and (○) absence of 15 mM glycolaldehyde. Data represent the average of triplicate measurements. Experiments were conducted at pH 8.1, 30°C, with 25 mM NaCl and light was supplied at 300 μmol photons.m^{-2}.s^{-1}. The [chl] ranged from 8 - 10 μg.mL^{-1}. The initial [DIC] was 20 μM with a specific activity of 50 μCi.$\mu$$mol^{-1}$.

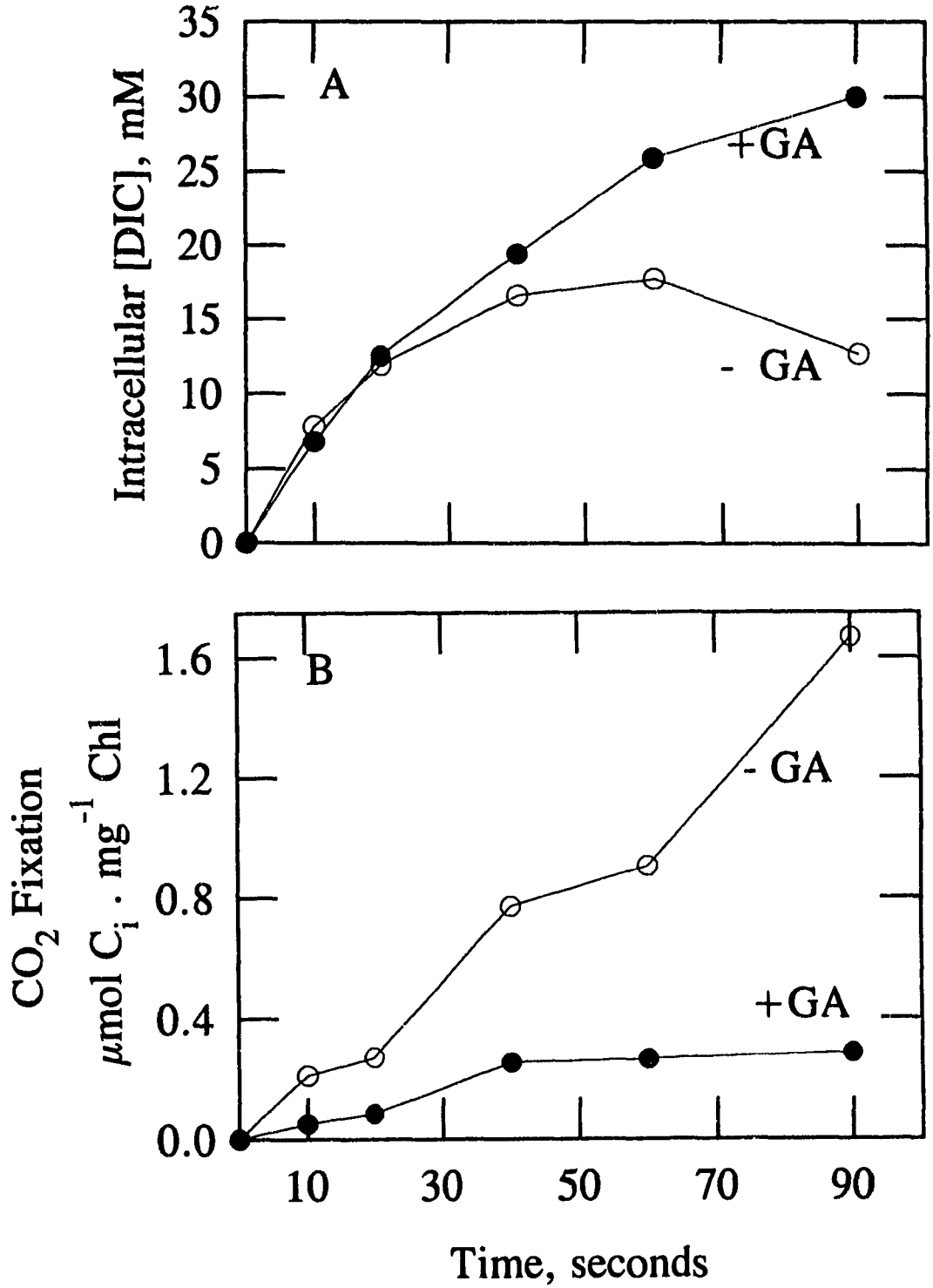
A
Intracellular [DIC], mM
35
30
25
20
15
10
5
0
+GA
- GA
B
CO_2 Fixation
μmol C_i . mg^{-1} Chl
1.6
1.2
0.8
0.4
0.0
- GA
+GA
10
30
50
70
90
Time, seconds

8b) prevented the drawdown of the internal DIC pool, resulting in a larger steady state internal DIC pool (Fig. 8a). The fact that the larger DIC pool was not reflected in a corresponding increase in chl a fluorescence quenching indicates that some portion of the quenching was associated with electron flow to $NADP^+$ and beyond.

INTERACTION BETWEEN EXTRACELLULAR pH AND Na^+

The photosynthetic response of air-grown cells to Na^+ is shown in Fig. 9. At a fixed concentration of DIC (20 μM), increasing levels of Na^+ stimulated the rate of photosynthesis up to a saturation level beyond which further Na^+ addition had no effect. As shown in Fig. 9 (inset) the amount of Na^+ required for half saturation varied with the extracellular pH. The double reciprocal plot in the inset of Fig. 9 also indicates that there was no effect of extracellular pH on the V_{max} for photosynthesis at a fixed DIC. For the experiment shown in Fig. 9, at pH 8.1 the $K_{1/2}$ for Na^+ was 4.0 mM while at pH 9.6 it was 0.8 mM. A number of experiments were carried out to determine the trend of the relationship between the $K_{1/2}$ for Na^+ and extracellular pH at 20 μM DIC and the results are summarized in Fig. 10. This figure indicates that the photosynthetic affinity for Na^+ increased with increasing pH. The $K_{1/2}$ for Na^+ at around pH 8.0 was 5.5 $\pm$ 1.5 mM (n = 3) and declined to 1.3 $\pm$ 0.7 mM (n = 5) at around pH 9.5. Intermediate values of $K_{1/2}$ were found at intermediate pH. The inset to Fig. 10 depicts the variation of V_{max} for photosynthesis with extracellular pH at 20 μM DIC. The largest difference in V_{max} between two pH values would appear from the inset of Fig. 9 to be between pH 8.5 and pH 9.5, however, statistical analysis (ANOVA using the F-test) revealed that the the two means were not significantly different ($P < 0.05$). Furthermore, statistical analysis

FIGURE 9

Effect of Na^+ and pH on photosynthesis in air grown cells. Oxygen evolution was measured at 30°C and illumination was provided at 100 μmol photons.m^{-2}.s^{-1}. Measurements were carried out at (○) pH 8.1 and (●) pH 9.55. DIC was provided at an initial concentration of 20 μM. The $K_{1/2}$ for Na^+ was 4.0 and 0.8 mM at pH 8.1 and pH 9.55, respectively. The maximum rate of photosynthesis at 20 μM DIC was 100 μmol O_2.mg^{-1}chl.h^{-1} and 91 umol O_2.mg^{-1}chl.h^{-1} at pH 8.1 and pH 9.55, respectively. The $K_{1/2}$ and maximum rate of photosynthesis were determined by linear regression analysis of double reciprocal plots of the data (inset). The [chl] was between 9 and 10 μg chl.mL^{-1}.

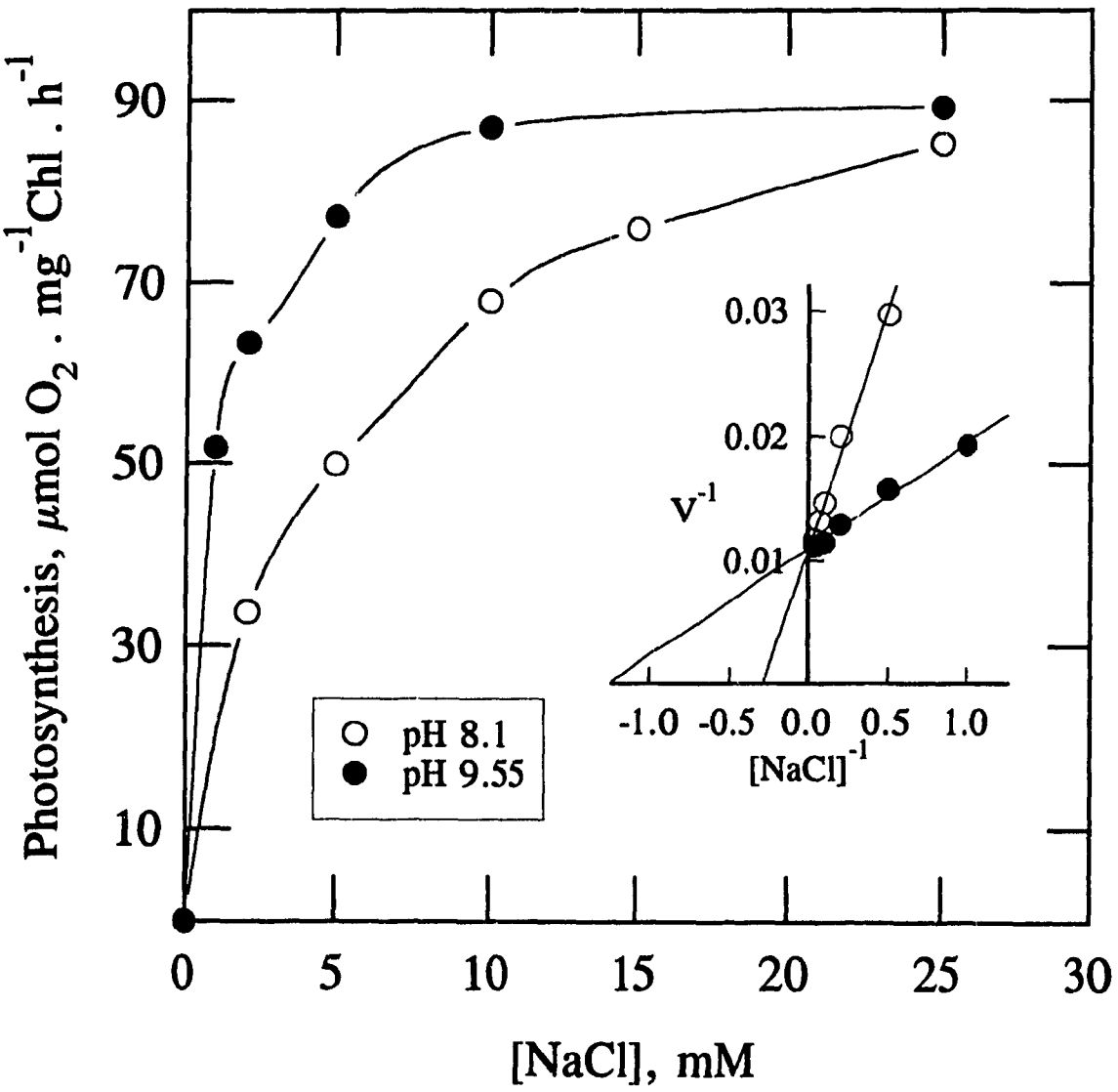
Photosynthesis, μmol O_2 . mg^{-1}Chl . h^{-1}
90
70
50
30
10
0
5
10
15
20
25
30
[NaCl], mM
pH 8.1
pH 9.55
0.03
0.02
0.01
V^{-1}
-1.0 -0.5 0.0 0.5 1.0
$[NaCl]^{-1}$

FIGURE 10

Effect of extracellular pH on $K_{1/2}$ for Na^+ and V_{max} (inset) for photosynthesis (measured as O_2 evolution) at 20 μM DIC. The extracellular pH was varied between 8.0 and 9.55 and extracellular Na^+ was varied between 1 - 25 mM. Kinetic parameters were determined from linear regression analysis of double reciprocal plots of the data. Experiments were carried out at 30C, illumination was provided at 100 μmol photons.m^{-2}.s^{-1}, and the [chl] ranged between 7 - 12 μg.mL^{-1}.

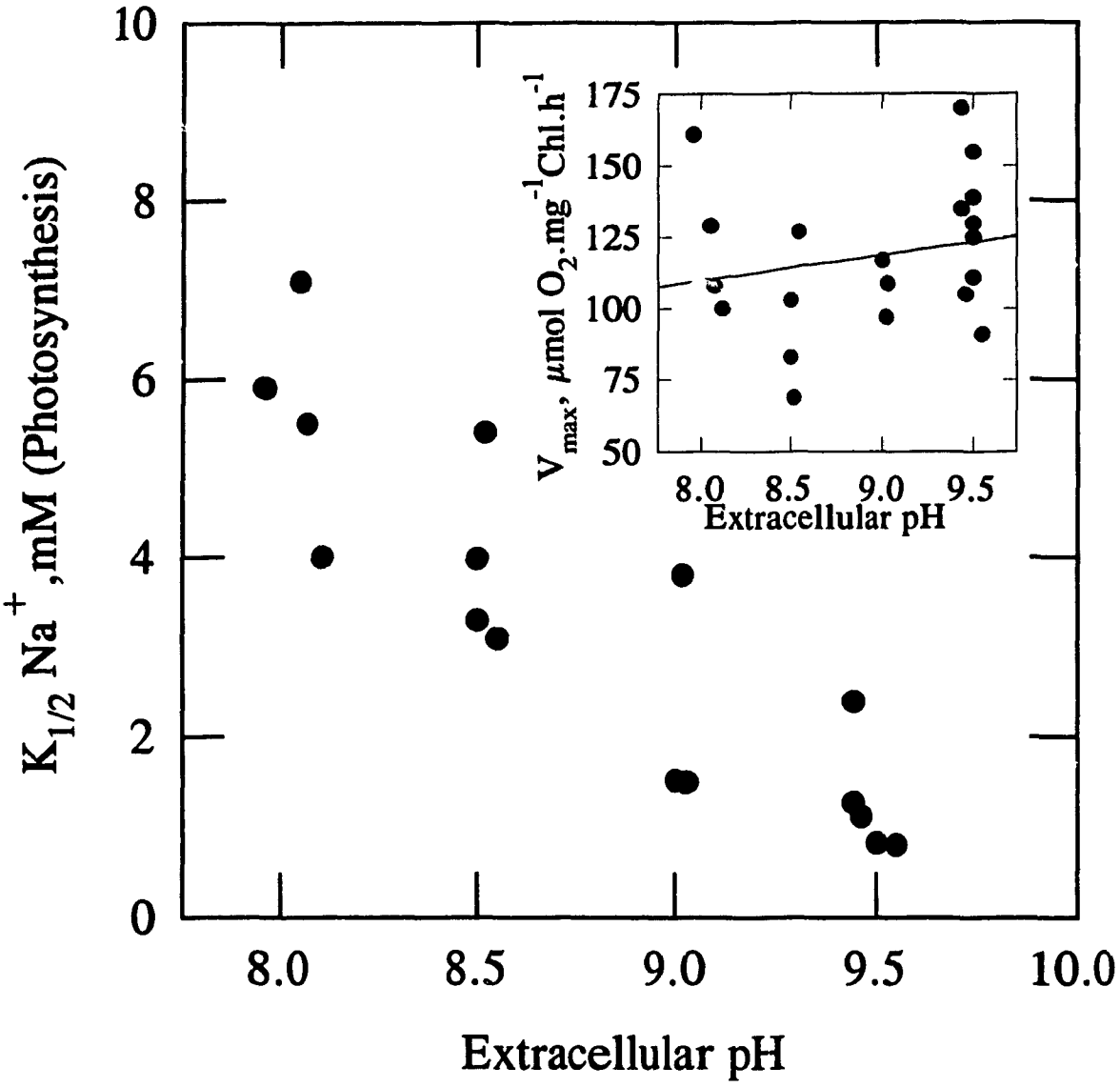
10
8
6
4
2
0
8.0
8.5
9.0
9.5
10.0
$K_{1/2}$ Na^+ ,mM (Photosynthesis)
Extracellular pH
175
150
125
100
75
50
V_{max}, μmol O_2.mg^{-1}Chl.h^{-1}
8.0
8.5
9.0
9.5
Extracellular pH

(Students-t) showed that the linear regression line through the data had a slope not significantly different from zero.

The changes in photosynthetic affinity for Na^+ with varying external pH presumably arose from changes in transport processes, since transport would appear to be the limiting factor in cyanobacterial photosynthesis at low DIC (Mayo et al. 1989). This possibility was investigated using both the silicon fluid centrifugation technique and chl a fluorescence quenching as an indirect monitor for transport. Using air-grown cells, with varying levels of [NaCl], and at constant DIC (20 μM), the initial rates (10 - 15 seconds) of quenching and HCO_3^- uptake (10 seconds) were plotted as a function of extracellular [NaCl] (Fig. 11a and b). The initial rates for both measurements were normalized as a % of the maximum rate obtained. The $K_{1/2}$ for Na^+ at pH 8.1 was 10.3 mM using the initial rate of fluorescence quenching and 5.5 mM using the silicone-fluid method (Fig. 11a). At pH 9.1 the $K_{1/2}$ for Na^+ was 2.6 mM using fluorescence quenching and 4.3 mM using the silicon-fluid method (Fig. 11b). The response of $K_{1/2}$ for Na^+ to extracellular pH for both fluorescence quenching and HCO_3^- transport is shown in Fig. 12. This figure shows that the apparent affinity of the HCO_3^- transport system for Na^+ increased with increasing extracellular pH. This response mirrored that of the $K_{1/2}Na^+$ for photosynthesis with varying pH (Fig 10). These results (Figs 10 & 12) are consistent with an effect of pH and Na^+ being exerted directly at the level of the transport mechanism in air grown cells.

FIGURE 11

Effect of Na^+ and pH on (●) initial rate of chl a fluorescence quenching and (○) initial rate of HCO_3^- uptake measured using the silicone fluid centrifugation technique. Initial rates (10 - 15 seconds) using both methods were determined at (A) pH 8.1 and (B) pH 9.1 (B). Measurements are normalized as a percent of the maximum rate obtained (at 25 mM NaCl). Maximum rates of HCO_3^- uptake at 20 μM DIC were 133 μmol C_i.mg chl^{-1}.hr^{-1} and 215 μmol C_i.mg chl^{-1}.hr^{-1} at pH 8.1 and pH 9.1, respectively. HCO_3^- uptake was measured at 30°C and with illumination at 300 μmol photons $m^{-2}.s^{-1}$. Fluorescence quenching was measured at 30°C and with illumination at 100 μmol photons.$m^{-2}.s^{-1}$. The [chl] ranged between 9 - 12.5 μg chl.mL^{-1}.

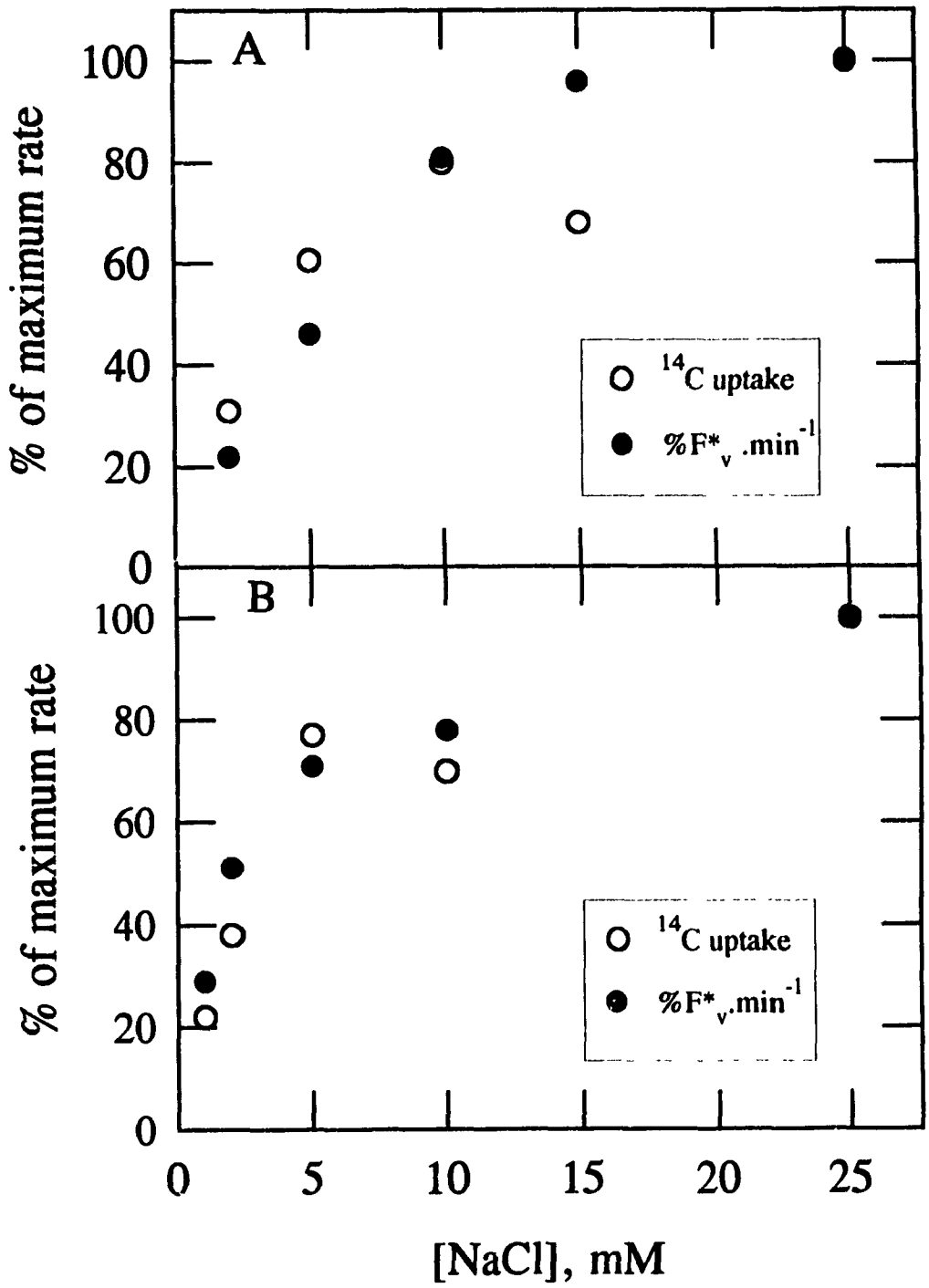
A
B
100
80
60
40
20
0
% of maximum rate
^{14}C uptake
%F*$_v$ .min^{-1}
0
5
10
15
20
25
[NaCl], mM

FIGURE 12

Effect of extracellular pH on $K_{1/2}^{Na+}$ for (○) initial rates of fluorescence quenching and (●) initial rates of HCO_3^- uptake measured using the silicon fluid centrifugation technique. The pH was varied between pH 8.0 and pH 9.55 and extracellular Na^+ was varied between 1 and 25 mM at a constant initial [DIC] (20 μM). $K_{1/2}$ was determined by linear regression analysis of double reciprocal plots. Experiments were carried out at 30°C, illumination was provided at 100 μmol photons.$m^{-2}.s^{-1}$ for fluorescence experiments and 300 μmol.$m^{-2}.s^{-1}$ for silicone fluid centrifugation experiments.

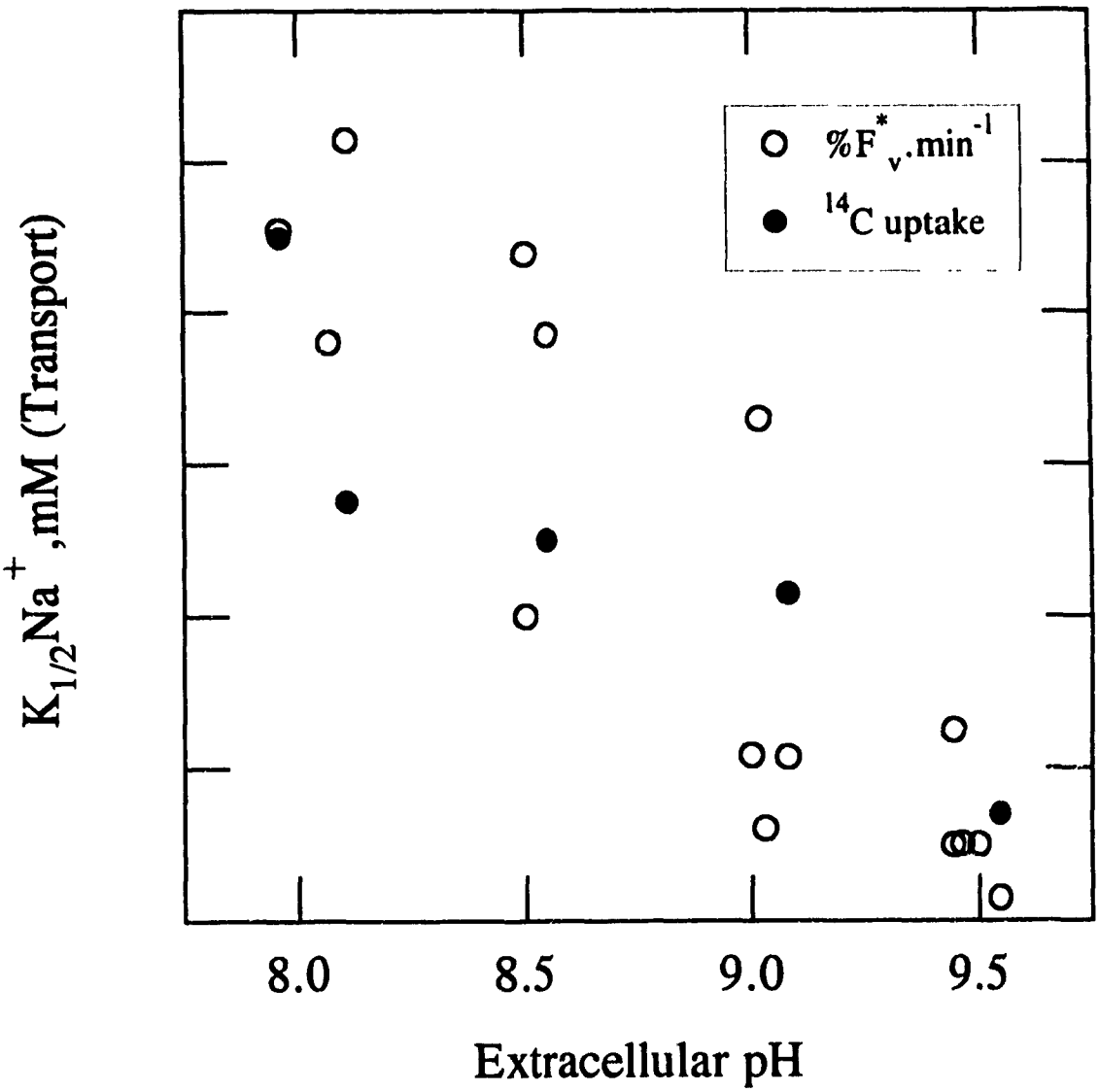
$K_{1/2}Na^+$,mM (Transport)
%F^*_v.min^{-1}
^{14}C uptake
8.0
8.5
9.0
9.5
Extracellular pH

RELATIONSHIP BETWEEN RATES OF CHL a FLUORESCENCE QUENCHING AND RATES OF HCO_3^- UPTAKE

The initial rate of chl a fluorescence quenching has been shown to be highly correlated with the initial rate of CO_2 disapearance from the medium as measured by mass spectrometry (Espie et al,1991). A series of experiments were performed to determine whether or not a similar correlation would apply under conditions where HCO_3^- transport was the primary means of DIC acquisition. The data are shown in Fig. 13a and b where the correlation between the initial rate of fluorescence quenching ($\%F'_v.mg^{-1}chl.n^{-1}$ on the y-axis and initial rate of HCO_3^- uptake (μmoles C_i. mg $chl^{-1}.hr^{-1}$) on the x-axis is depicted. The data were well correlated (r = .785) by linear regression (y = .188x + 21.8) (Fig 13a). The computed r^2 for the regression (0.62) indicated that 62 % of the variation in initial rates of fluorescence quenching could be explained by variation in the initial rate of HCO_3^- uptake. Statistical analysis (t-test) revealed that this correlation was highly significant ($p < .001$). The regression predicted that at zero rate of HCO_3^- transport there would still be a substantial rate of quenching (21.8 $\%F_v.mg^{-1}chl.h^{-1}$). In fact, at the CO_2 compensation point, where no net DIC transport occured, fluorescence was always near its maximum level and nc quenching independent of HCO_3^- transport under these circumstances (Figs 2 & 7, Espie and Kandasamy, 1992). Based on this observation, a forced-fit linear regression through the origin was performed (Fig 13b). The correlation co-efficient for the regression through the origin (Fig 13b) indicated a better fit to the data (r = 0.957) than for the simple linear regression (Fig 13a).

The large y-intercept predicted by simple linear regression (Fig 13a) can perhaps

FIGURE 13

Relationship between the initial rate of chl a fluorescence quenching ($\%F^{*}_{v}.min^{-1}.mg^{-1}$ chl) as measured using the PAM fluorometer and initial rate of HCO_3^- transport as measured by the silicone fluid centrifugation method. The data were obtained from eight separate experiments using six separate batches of air-grown cells. For each point, parallel measurements of fluorescence quenching and transport were made. The initial rates were measured at various HCO_3^- (5 - 100 μM), Na^+ (1 - 25 mM), and pH (8.0 - 9.55). The temperature was maintained at 30°C and illumination was provided at 100 μmol photons.$m^{-2}.s^{-1}$ for fluorescence measurements and 300 μmol photons.$m^{-2}.s^{-1}$ for HCO_3^{-1} uptake experiments. The data were correlated by (A) simple linear regression or (B) linear regression through the origin.

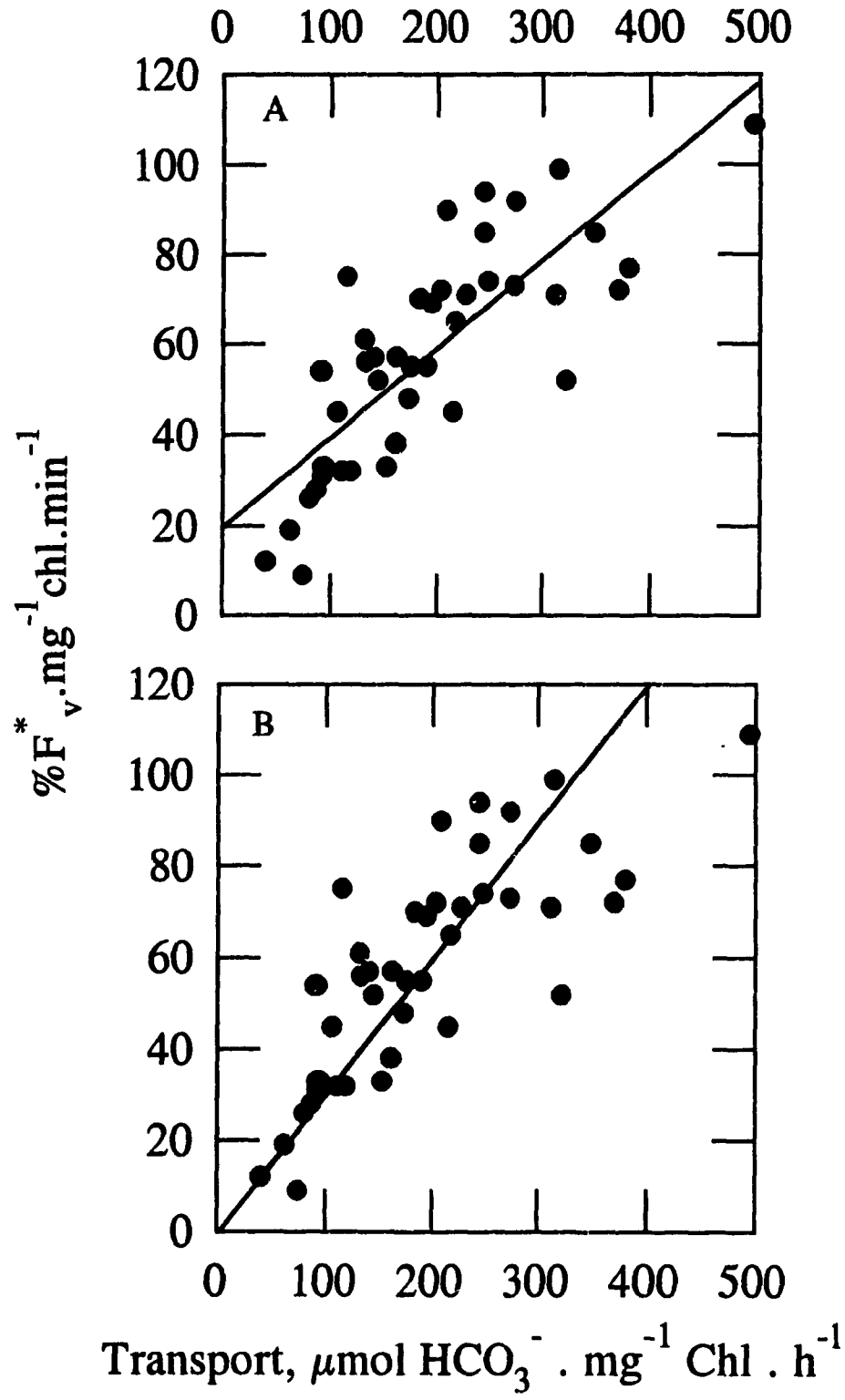
0 100 200 300 400 500
120
100
80
60
40
20
0
A
B
$\%F^*_v.mg^{-1}chl.min^{-1}$
Transport, μmol HCO_3^- . mg^{-1} Chl . h^{-1}

be explained if it is assumed that the fluorescence quenching technique loses some of its resolution at very high transport rates, leading to an underestimation of the transport rate at very high quenching rates. If this is the case then some of the variation in quenching rates which is not accounted for by changes in the transport rates might also be due to a loss of resolution at high quenching rates. A recent report (Miller et al,1991) has shown that more chl a fluorescence quenching was evident in the presence of O_2 and CO_2 than in the presence of CO_2 alone. The experiments shown in Fig 13 were performed at O_2 concentrations between 20 and 100 μM to control for the effects of O_2. Clamping the O_2 concentration at a fixed and constant level was not possible due to ongoing photosynthesis. Chl a fluorescence quenching was partially dependent on electron flow to CO_2 rather than strictly dependent on the rate of HCO_3^- transport (Figs 7 - 8). These factors were probably responsible for the residual variability in chl a fluorescence quenching which cannot be accounted for by variability in HCO_3^- transport rates. Nonetheless, the results shown in Fig. 13 indicate that there was a significant correlation between initial rates measured using these two methods.

PHOTOSYNTHESIS IN LOW DIC (30 μL.L^{-1} CO_2) GROWN CELLS

The photosynthetic response to extracellular DIC of cells grown at pH 8.0 and bubbled with low CO_2 (30 μL.L^{-1} CO_2) is shown in Figs. 14 and 15. Fig. 14 depicts the rates of photosynthesis as measured by O_2 evolution in the presence and absence of 25 mM NaCl at pH 8.0. At 10 μM DIC, the CO_2 supply rate from HCO_3^- dehydration would initially be 1.3 nmoles.ml^{-1}.min^{-1}. The actual rate of photosynthesis observed in the absence of Na^+ was 9.4 nmoles O_2ml^{-1}.min^{-1}. The rate of photosynthesis at 10 μM

FIGURE 14

DIC response curves for photosynthesis (measured as O_2 evolution) in 30 $\mu L.L^{-1}$ CO_2 grown cells in the (●) presence and (○) absence of 25 mM NaCl at pH 8.0. The cells were grown in buffered (25 mM BTP/HCl, pH 8.0) Allen's medium bubbled with 30 $\mu L.L^{-1}$ CO_2 and were harvested at 6 - 8 μg chl.mL^{-1}. For the experiment shown, linear regression through double-reciprocal plots of the data resulted in $K_{1/2}^{DIC}$ values of 6.0 and 8.5 μM in the presence and absence of 25 mM Na^+, respectively. Maximum photosynthetic rates predicted by double-reciprocal plots were 143 and 141 $\mu mol\ O_2.mg^{-1}$ chl.hr^{-1} in the presence and absence of 25 mM Na^+, respectively.

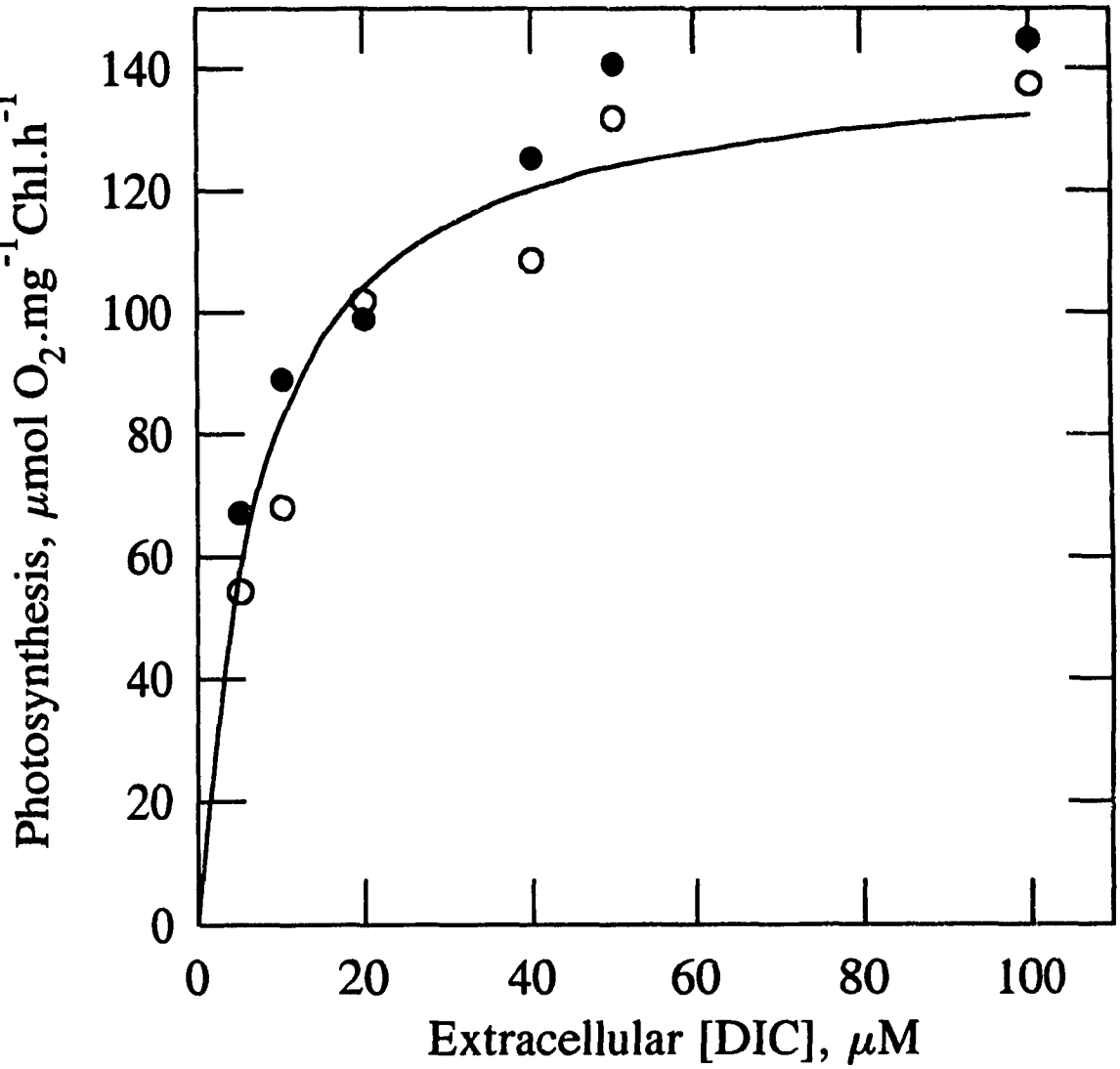
Photosynthesis, μmol O_2.mg^{-1}Chl.h^{-1}
0
20
40
60
80
100
120
140
0
20
40
60
80
100
Extracellular [DIC], μM

FIGURE 15

DIC response curve for photosynthesis (measured as O_2 evolution) in 30 $\mu L.L^{-1}$ CO_2 grown cells in the (○) presence and (●) absence of 25 mM NaCl at pH 9.5. The cells were grown in buffered (25 mM BTP/HCl, pH 8.0) Allen's medium with 30 $\mu L.L^{-1}$ CO_2 and were harvested at 6 - 8 μg chl.mL^{-1}. For the experiment shown, linear regression through double reciprocal plots of the data resulted in $K_{1/2}^{DIC}$ values of 5.4 and 8.1 μM in the presence and absence of 25 mM Na^+, respectively. Maximum photosynthetic rates predicted by double - reciprocal plots were 145 and 163 μmol $C_i.mg^{-1}$ chl.h^{-1} in the presence and absence of 25 mM Na^+ respectively.

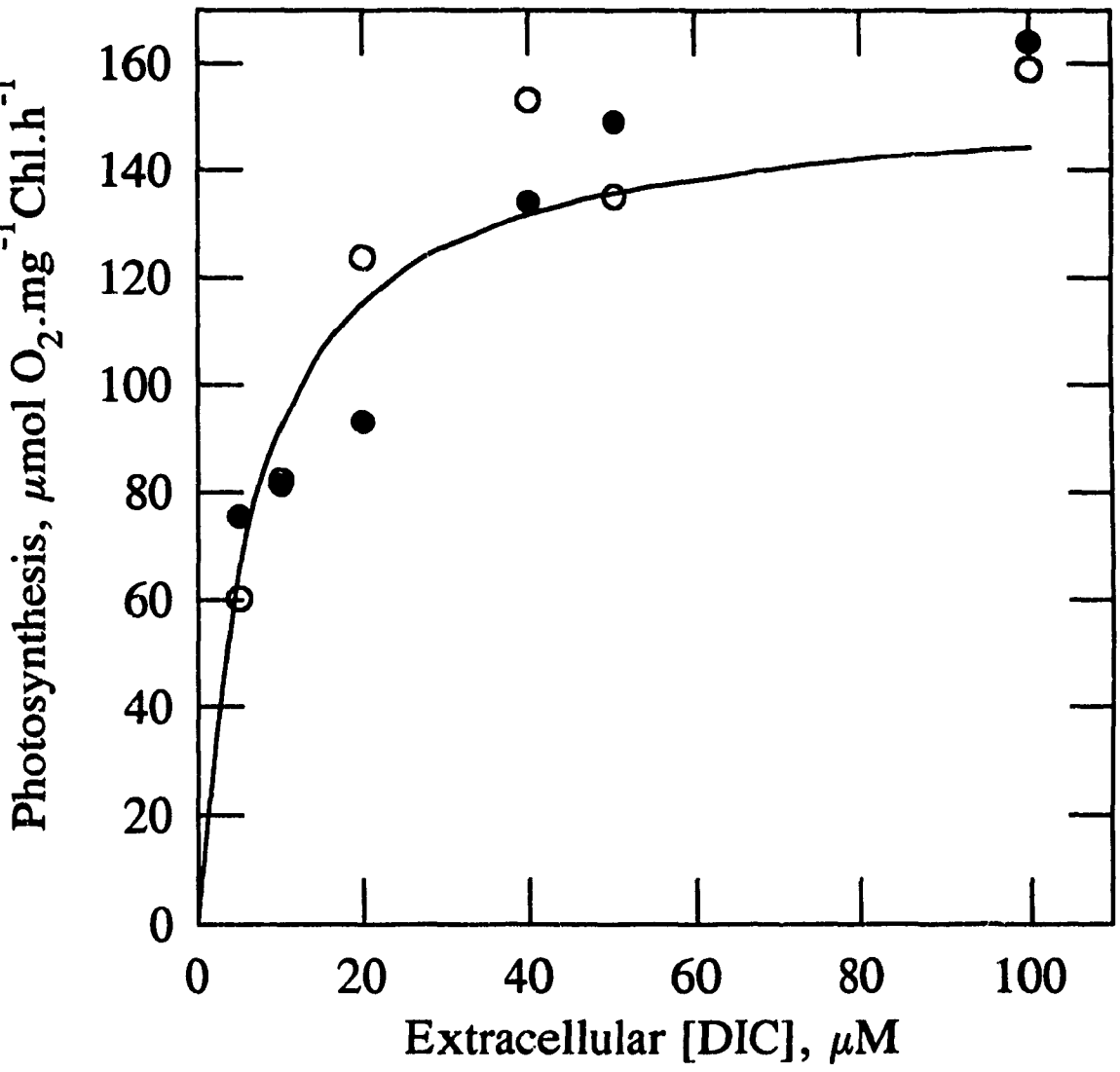
Photosynthesis, μmol O_2.mg^{-1}Chl.h^{-1}
160
140
120
100
80
60
40
20
0
0
20
40
60
80
100
Extracellular [DIC], μM

DIC, in the absence of Na^+, thus exceeded the rate of photosynthesis which could be sustained by CO_2 uptake by 7.2 fold. Over the range of external DIC from 5-100 μM, and in the absence of added Na^+, low DIC grown cells were able to photosynthesize at rates which were considerably in excess of the rate of CO_2 supply from HCO_3^- dehydration (Fig 14). The rate of photosynthesis was not greatly stimulated by the addition of 25 mM NaCl. The average stimulation for the data shown in Fig. 14 was 1.14 fold and did not exceed 1.3 fold.

When photosynthesis was measured at an extracellular pH of 9.5 (Fig. 15), there was no evidence of Na^+ stimulation greater than that which was seen at pH 8.0. The average Na^+ stimulation by 25 mM for the range of DIC between 5 - 100 μM was 1.1 fold and did not exceed 1.3 fold. Since the rate of CO_2 supply from HCO_3^- is known to decrease with increasing pH (Miller and Colman,1980) the factor by which the rate of photosynthesis exceeded the CO_2 supply rate was more pronounced at pH 9.5 than at pH 8.0. Accordingly at pH 9.5, with 10 μM DIC, the rate of photosynthesis exceeded the CO_2 supply rate by 35 fold compared to 7 fold at pH 8.0. The $K_{1/2}^{DIC}$ and V_{max} were not greatly affected by 25 mM NaCl at either pH 8.0 or 9.5 (Figs. 14 and 15). Cells grown at 30 $\mu L.L^{-1}$ CO_2 under the same conditions with the exception of being buffered during growth at pH 9.5 exhibited identical photosynthetic kinetics with respect to Na^+ and DIC (data not shown).

These low DIC grown cells would thus appear to be very similar to standing culture cells, which exhibit Na^+ independent HCO_3^- transport (Espie and Canvin,1987; Espie and Kandasamy, 1992). Standing culture cells have been shown to be devoid of

any measureable extracellular carbonic anhydrase activity by the isotopic disequilibrium method (Espie and Canvin, 1987). A conventional electrometric assay for the presence of extracellular carbonic anhydrase activity indicated that this enzyme was not present in the extracellular space of low DIC grown cells (data not shown). Mass spectrometry has also shown that 30 $\mu L.L^{-1}$ cells of Synechococcus PCC7942 lack extracellular CA (Badger and Price,1989). Since the rate of CO_2 formation from HCO_3^- dehydration was not catalyzed, photosynthesis in excess of the dehydration rate provides strong evidence for the presence of a high affinity Na^+ independent HCO_3^- transport mechanism in 30 $\mu L.L^{-1}$ CO_2 grown cells.

GROWTH DIC AND PHOTOSYNTHESIS

Table 1 outlines some of the features which distinguish Synechococcus UTEX 625 grown under three different conditions (ie. air-grown, standing culture, and 30 $\mu L.L^{-1}$ CO_2 grown cells). There was a significant decline in the $K_{1/2}^{DIC}$ for photosynthesis which corresponded to a decline in the measured growth DIC. This response of photosynthetic affinity for DIC in response to exogenous DIC is consistent with the results obtained by Mayo et al (1986) for Synechococcus UTEX 625 grown in batch culture. In contrast there was no pattern relating growth rate to the exogenous DIC concentration. This can be explained if it is assumed that the growth rate varied according to the rate of CO_2 supply to the medium. The 25 fold difference in the growth rates between standing culture cells and air-grown cells tends to support this assumption since the major difference in growth conditions between these two cell types was the rate of air supply to the medium. Air-grown cells were supplied with 50 μmol photon$\cdot m^{-2}\cdot s^{-1}$ of light during

TABLE 1

Photosynthetic parameters ($K_{1/2}^{DIC}$ and Na^+ stimulation) and growth rates of Synechococcus UTEX 625 grown under various growth DIC. All measurements carried out at pH 8.0.

CELL TYPE	$K_{1/2}^{DIC}$	MEASURED DIC	μ (d^{-1})	Na^+ STIMULATION (25 mM)
30 $\mu L.L^{-1}$ CO_2	9.7 ± 0.5 (n = 3)	3 μM	0.31 ± 0.09 (n = 3)	1.0 - 1.3
SCC	19.5 ± 6.5 (n = 4)	21 μM[a]	0.09[b]	1.0 - 1.6
AGC	39.0 ± 13 (n = 8)	60 - 200 μM[a]	2.22 ± 0.28 (n = 2)	7 - 10

[a] McKay et al., in press

[b] Kandasamy, R., M.Sc. thesis, 1991

growth, compared to 25 μmol photon$\cdot m^{-2}\cdot s^{-1}$ for standing culture cells, therefore the possibility that the difference in the growth rate was due in part to differences in light intensity cannot be discounted. However this possibility seems remote in view of the fact that the light intensity dose response for photosynthesis shows a lower than two-fold stimulation of photosynthesis between 25 and 50 μmol photons$\cdot m^{-2}\cdot s^{-1}$ for both high and low DIC grown cells (Badger and Andrews,1982). The fact that 30 $\mu L.L^{-1}$ CO_2 grown cells, which were supplied with 0.003 % CO_2 (v/v) at a high flow rate (250 mL.$\cdot min^{-1}$), exhibited growth rates which were 3 times higher than standing culture cells, which were provided with 0.03 % CO_2 (v/v) at a very low rate (diffusion through a foam stopper) also supports the hypothesis that growth rate is determined in part by the CO_2 supply rate. It can be concluded that the photosynthetic affinity for DIC was correlated with exogenous DIC, while the growth rate was dependent on a complex interaction between the DIC supply rate and photosynthetic affinity for DIC.

The Na^+ stimulation of photosynthesis at pH 8.0 and at low DIC (5 - 100 uM) followed a graded response with respect to the growth DIC (Table 1). Air-grown cells, which exhibited partially induced high affinity kinetics, are strictly and specifically dependent on the Na^+ ion for HCO_3^- transport (Miller et al,1984; Espie and Canvin,1987; Figs. 3 and 4). In contrast 30 $\mu L.L^{-1}$ cells, which exhibited fully induced high affinity kinetics, typically showed a Na^+ stimulation which did not exceed 1.3 fold. Standing culture cells appeared to be intermediate with respect to both photosynthetic affinity for DIC, and Na^+ stimulation of photosynthesis, which can be as high as 1.6 fold (Espie and Canvin,1987; Espie and Kandasamy, 1992). It should be noted that dilution

of log - phase 30 $\mu L.L^{-1}$ CO_2 grown cells into unbuffered Allen's medium, followed by bubbling with air (0.03 % CO_2 v/v) resulted in the loss of Na^+ independent HCO_3^- transport (data not shown).

THE EFFECT OF ETHOXYZOLAMIDE ON PHOTOSYNTHESIS AND DIC TRANSPORT IN STANDING CULTURE AND 30 $\mu L.L^{-1}$ CO_2 GROWN CELLS

Previous studies have shown that a sulfonamide inhibitor of carbonic anhydrase, ethoxyzolamide (EZA), inhibited CO_2 and HCO_3^- transport in both high and low DIC grown cells of Synechococcus PCC7942 (Price and Badger,1989a). An extensive study of the effect of EZA and Na^+ on standing culture cell photosynthesis and chl a fluorescence quenching has also recently been conducted by Tyrrell and Espie (unpublished). To facilitate comparison of the results of EZA and Na^+ treatment on 30 $\mu L.L^{-1}$ CO_2 grown cells with standing culture cells I have repeated some of the work of Tyrrell and Espie (as indicated).

Figure 16 shows the effects of EZA on initial rates of fluorescence quenching (Fig. 16,a and c) and photosynthesis (Fig. 16,b and d) in both 30 $\mu L.L^{-1}$ CO_2 grown cells (Fig. 16 a and b) and standing culture cells (Tyrrell and Espie, unpublished; Fig. 16, c and d), when HCO_3^- was added as the predominant DIC species. In all cases, the inhibition by EZA in the range of concentration between 5 and 200 μM EZA could be partially reversed by the addition of 25 mM NaCl. Photosynthesis was less sensitive to EZA inhibition than was the initial rate of fluorescence quenching. The extent of fluorescence quenching, however, was inhibited to the same degree as photosynthesis (data not shown). The relief of EZA inhibition by 25 mM Na^+ was more pronounced in

standing culture cells than in 30 $\mu L.L^{-1}$ CO_2 grown cells. This applied to both photosynthesis and the initial rate of fluorescence quenching. It has already been shown that both standing culture and 30 $\mu L.L^{-1}$ CO_2 grown cells possess residual levels of Na^+ dependent HCO_3^- transport (Espie and Kandasamy, 1992; Figs. 14 and 15). The restoration of both photosynthesis and fluorescence quenching by Na^+ suggests that the Na^+ dependent HCO_3^- transport mechanism was less sensitive to EZA inhibition than the Na^+ independent mechanism. The larger relief afforded by 25 mM NaCl in standing culture cells as compared to 30 $\mu L.L^{-1}$ CO_2 grown cells is consistent with the lower levels of Na^+ stimulation of photosynthesis of 30 $\mu L.L^{-1}$ CO_2 grown cells compared to standing culture cells (Figs 14 and 15; Table 1).

In standing culture cells, 50 % inhibition of photosynthesis was estimated to occur at 35 μM EZA in the absence of mM levels of NaCl (Fig. 16d). The stimulation by 25 mM NaCl at this concentration of EZA was approximately 1.5 fold. At 100 μM EZA, the Na^+ stimulation increased to 2.6 fold. Similar results were obtained by Tyrrell and Espie (pers. comm.). In 30 $\mu L.L^{-1}$ CO_2 grown cells, 50 % inhibition of photosynthesis was also estimated to occur at 35 μM EZA in the absence of mM levels of Na^+ (Fig.16b). The stimulation by 25 mM Na^+ was approximately 1.2 fold at 35 μM EZA. At 90 μM EZA, this stimulation increased to 1.8 fold. These observations also applied equally for measurements of the initial rate of fluorescence quenching (Fig.16, a and c). These observations led to the question of whether or not the increased stimulation by 25 mM Na^+ at progressively higher EZA concentrations was due to a feedback mechanism which increased the activity of the Na^+ dependent mechanism under conditions where the

FIGURE 16

Effect of ethoxyzolamide (EZA) on (A and C) the initial rate of chl a fluorescence quenching and (B and D) photosynthesis in (A and B) 30 $\mu L.L^{-1}$ CO_2 grown cells and (C and D) standing culture cells under conditions where HCO_3^- transport was the primary means of DIC acquisition. The initial DIC provided was 10 μM for 30 $\mu L.L^{-1}$ CO_2 grown cells (A and B) and 20 μM for standing culture cells (C and D). Experiments were carried out at pH 8.0, 30°C, in the (●, ▲) presence of 100 μM Na^+ and in the (○, △) presence of 25 mM Na^+. EZA was added from stock solutions of dimethylsulfoxide (DMSO) such that the DMSO concentration did not exceed 1 % (v/v). Light was provided at 100 μmol photons.$m^{-2}.s^{-1}$ and the [chl] ranged between 13 - 14 μg chl.mL^{-1} for 30 $\mu L.L^{-1}$ CO_2 grown cells and 8 - 11 μg chl.mL^{-1} for standing culture cells.

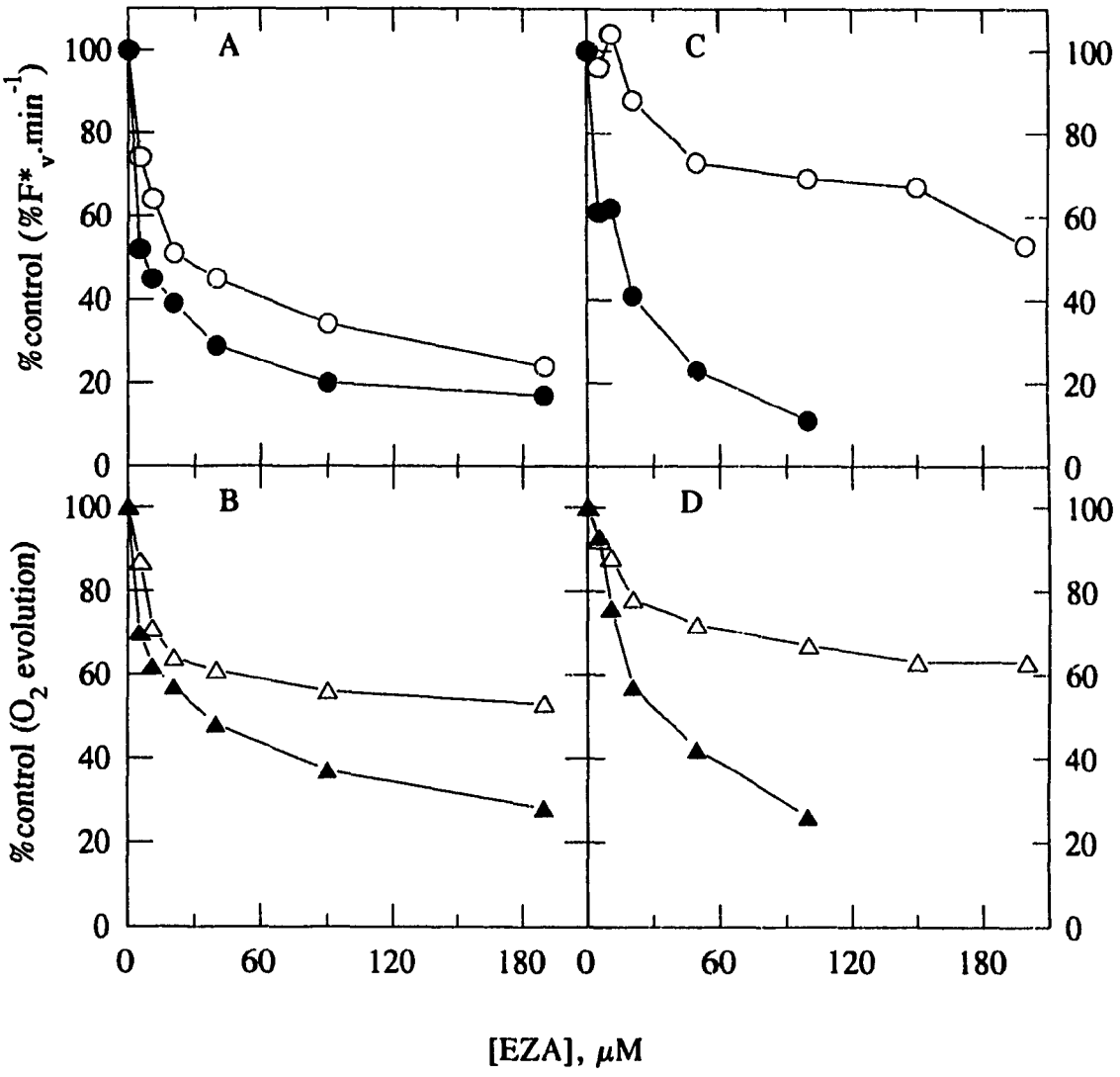
A
B
C
D
100
80
60
40
20
0
0
60
120
180
%control (%F*v.min-1)
%control (O2 evolution)
[EZA], μM

Na^+ independent mechanism was progressively inhibited. It should be noted, however, that the increased stimulation by Na^+ at progressively higher EZA concentrations, over and above the stimulation which was seen in the absence of EZA, can be entirely accounted for by a model where the Na^+ dependent pathway was fully and equally active at all concentrations of EZA (as long as 25 mM Na^+ was present). As the EZA concentration was increased, and in the presence of 25 mM Na^+, the proportion of sites which were insensitive to EZA accounted for a progressively greater proportion of the total photosynthetic or fluorescence quenching activity, resulting in an increase in the Na^+ stimulation as the EZA concentration was increased.

The inhibition of the initial rate of fluorescence quenching by μM amounts of EZA (Fig. 16, a and c) is strong evidence that EZA exerts its effect at the site of DIC uptake. The effect of EZA on the initial rate (10 sec. time points) of ^{14}C labelled HCO_3^- uptake in standing culture cells is shown in Fig. 17. These results confirm that EZA inhibits photosynthesis and fluorescence quenching by inhibiting the Na^+ independent HCO_3^- transport mechanism. The relief of inhibition by 25 mM Na^+ was also evident in direct measurements of HCO_3^- transport (Fig 17). In the absence of mM levels of Na^+, 50 % inhibition can be estimated to occur at between 30 and 40 μM EZA, which is consistent with the results obtained for the inhibition of photosynthesis in standing culture cells (Fig. 16d). The rate of ^{14}C-HCO_3^- uptake was less sensitive to inhibition by EZA than the initial rate of fluorescence quenching (Fig. 16c and Fig. 17). This could either be due to an effect of EZA on the ability of chlorophyll fluorescence to monitor transport or due to the differences in experimental conditions for the two different systems. This

FIGURE 17

Effects of ethoxyzolamide on the initial rate (10 second time points) of HCO_3^- uptake in standing culture cells in the (●) presence of 25 mM Na^+ and in the (○) presence of 100 μM Na^+. Measurements were made using the silicone fluid centrifugation technique and ^{14}C labelled HCO_3^-. Ethoxyzolamide was added from stock solutions of DMSO so that a constant (1 % v/v) amount of DMSO was added to each treatment, including the controls. Control rates of HCO_3^- uptake were 120 and 117 μmol C.mg $chl^{-1}.hr^{-1}$ in the presence of 100 μM and 25 mM Na^+ respectively. The initial DIC was 20 μM with a specific activity of 54 $\mu Ci.\mu mol^{-1}$. The experiment was conducted at pH 8.0, 30°C, and light was provided at 300 μmol photons.$m^{-2}.s^{-1}$. Data shown are the average of triplicate measurements.

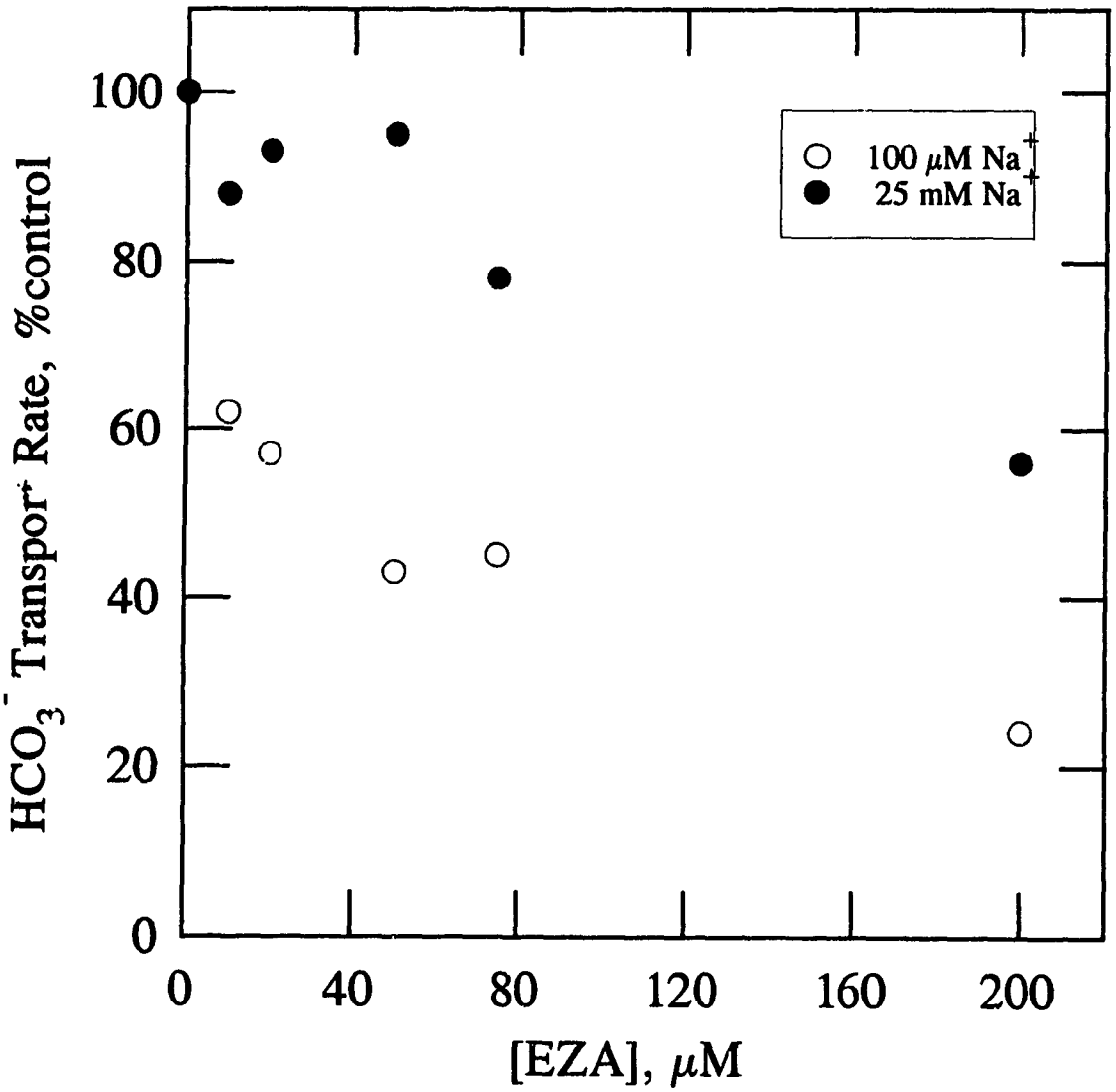
100
80
60
40
20
0
0
40
80
120
160
200
HCO_3^- Transport Rate, %control
[EZA], μM
100 μM Na$^+$
25 mM Na$^+$

question was not pursued further.

The results also indicate that, in this case, there was no apparent stimulation of HCO_3^- uptake by 25 mM Na^+ in the absence of EZA (Fig 17, legend). Since there was a relief of EZA inhibition upon the addition of 25 mM Na^+, these cells do possess Na^+ dependent HCO_3^- transport capacity. As indicated in Table 1, it is sometimes observed that there is no apparent stimulation of photosynthesis by 25 mM Na^+ in both standing culture and 30 $\mu L.L^{-1}$ CO_2 grown cells. The variability between batches of cells in their Na^+ dependent HCO_3^- capacity is probably due to variability in the growth DIC (Table 1).

The effects of EZA and Na^+ on the maximum pool size attained by standing culture cells are shown in Table 2. When HCO_3^- (10 μM) was added as the predominant DIC species, and with 100 μM Na^+ present, the addition of 75 μM EZA was sufficient to reduce the maximum pool size by 56 % (Table 2). When 75 μM EZA was added in the presence of 25 mM Na^+, the maximum pool size was inhibited by only 32 % (Table 2). Similarly, with 400 μM EZA present, 63 % inhibition of maximum pool formation was observed in the presence of 25 mM Na^+ while in the presence of 100 μM Na^+, the maximum pool size was inhibited by 83 % (Table 2). Furthermore, in the absence of 25 mM Na^+, 50% inhibition of pool formation was obtained at between 50 and 75 μM EZA whereas 50% inhibition of pool formation in the presence of 25 mM Na^+ required over 200 μM EZA (Table 2). These results confirm that the effect of EZA on photosynthesis in standing culture cells (Fig 16d) was due to a reduction in the ability of the cells to form the intracellular DIC pool, through an impairment of the transport mechanism,

TABLE 2

Effect of EZA and Na^+ on the maximum internal DIC in standing culture cells presented with 20 μM DIC at pH 8.0. Shown are the means $\pm$ standard error for triplicate measurements.

[EZA], μM	MAXIMUM INTERNAL [DIC], mM	
	100 μM Na^+	25 mM Na^+
0	7.94 $\pm$ 3.7	9.48 $\pm$ 3.1
10	5.67 $\pm$ 2.7	8.83 $\pm$ 2.25
50	4.60 $\pm$ 1.3	9.17 $\pm$ 2.8
75	3.44 $\pm$ 0.1	7.49 $\pm$ 1.0
200	2.86 $\pm$ 0.3	5.62 $\pm$ 1.9
400	1.38 $\pm$ 0.04	4.07 $\pm$ 0.6

rather than through an inability of the cells to utilize the pool for photosynthesis, as might be expected if intracellular carbonic anhydrase was the main site of inhibition by EZA. These results also confirm that the main effect of 25 mM Na^+ was to enhance the ability of the cells to form and maintain an intracellular DIC pool through a Na^+ dependent mechanism rather than through an effect of Na^+ on the ability of the cells to utilize the pool for photosynthesis. It should also be noted that both the inhibition of Na^+ independent HCO_3^- transport by EZA and the relief of this effect by Na^+ were evident and indeed predicted by the chl a fluorescence quenching technique (Fig 16,c and d).

THE EFFECT OF EZA ON PHOTOSYNTHESIS AND FLUORESCENCE QUENCHING IN AIR - GROWN CELLS

The apparent relief of EZA mediated inhibition of photosynthesis and HCO_3^- transport by 25 mM Na^+ in 30 $\mu L.L^{-1}$ CO_2 grown and standing culture cells can be attributed to the Na^+ dependent HCO_3^- transport activity which both of these cell types possess. Air-grown cells are strictly and specifically dependent on mM levels of Na^+ for HCO_3^- transport (Miller et al.,1984; Reinhold et al.,1984; Figs. 3 and 4) and therefore possess only the Na^+ dependent mechanism for transporting HCO_3^-. It was, therefore, desirable to examine the effects of EZA on photosynthesis and fluorescence quenching in air-grown cells. These results are depicted in Fig. 18 and they show that air-grown cells were relatively insensitive to inhibition by EZA in the range of EZA concentrations from 20 - 200 μM. At 200 μM EZA, the rate of photosynthesis in air-grown cells was inhibited by 30 % (Fig. 18) whereas in standing culture cells, the rate of photosynthesis was inhibited by 75 % and 35 % in the absence and presence of 25 mM Na^+,

FIGURE 18

Effect of ethoxyzolamide on (○) photosynthesis and (●) the initial rate of chl a fluorescence quenching in air grown cells. Experiments were conducted at pH 8.0, 30°C and the initial [DIC] was 20 μM. Na^+ was present throughout at 25 mM. EZA was added from stock solutions of DMSO such that the final concentration was less than 1 % (v/v) DMSO. The control rate of photosynthesis was 64 μmol O_2.mg^{-1} chl.h^{-1}. Light was provided at 100 μmol photons.m^{-2}.s^{-1} and the [chl] was 13 μg.mL^{-1}.

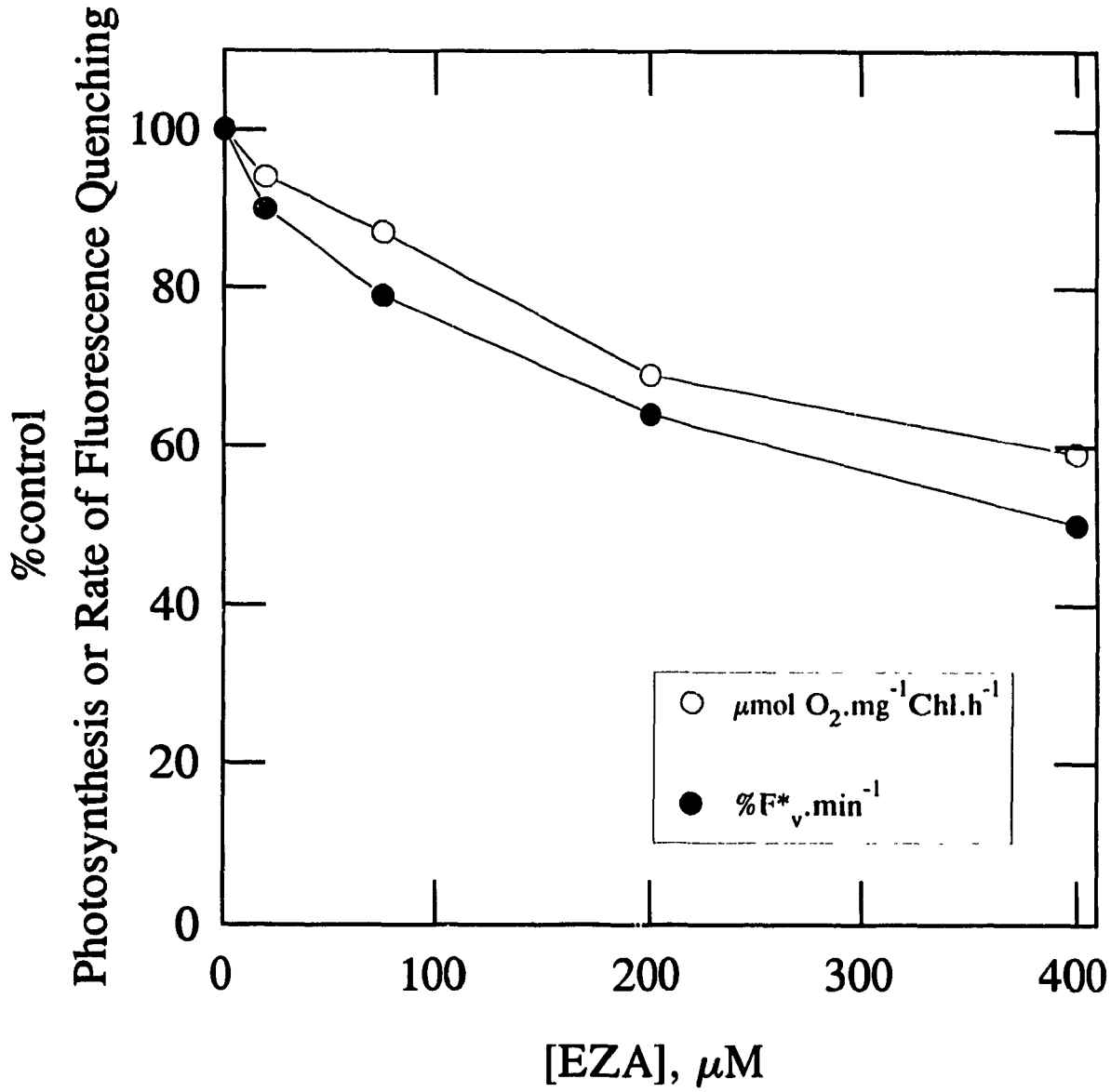
%control
Photosynthesis or Rate of Fluorescence Quenching
100
80
60
40
20
0
0
100
200
300
400
[EZA], μM
μmol O2.mg-1Chl.h-1
%F*v.min-1

respectively (Fig 16d). Similarly, the initial rate of fluorescence quenching in air-grown cells was relatively unaffected by low levels of EZA (20-100 μM). At 200 μM EZA, the initial rate of fluorescence quenching in air-grown cells was inhibited by 30 % (Fig. 18) whereas in standing culture cells the initial rate of quenching was reduced by 47 % and >75 % in the presence and absence of 25 mM Na^+ (Fig.16c), respectively.

THE EFFECT OF EZA ON HCO_3^- TRANSPORT IN AIR-GROWN CELLS

The relatively smaller effect of low concentrations of EZA (20 - 100 μM) on the initial rate of fluorescence quenching in air-grown cells (Fig 18), and the relief from EZA inhibition of HCO_3^- transport by 25 mM Na^+ in standing culture and 30 $\mu L.L^{-1}$ cells (Figs. 16 and 17), are evidence that the Na^+ dependent mechanism is much less sensitive to EZA inhibition than the Na^+ independent mechanism of HCO_3^- transport. Direct measurements of intracellular DIC accumulation and CO_2 fixation in the presence of 0 - 400 μM EZA and 25 mM Na^+ in air-grown cells confirmed these findings (Fig. 19). These results indicate that 75 μM EZA had virtually no effect on intracellular DIC pool formation (Fig. 19a) and little effect on C_i fixation (Fig 19b). Even at 400 μM EZA, which was sufficient to reduce photosynthesis by 90 % in standing culture cells (when HCO_3^- was added) in the absence of Na^+ (Tyrrell and Espie, unpublished results), the maximum pool formation in air-grown cells in the presence of 25 mM Na^+ was reduced by less than 50 % (Fig 19a). Similarly, the rate of C_i fixation was only reduced by approximately 50 % in the presence of 400 μM EZA (Fig 19b).

The previously documented evidence for EZA inhibition of CO_2 and HCO_3^- transport in Synechococcus PCC 7942 was interpreted as supporting a mechanism for

FIGURE 19

Effect of EZA on (A) intracellular DIC accumulation and (B) carbon fixation in air grown cells as measured using the silicone fluid centrifugation technique with ^{14}C labelled HCO_3^-. EZA was added at (○) 0, (●) 75, (▽) 200, and (▼) 400 μM from stock solutions with DMSO (present at 1 % v/v throughout). Experiments were conducted at pH 8.0, 30°C, and with 25 mM Na^+. HCO_3^- was added at an initial concentration of 10 μM with specific activity 35.3 $\mu Ci.\mu mol^{-1}$. The [chl] ranged between 4.9 and 6.8 μg chl.mL^{-1}. Data are the average of triplicate determinations.

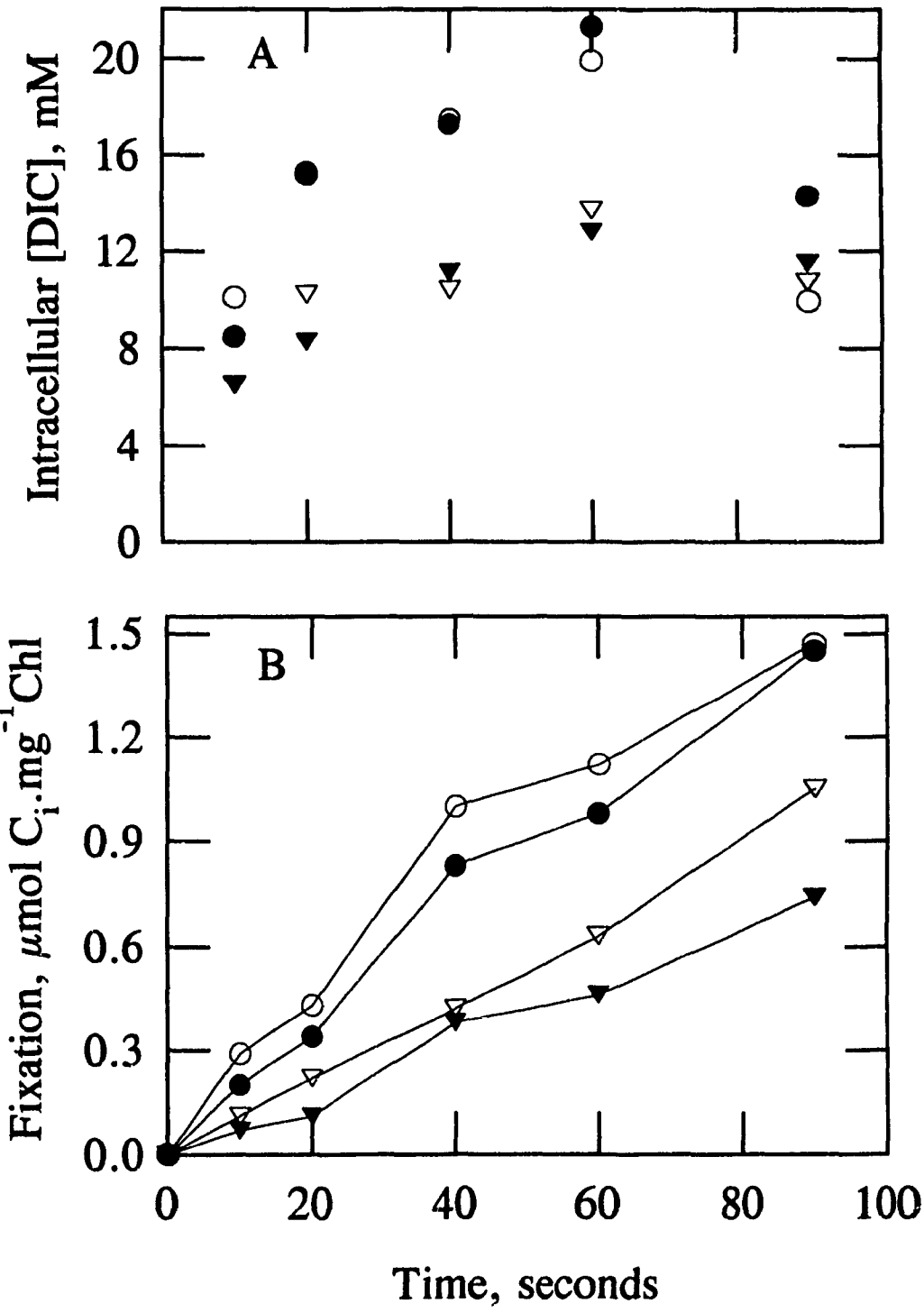
A
Intracellular [DIC], mM
20
16
12
8
4
0
B
Fixation, μmol C_i.mg^{-1}Chl
1.5
1.2
0.9
0.6
0.3
0.0
0
20
40
60
80
100
Time, seconds

HCO_3^- transport which involved a "front-end mechanism", converting HCO_3^- to CO_2 prior to the translocation step (Fig 1a; Price and Badger,1989a). The results presented in Figs. 16 - 19 and the data of Espie and Kandasamy (1992) and Tyrrell and Espie (unpublished) indicate that the situation is more complex than the model proposed by Price and Badger (1989a) in that there are two separate and distinct mechanisms for transporting HCO_3^-. One mechanism was independent of mM levels of Na^+ and susceptible to inhibition by low doses of EZA (< 50 μM) while the other was specifically dependent on mM levels of Na^+ but relatively insensitive to low levels of EZA. In view of the inhibition of Na^+ independent HCO_3^- transport by low concentrations of EZA, this transport mechanism is more likely to include a "carbonic anhydrase - like step", as proposed by Price and Badger (1989a) in its reaction sequence than the Na^+ dependent mechanism.

INHIBITION OF CO_2 AND HCO_3^- TRANSPORT BY EZA

EZA has been reported to inhibit CO_2 and HCO_3^- transport equally well in Synechococcus PCC7942 (Price and Badger, 1989a). The experiments supporting this claim were conducted with 100 μM CO_2 and 100 μM HCO_3^- at pH 8.0 (Price and Badger,1989a). At pH 8.0 and at 30 °C, the hydration of CO_2 is relatively rapid ($t_{1/2}$ = 5 - 8 sec., Miller et al,1988b). The uptake experiments performed by Price and Badger (1989a) utilizing 100 μM CO_2 as the "active species" probably reflected a large component of HCO_3^- uptake. When CO_2 was provided at an initial concentration of 10 μM, uptake was rapid and the intracellular DIC pool reached its maximum level within 10 seconds (Miller et al,1988b). The rapid depletion of extracellular CO_2 was due to the

FIGURE 20

Effect of 0 - 400 μM EZA on the initial rate of chl fluorescence quenching induced by (○) 10 μM CO_2 or (●) 10 μM HCO_3^- in 30 μL.L^{-1} CO_2 grown cells. EZA was added from stock solutions made up in DMSO. Experiments were performed with 100 μM NaCl present at pH 8.0, 30°C, and light was supplied at 100 μmol photon.m^{-2}.s^{-1}. The [chl] ranged between 8 and 12 μg.mL^{-1}.

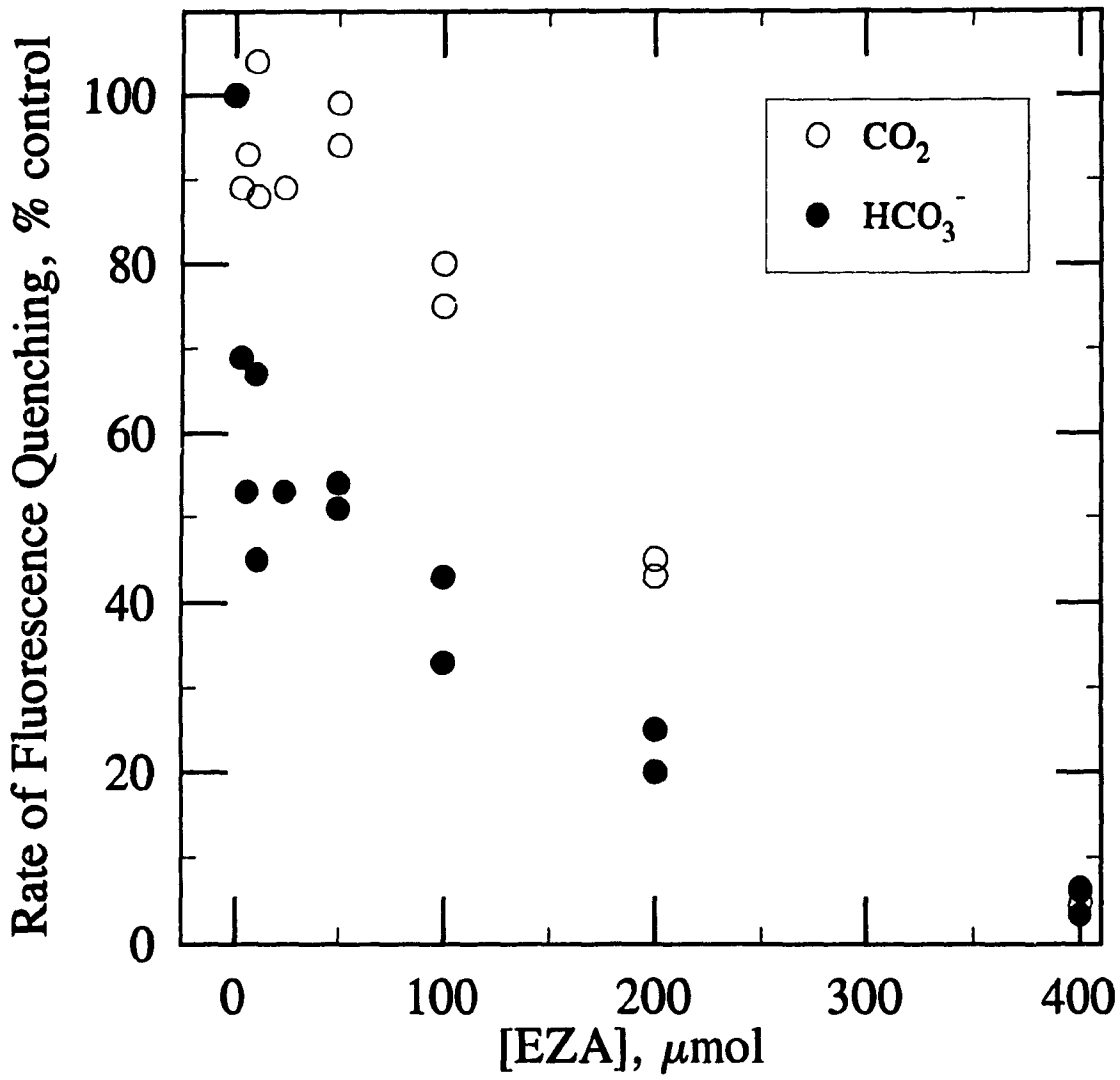
Rate of Fluorescence Quenching, % control
100
80
60
40
20
0
0
100
200
300
400
[EZA], μmol
CO2
HCO3-

high affinity CO_2 transport system ($K_{1/2}$ CO_2 = 0.2 μM, Espie et al,1991). This rapid depletion ensured that extracellular hydration of CO_2 (to form HCO_3^-) was kept at a minimum. Consequently, CO_2 uptake is more accurately determined at 10 μM CO_2 than at 100 μM CO_2. In order to determine whether CO_2 and HCO_3^- transport were inhibited to the same extent by EZA, 10 μM CO_2 or HCO_3^- was added to 30 $\mu L.L^{-1}$ cells in the presence of 100 μM NaCl and with varying levels of EZA (Fig. 20). These results indicate that the initial rate of fluorescence quenching was much more sensitive to EZA when HCO_3^- was added than when equal amounts of CO_2 were added (Fig.20). The presence of as low as 5 μM EZA inhibited fluorescence quenching by 50 % when HCO_3^- was added. In contrast, 200 μM EZA was required to inhibit fluorescence quenching by 50 % when CO_2 was added to initiate quenching (Fig. 20). Very similar results have been found for standing culture cells (Tyrrell and Espie, unpublished results).

When uptake was initiated using ^{14}C labelled CO_2, direct measurements of pool formation and carbon fixation revealed that 75 μM EZA had a relatively negligible effect on CO_2 transport in standing culture cells (Fig 21, a and b). The presence of 400 μM EZA resulted in a lag phase in intracellular DIC pool formation and the maximum pool size was reduced by 67 % compared to the control (Fig 21a). The rate of carbon fixation was reduced by 72 % in the presence of 400 μM EZA (Fig 21b). In the absence of inhibitor, as well as with 75 μM EZA present, pool formation was essentially complete by the first sampling time (10 sec.), in agreement with previous results utilizing low CO_2 (10 μM) to initiate uptake (Miller et al, 1988b).

Since the Na^+ independent HCO_3^- transport mechanism was inhibited by more

FIGURE 21

Effect of (○) 0, (●) 75, and (▽) 400 μM EZA on (A) internal DIC pool formation and (B) carbon fixation in standing culture cells as measured using the silicon fluid centrifugation technique. Transport was initiated using 10 μM CO_2 (spec. act = 56 $\mu Ci.\mu mol^{-1}$, added from a stock solution of CO_2 in 10 mM phthallic acid, pH 4.0). Experiments were conducted at pH 8.0, 30°C and with 100 μM Na^+ present. Light was provided at 300 μmol photons.$m^{-2}.s^{-1}$. The chl ranged from 10 - 13 $\mu g.mL^{-1}$. Data are the average of triplicate determinations.

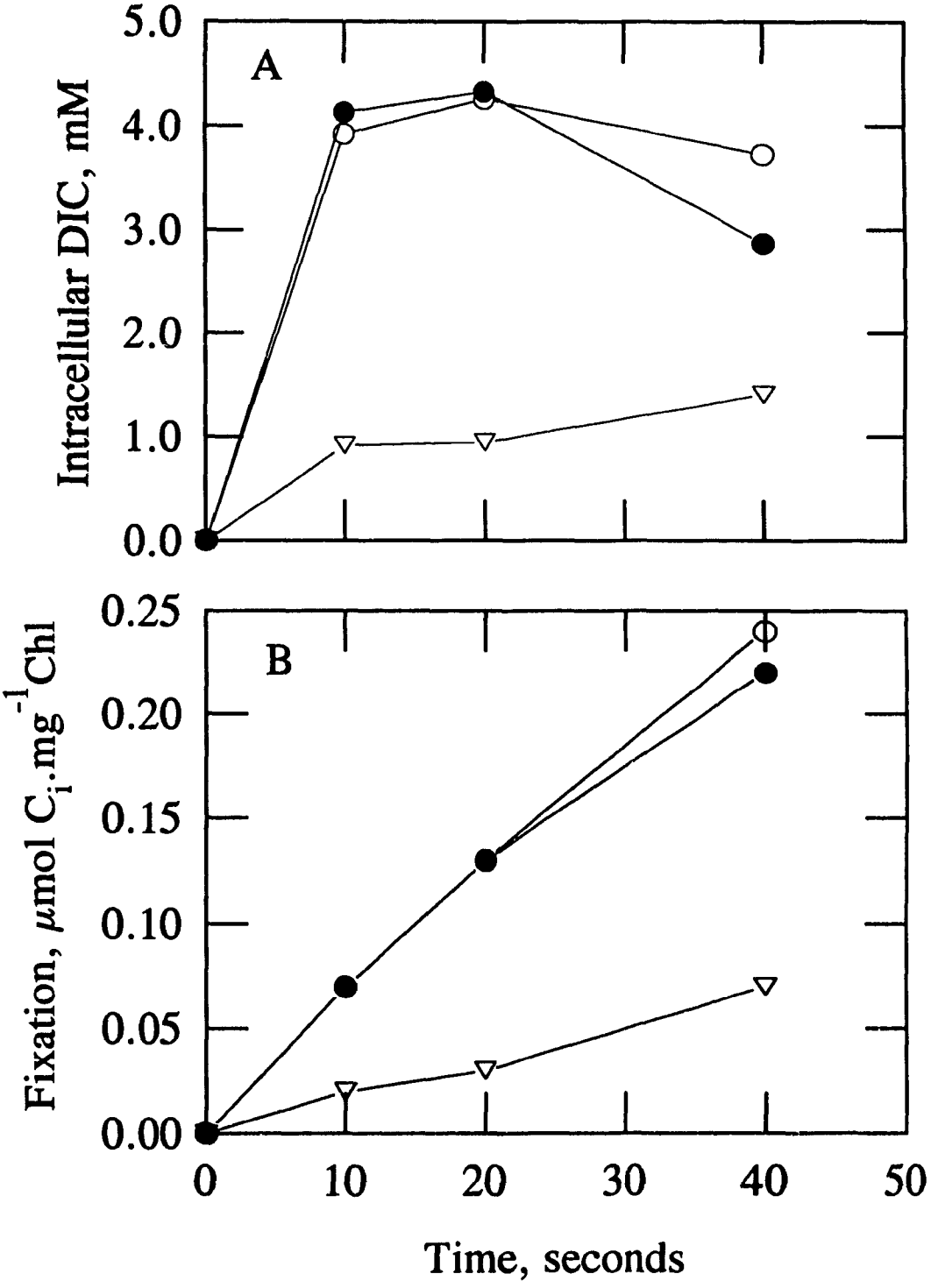
A
B
Intracellular DIC, mM
Fixation, μmol C_i.mg^{-1}Chl
Time, seconds
5.0
4.0
3.0
2.0
1.0
0.0
0.25
0.20
0.15
0.10
0.05
0.00
0
10
20
30
40
50

than 50 % in the presence of 75 μM EZA (Figs 16 & 17, Table 2), the lack of inhibition of pool formation initiated by CO_2 pulsing in the presence of 75 μM EZA indicated that there was virtually no HCO_3^- transport occuring under these conditions. It follows that CO_2 transport was much less sensitive to 75 μM EZA than was Na^+ independent HCO_3^- transport when both were presented at low (10 - 20 μM) concentrations. Only at higher concentrations of EZA (>400 μM) was there evidence for an equal inhibitory effect of EZA on both CO_2 and HCO_3^- transport (Fig 20). Experiments using mass spectrometry to monitor CO_2 dissapearence from the medium have confirmed that relatively low levels of EZA (<100 μM) do not affect CO_2 transport in air-grown cells in either the absence or presence of 25 mM Na^+ (Tyrrell, Skleryk, and Espie, unpublished results).

EFFECT OF EZA ON Na^+ INDEPENDENT HCO_3^- TRANSPORT KINETICS

The effect of 75 and 200 μM EZA on the HCO_3^- transport kinetics of 30 $\mu L.L^{-1}$ CO_2 grown cells is shown in Fig 22, a and b. The addition of 75 μM EZA in the presence of 100 μM Na^+ resulted in a maximum inhibition of the initial transport rate of 60 % while the addition of 200 μM EZA resulted in a maximum inhibition of 75 % (Fig 22a). In the presence of 25 mM Na^+, the maximum inhibition of transport was 30 % with 75 μM EZA present and 50 % with 200 μM EZA present (Fig 22b). Thus, the transport-substrate relation for HCO_3^- transport was affected in a dose dependent fashion by EZA. The partial relief of EZA mediated inhibition of HCO_3^- transport by 25 mM Na^+ in 30 $\mu L.L^{-1}$ CO_2 grown cells inferred from fluorescence experiments (Fig 16a) was confirmed using direct measurements of HCO_3^- transport and was shown to be valid in the range of HCO_3^- from 10-100 μM (Fig 22, a and b). In the absence of EZA, the

FIGURE 22

Effect of (○) 0, (●) 75, and (▽) 200 μM EZA on the DIC dose response of transport in the presence of (A) 100 μM and (B) 25 mM Na^+ in 30 $\mu L.L^{-1}$ CO_2 grown cells. The initial rate of HCO_3^- transport (10 sec. time points) was measured using the silicone fluid centrifugation technique. HCO_3^- was added from three different stock solutions of 50, 200, and 500 μM DIC having specific activities of 27, 50, and 55 $\mu Ci.\mu mol^{-1}$, respectively. The experiments were conducted at pH 8.0, 30°C, and the light was supplied at 300 μmol photons.$m^{-2}.s^{-1}$. The chl ranged from 7 - 15 $\mu g.mL^{-1}$. Data shown are the average of triplicate measurements.

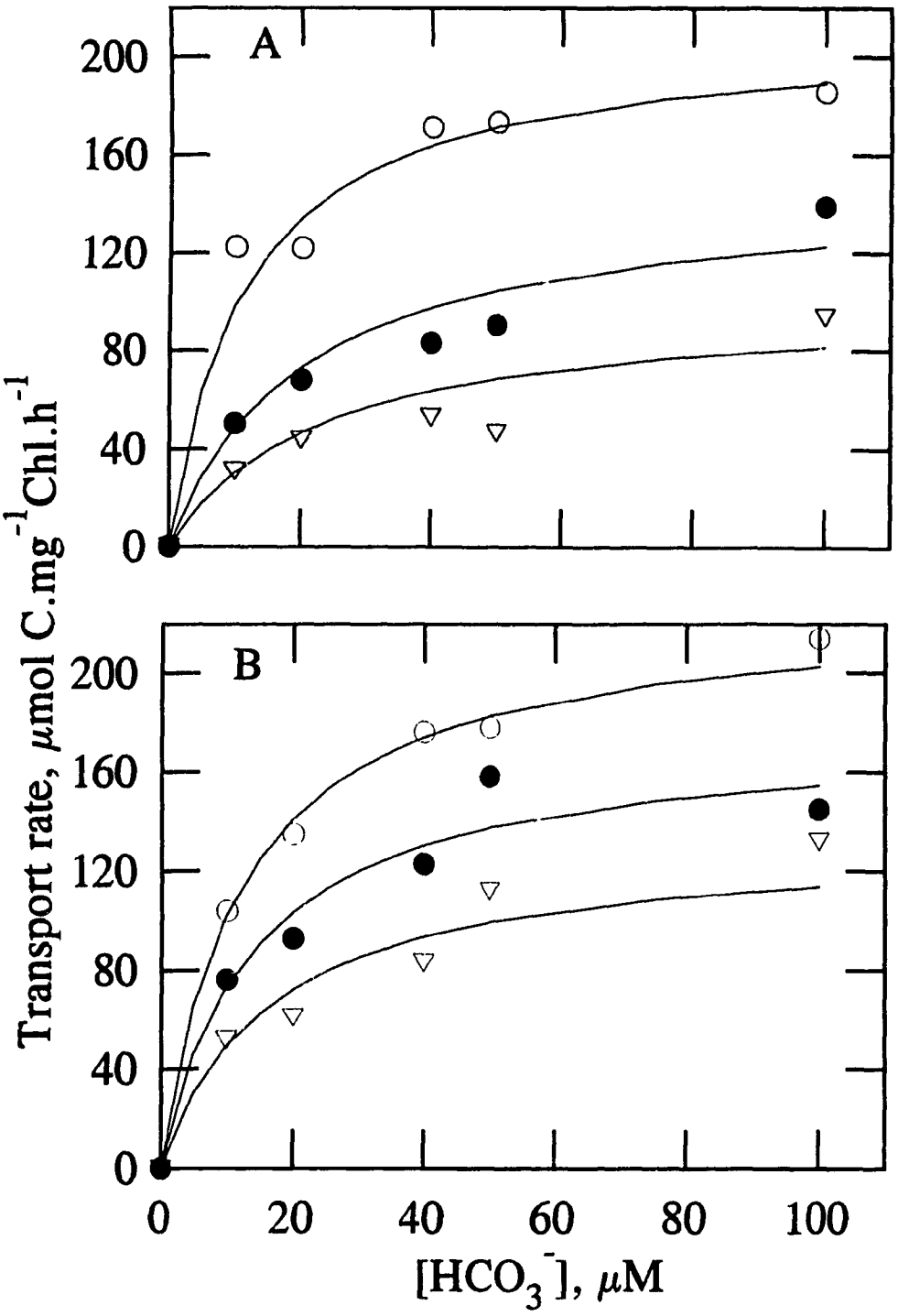
A
B
200
160
120
80
40
0
0
20
40
60
80
100
Transport rate, μmol C.mg-1Chl.h-1
[HCO3-], μM

FIGURE 23

Double reciprocal plots of transport vs [HCO_3^{-1}] in 30 $\mu L.L^{-1}$ CO_2 grown cells with (○) 0, (●) 75, and (▽) 200 μM EZA in the presence of (A) 100 μM and (B) 25 mM Na^+. The $K_{1/2}^{HCO3-}$ were found by linear regression to be: (A) 11.3, 20.2, and 22.9 μM with 0, 75, and 200 μM EZA present, respectively. (B) 12.2, 14.0, and 16.9 μM with 0, 75, and 200 μM EZA present respectively. The V_{max} were found to be (in μmol C_i. $mg^{-1}chl.h^{-1}$) (A) 210, 147, and 100 with 0, 75, and 200 μM EZA present respectively, (B) 227, 176, and 133 with 0, 75, and 200 μM EZA present respectively.

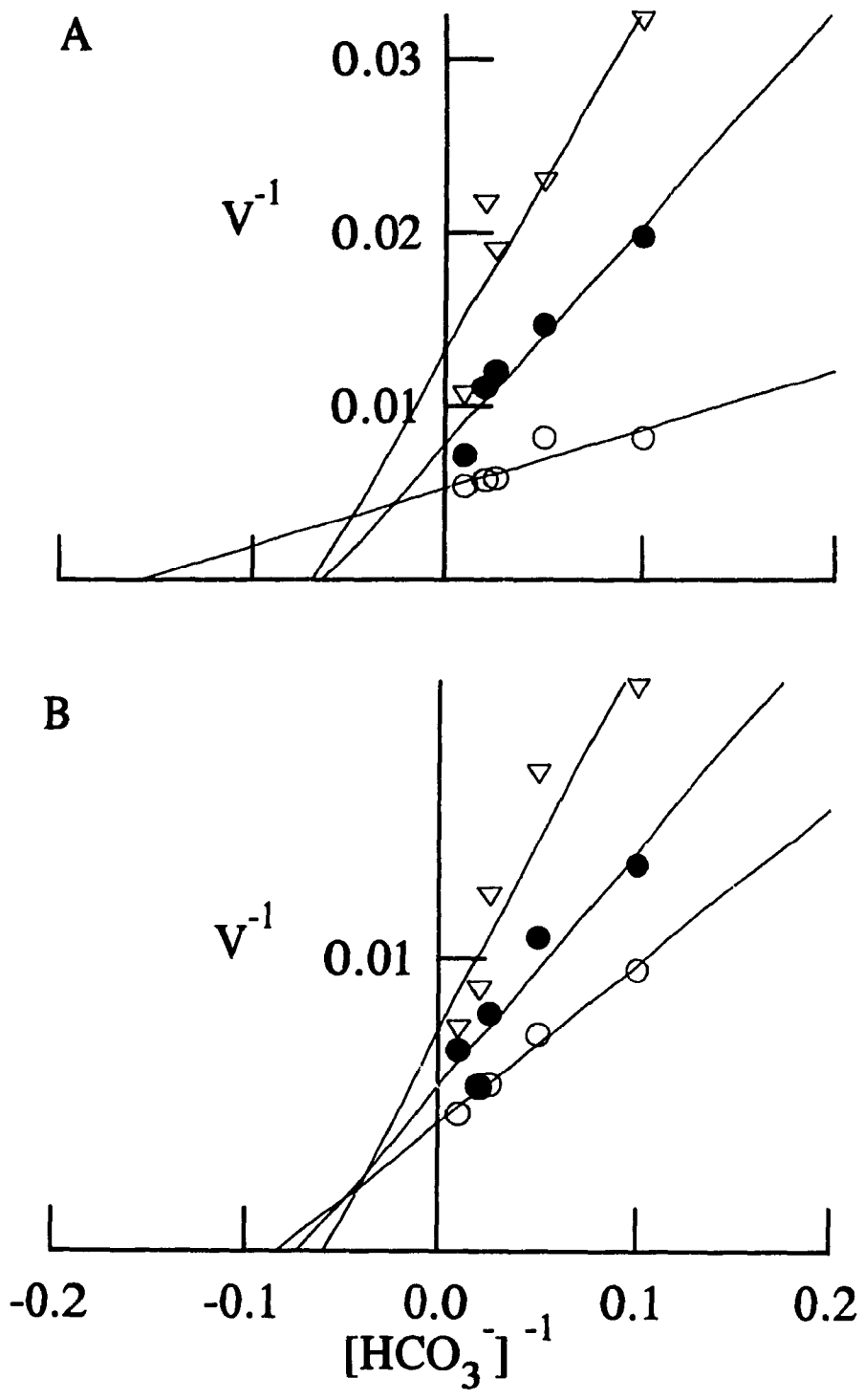
A
0.03
V^{-1}
0.02
0.01
B
V^{-1}
0.01
-0.2
-0.1
0.0
0.1
0.2
$[HCO_3^-]^{-1}$

FIGURE 24

Plots of $K_{1/2}$:V_{max} versus [EZA] for the kinetic parameters obtained from Figure 23 by linear regression analysis. The K_i for transport was found to be (○) 70 μM EZA in the presence of 100 μM Na^+ and (●) 142 μM EZA in the presence of 25 mM Na^+.

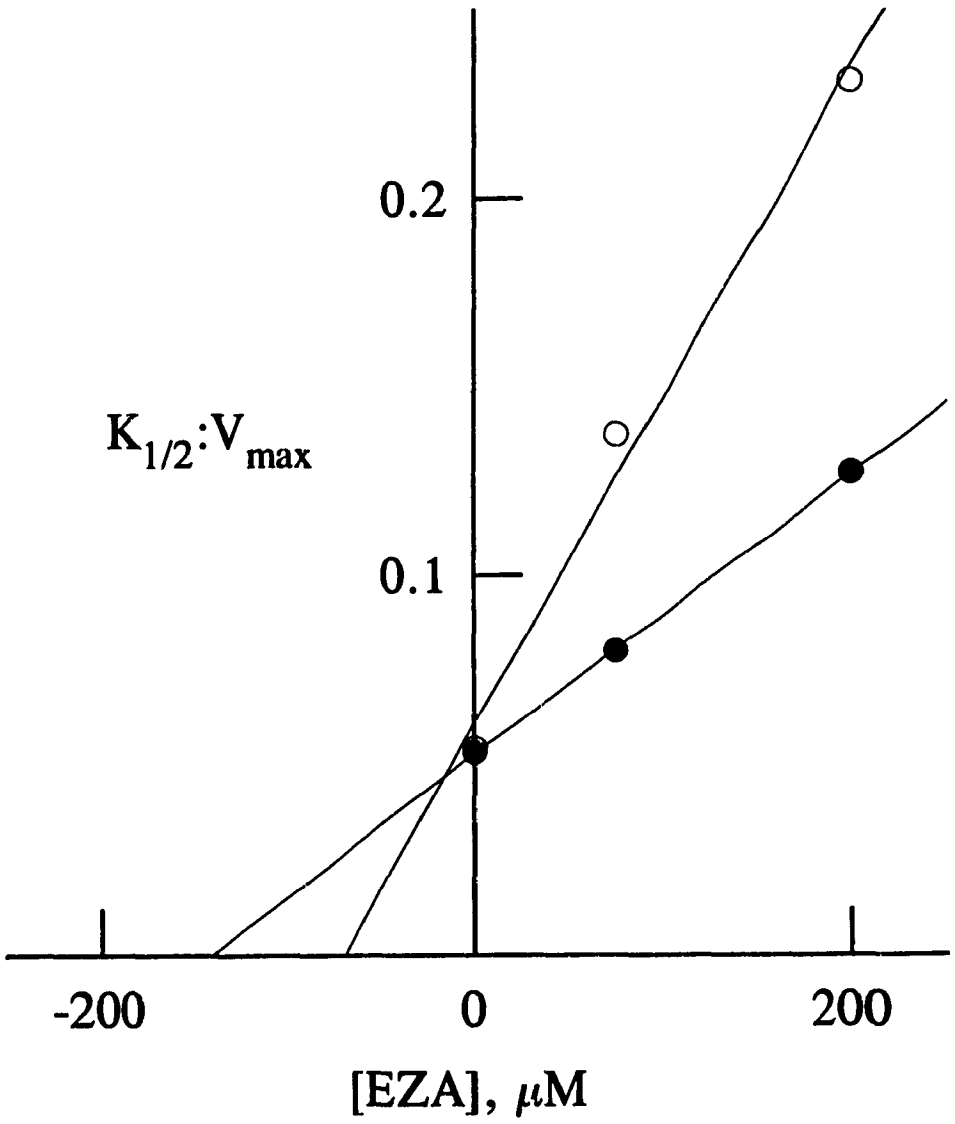
0.2
0.1
$K_{1/2}:V_{max}$
-200
0
200
[EZA], μM

stimulation of HCO_3^- transport by 25 mM Na^+ was less than 1.3 fold at all concentrations of HCO_3^- tested (Fig 22, a and b). This is consistent with the lack of substantial Na^+ stimulation observed for both photosynthesis and fluorescence quenching in 30 $\mu L.L^{-1}$ cells (Figs 14-16, Table 1). In the presence of 200 μM EZA, the Na^+ stimulation varied between 1.4 and 2.4 fold, thus confirming the fluorescence results of Fig 16a, which indicated that the Na^+ stimulation of fluorescence quenching in 30 $\mu L.L^{-1}$ CO_2 grown cells increased with increasing EZA concentration.

Double reciprocal re-plots of the data shown in Fig. 22 are shown in Fig. 23. The effect of EZA, both in the presence and absence of 25 mM NaCl, was to increase the $K_{1/2}^{HCO3-}$ and to lower the V_{max} for transport (Fig. 23). The pattern of inhibition can therefore best be described as mixed non-competitive (Segel, 1988). The apparent K_I can be estimated by plotting the ratio of $K_{1/2}$:V_{max} versus the inhibitor concentration, as is shown in Fig. 24. The K_I in the absence of 25 mM Na^+ was 57 μM EZA whereas in the presence of 25 mM Na^+ it was found to be 142 μM (Fig 24).

The effect of 20, 75, and 200 μM EZA on the HCO_3^- transport kinetics of standing culture cells in the presence of 100 μM Na^+ is shown in Fig 25. Increasing the EZA concentration in the range 20-200 μM was increasingly inhibitory for HCO_3^- transport in the range of HCO_3^- concentrations 5-50 μM. The presence of 20 μM EZA resulted in a maximum inhibition of transport of 47 % whereas with 200 μM EZA present the maximum inhibition observed was 79 % (Fig. 25). A double reciprocal plot of the data in Fig 25 is shown in Fig 26. The effect of EZA was to increase the $K_{1/2}^{HCO3-}$ while lowering the V_{max} (Fig 26). The $K_{1/2}^{HCO3-}$ for transport was observed to increase

FIGURE 25

Effect of (○) 0, (●) 20, (▽) 75, and (▼) 200 μM EZA on the HCO_3^- dose response of transport in the presence of 100 μM Na^+ in standing culture cells. The initial rate of HCO_3^- transport (10 sec time points) was measured using the silicone fluid centrifugation technique. HCO_3^- was added from three different stock solutions of 50, 200 and 500 μM DIC having specific activities of 40, 50, and 54 $\mu Ci.\mu mol^{-1}$, respectively. The experiments were conducted at pH 8.0, 30°C, and light was supplied at 300 μmol photons.$m^{-2}.s^{-1}$. The chl ranged from 8 - 12 $\mu g.mL^{-1}$. Data shown are the average of triplicate measurements.

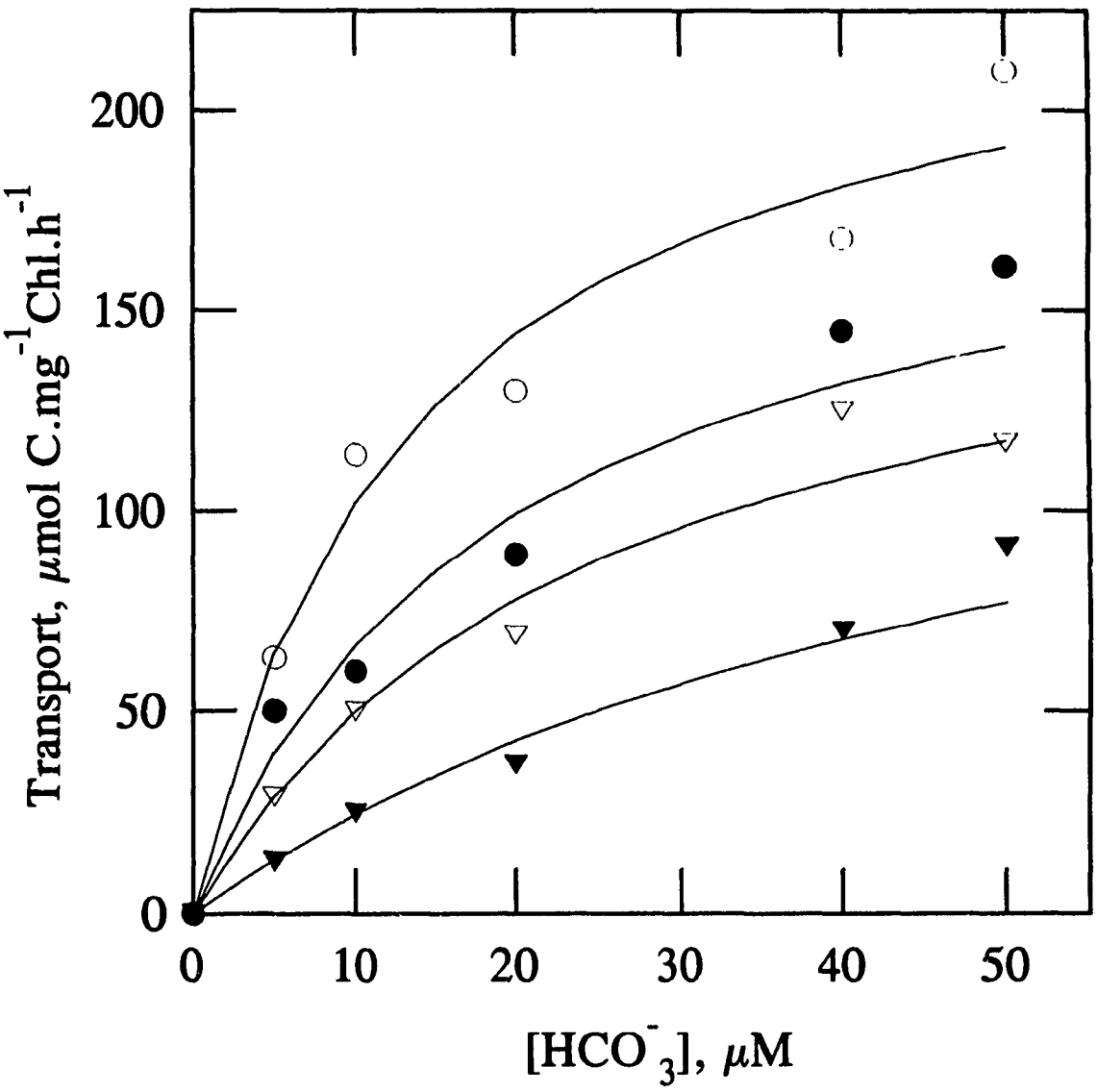
Transport, μmol C.mg-1Chl.h-1
200
150
100
50
0
0
10
20
30
40
50
[HCO-3], μM

FIGURE 26

Double reciprocal plots of the data shown in Figure 25. The $K_{1/2}^{HCO3-}$ for transport were determined by linear regression analysis to be; 13.9, 19.5, 25.4, and 57.1 μM in the presence of (○) 0, (●) 20, (▽) 75, and (▼) 200 μM EZA, respectively. The V_{max} for transport (μmol HCO_3^-.mg^{-1}chl.h^{-1}) were found to be 244, 196, 177, and 165 in the presence of 0, 20, 75, and 200 μM EZA, respectively.

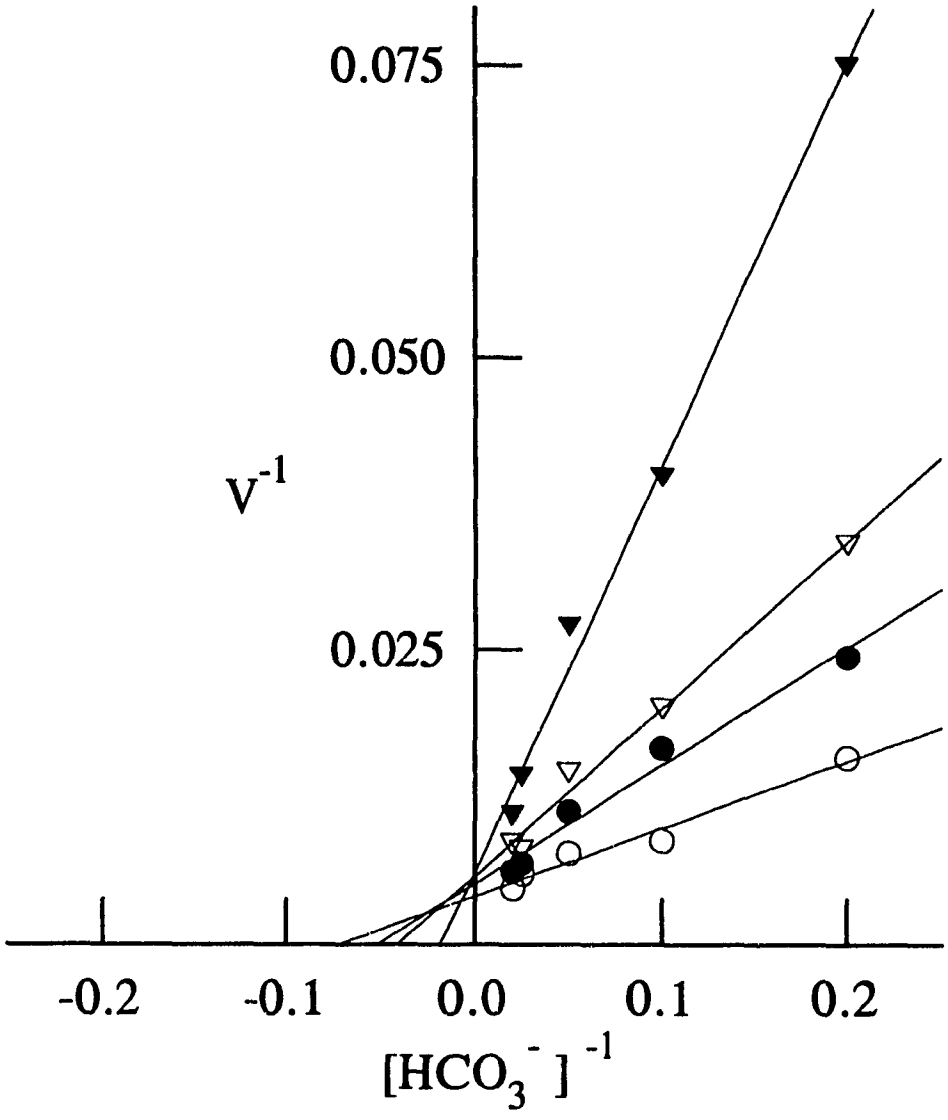
0.075
0.050
0.025
V^{-1}
-0.2
-0.1
0.0
0.1
0.2
$[HCO_3^-]^{-1}$

FIGURE 27

Plot of the $K_{1/2}$:V_{max} versus [EZA] for the kinetic parameters obtained from Figure 26 by linear regression analysis. The K_I for EZA was found to be 41.3 by extrapolation of the linear regression to the x - axis.

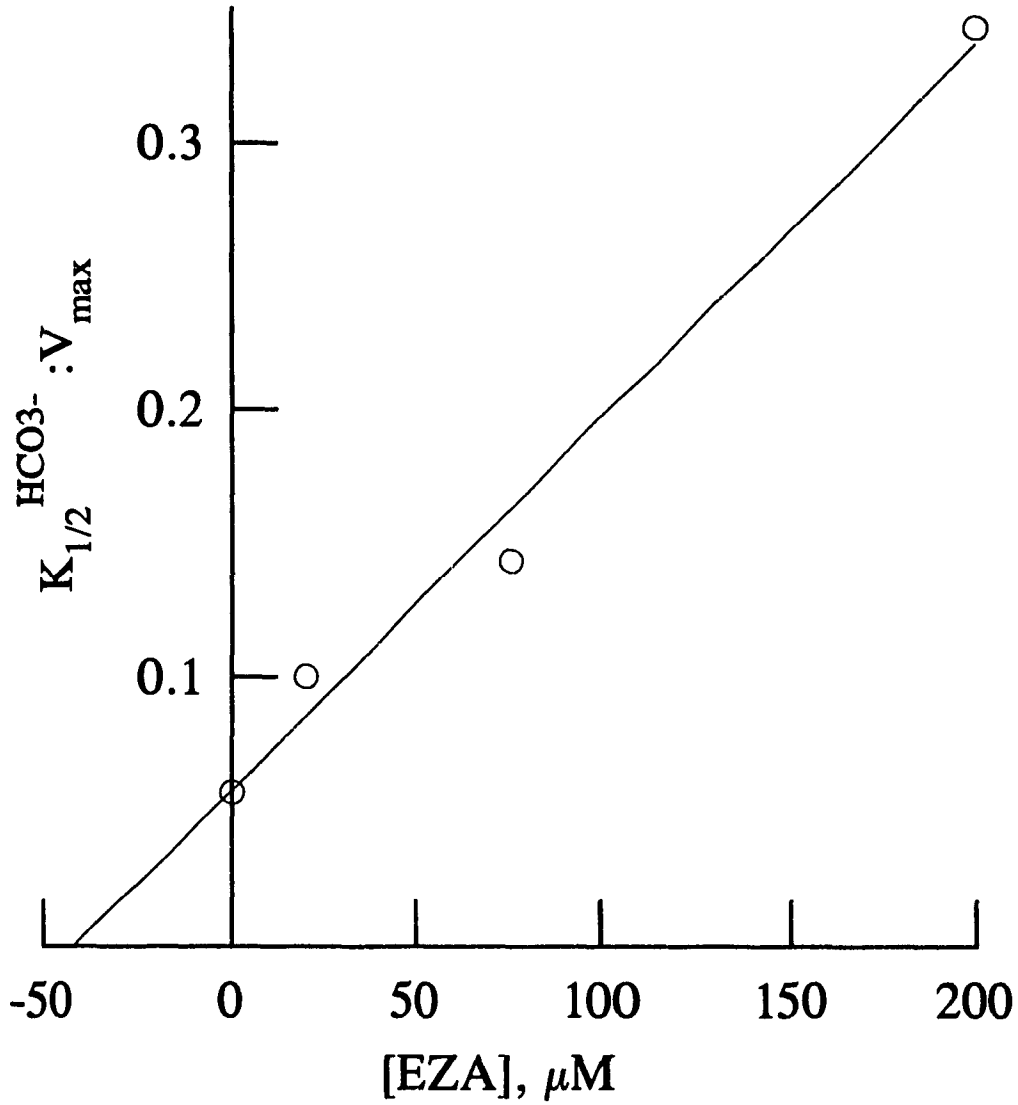
0.3
0.2
0.1
$K_{1/2}^{HCO3-}$:V_{max}
-50
0
50
100
150
200
[EZA], μM

from 14 μM DIC in the absence of EZA to 57 μM DIC in the presence of 200 μM EZA. Similarly, the V_{max} for transport was observed to decrease from 243 to 165 μmol C.mg^{-1} chl.h^{-1} in the absence and presence of 200 μM EZA, respectively. Intermediate increases in $K_{1/2}^{HCO3-}$ and decreases in V_{max} for transport were observed at intermediate concentrations of EZA. The inhibitory pattern can be best described as mixed non - competitive, and is similar to the situation for 30 μL.L^{-1} cells (Figs. 23 - 24). The K_I for EZA inhibition in standing culture cells was estimated by plotting the ratio of $K_{1/2}^{HCO3-}$:V_{max} versus EZA and, in the absence of 25 mM Na^+, the K_I was estimated to be 41 μM (Fig 27).

INHIBITORY SPECIES OF EZA

EZA is a sulfonamide drug with a pK_A of 8.1 (Maren, 1967). The sulfonamides (including EZA) have been shown to bind to the active site Zn^{2+} ion of carbonic anhydrase through the deprotonated sulfonamido nitrogen (Coleman, 1975). In the case of ethoxyzolamide, the deprotonated active inhibitory species is negatively charged. It was therefore of interest to verify the pH dependence of EZA inhibition of the Na^+ independent HCO_3^- transport mechanism. The chl a fluorescence quenching technique was used as a monitor for HCO_3^- transport and the results of an experiment conducted at pH 8.0 and 9.6 with total EZA in the range 5-200 μM are shown in Fig. 28. The inhibition by EZA of the initial rate of fluorescence quenching was more evident at pH 8.0 than for an equal concentration of EZA at pH 9.6. Experiments conducted in the pH range 8.0 - 9.5 will have less of the protonated species in solution as the pH is increased. To investigate the pH dependence of inhibition in more detail, measurements of the initial

FIGURE 28

Effect of EZA on the initial rate of chl a fluorescence quenching in 30 $\mu L.L^{-1}$ CO_2 grown cells at (○) pH 8.0 and at (●) pH 9.5. EZA was added from stock solutions made up in DMSO. Experiments were conducted at 30°C, with 100 μM Na^+ present. Transport was initiated by the addition of 10 μM DIC. Light was provided at 100 $\mu mol\ photons.m^{-2}.s^{-1}$. The chl ranged from 10 - 11 $\mu g.mL^{-1}$.

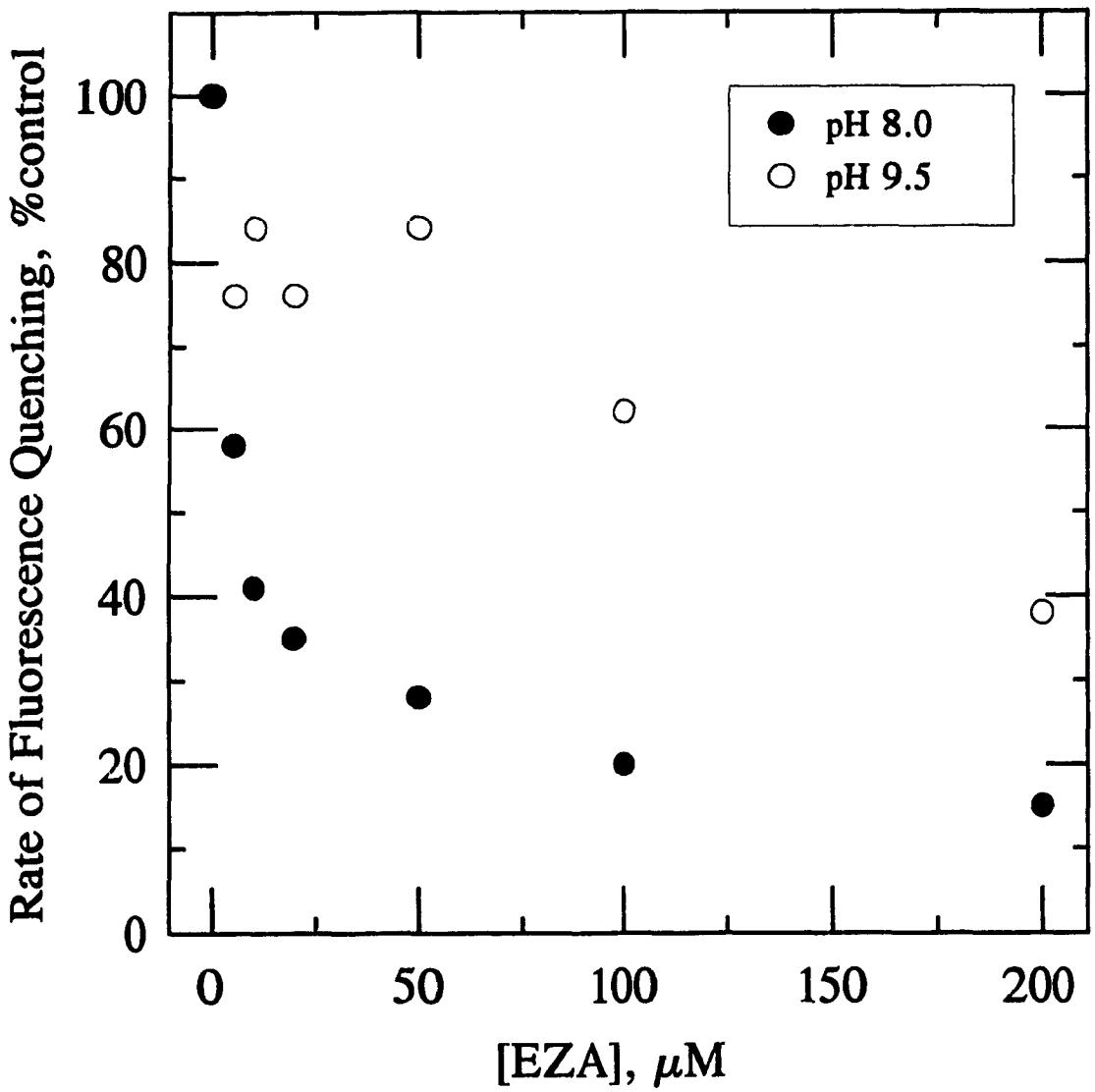
Rate of Fluorescence Quenching, %control
100
80
60
40
20
0
0
50
100
150
200
[EZA], μM
pH 8.0
pH 9.5

FIGURE 29

Effect of $EZAH_2$ and $EZAH^-$ on the initial rate of chl a fluorescence quenching in 30 $\mu L.L^{-1}$ CO_2 grown cells. Experiments were conducted as in Figure 28 at (○) pH 7.97, (●) pH 8.56, (▽) pH 9.07, and (▼) pH 9.56, with 10 μM DIC and over a range of total EZA from 0 -200 μM. The data were plotted as a function of (A) $EZAH_2$ or (B) as $EZAH^-$ using a pKa for EZA of 8.1. The chl ranged from 9 - 13 $\mu g.mL^{-1}$.

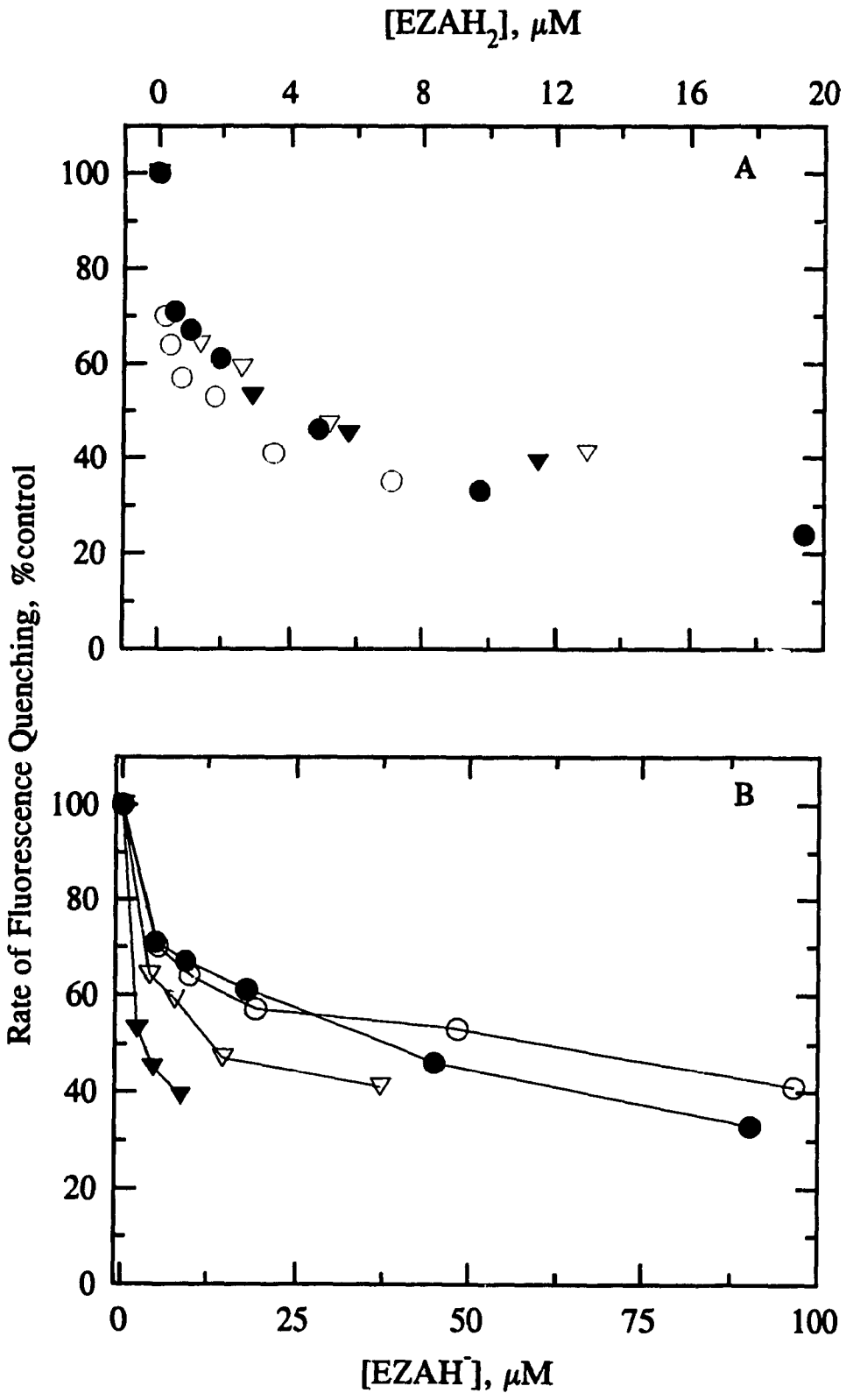
[EZAH2], μM
0
4
8
12
16
20
A
100
80
60
40
20
0
B
100
80
60
40
20
0
0
25
50
75
100
Rate of Fluorescence Quenching, %control
[EZAH-], μM

rate of fluorescence quenching were conducted at four different pH_o in the range from 7.97 to 9.54 and with total EZA from 0 - 200 μM ($[EZAH_2]:[EZAH^-]$ = 1.35 to 0.036, respectively) (Fig 29). When the initial rate of fluorescence quenching (expressed as a percentage of the control) was plotted as a function of the protonated species ($EZAH_2$), the data fell along a single inhibition curve (Fig 29a). The same data plotted as a function of the charged species revealed four separate pH dependent inhibition curves (Fig 29b). It can be concluded that the protonated species of EZA plays a central role in the inhibition of Na^+ independent HCO_3^- transport.

DISCUSSION

RELATION BETWEEN DIC TRANSPORT AND CHL a FLUORESCENCE QUENCHING

The addition of increasing levels of Na^+ to air-grown cells of Synechococcus UTEX 625 at constant DIC and extracellular pH served to increase the maximum intracellular DIC concentration (Fig 3). Corresponding measurements of chl a fluorescence revealed that the extent of fluorescence quenching was responsive to Na^+ over the same range of external Na^+ (Fig 4; Espie and Kandasamy, 1992). Previous results have indicated that the calculated internal DIC, based on measurements using mass spectrometry, was linearly related to the change in F'_v when both were measured simultaneously (Miller et al., 1991; Espie and Kandasamy, 1992). The data shown in Fig. 3 represent a direct measurement of the internal DIC concentration using the silicone fluid centrifugation technique and were obtained under conditions where HCO_3^- transport was the main route for DIC transport. The correlation between the maximum extent of quenching, and the maximum internal DIC pool, shown in Fig 5, thus extends and confirms previous correlations which were obtained under conditions where either CO_2 transport or both CO_2 and HCO_3^- transport were the operative pathways for DIC uptake (Miller et al., 1991; Espie et al., 1991; Espie and Kandasamy, 1992). The use of chl a fluorescence thus provides a reliable indicator of changes in the magnitude of the internal DIC pool, regardless of the transport mechanism involved or the DIC species being transported.

The underlying basis for the relation between the magnitude of change in chl a

fluorescence yield and the internal DIC concentration is not known. One possibility is the "HCO_3^- effect", which involves a direct physical effect of HCO_3^- on photosynthetic electron flow through Q_A and Q_B in PS II (Blubaugh and Govindjee, 1988). A requirement for HCO_3^- in photosynthetic electron transport has been demonstrated with isolated thylakoids from the cyanobacterium Synechocystis PCC 6803 (Cao and Govindjee, 1988). The requirement for HCO_3^- in electron transport in higher plants and algae has been proposed as being due to its role as; (a) a ligand to the non-heme iron found between Q_A and Q_B which acts to keep the D1 and D2 subunits of PS II in their proper functional conformation (b) a source of protons for the protonation of $Q_B^=$ to Q_BH_2 (Blubaugh and Govindjee, 1988). Since the inhibition of Q_A^- oxidation in Synechocystis PCC 6803 by HCO_3^- depletion in the presence of formate is reversed by mM levels of HCO_3^- (Cao and Govindjee, 1988), it has been speculated that the "HCO_3^- effect" could be the basis for the correlation between the internal DIC concentration and chl a fluorescence quenching (Miller et al., 1991). If binding of HCO_3^- between Q_A and Q_B is the basis for the observed changes in chl fluorescence, the K_D for binding must be several orders of magnitude higher in Synechococcus UTEX 625 than in spinach, where it was found to be on the order of 35 - 60 μM (Blubaugh and Govindjee, 1988). By contrast, chl a fluorescence quenching responds linearly to internal DIC in the mM range (Fig 5; Miller et al., 1991; Espie et al., 1991; Espie and Kandasamy, 1992).

Chl a fluorescence quenching in higher plants and algae is due mainly to two components, termed Q_q and Q_E (Sivak and Walker, 1985). Q_q reflects changes in the red-ox status of Q_A and can be correlated with rates of CO_2 fixation (Sivak and Walker,

1985; Genty et al., 1989; Holmes et al., 1989). The rapid and monophasic recovery of fluorescence yield by a saturating flash of high-intensity light (Fig 7; Miller et al., 1991) or by the addition of DCMU (Miller et al., 1991) indicates that chl a fluorescence quenching in Synechococcus UTEX 625 is due to Q_q (photochemical quenching). Q_E, or non-photochemical quenching, due to the build up of the proton-motive force across the thylakoid membrane, has not been observed in cyanobacteria (Miller and Canvin, 1987).

The fact that the maximum extent of quenching was positively correlated with the rate of photosynthesis as measured by O_2 evolution (Fig 6) would appear to confirm that Q_q in Synechococcus was dependent on the rate of CO_2 fixation, as in higher plants and algae. The results in Figs 7 and 8 indicate that chl a fluorescence quenching occured even under conditions where CO_2 fixation was prevented by the presence of glycolaldehyde, a Calvin cycle inhibitor. Furthermore, DIC transport was not inhibited by glycolaldehyde (Fig 8; Miller and Canvin, 1989). It has previously been shown that the relation between fluorescence quenching and internal DIC remained valid under conditions where CO_2 fixation was inhibited (Miller et al., 1988a). Direct measurements of O_2 uptake while DIC transport was occuring in the presence of iodoacetimide, another Calvin cycle inhibitor, indicated that photosynthetic electron flow was diverted to O_2 by a Mehler type reaction, thus providing a means for the re-oxidation of Q_A (Miller et al., 1988c).

Since the rate of photosynthesis depends on the internal DIC pool in a dose dependent fashion (Kaplan et al., 1980; Shelp and Canvin, 1984), the linear relation between the extent of chl a fluorescence quenching and the rate of O_2 evolution (Fig 6)

provides an indirect confirmation of the ability of chl a fluorescence to monitor changes in the internal DIC. Since chl a fluorescence is quenched even in the absence of CO_2 fixation (Fig 7), the ability of chl fluorescence to monitor the internal DIC is largely independent of events associated with CO_2 fixation. This does not mean that CO_2 fixation does not result in some fluorescence quenching as electron flow from H_2O to $NADP^+$ will surely oxidize Q_A. Rather, it would appear (Figs 7 & 8) that only a small portion of the fluorescence quenching observed during active photosynthesis ($NADP^+$ reduction) is due to CO_2 fixation and the majority is due to DIC accumulation. Both the absence of Q_E and the relative independence of Q_q and CO_2 fixation are in direct contrast with chl a fluorescence in higher plants and algae (Sivak and Walker, 1985; Miller et al., 1991).

The relative independence between carbon fixation and chl a fluorescence quenching allows for the use of measurements of the initial rate of chl a fluorescence quenching to be used as estimates of the initial rate of DIC uptake (Miller et al., 1991; Espie et al., 1991). The correlation between the initial rate of Na^+ dependent HCO_3^- transport as measured using the silicone fluid centrifugation technique, and the initial rate of chl a fluorescence quenching was determined using simple linear regression (Fig 13a) and a forced fit linear regression through the origin (Fig 13b). The highly significant (Students - t, $P < 0.001$) correlation co-efficient for the simple linear regression (Fig 13a, $r = 0.79$) attests to the ability of measurements of the initial rate of chl a fluorescence quenching to provide estimates of HCO_3^- transport rates. The residual variability in $\%F^{\bullet}_{v}.mg^{-1}chl.min^{-1}$ which is unaccounted for by variation in the transport rate ($1 - r^2 = .36$) might be due to varying levels of O_2 in the medium since

photoreduction of O_2, and therefore O_2 dependent photosynthetic electron transport has been found to be significant under conditions where DIC transport is occuring (Miller et al., 1991).

Since fluorescence quenching independent of HCO_3^- transport does not occur at the CO_2 compensation point (Figs 2 & 7; Espie and Kandasamy, 1992), a relation between initial rates of fluorescence quenching and HCO_3^- transport can be expected to intercept the y-axis at the origin. A linear regression based on this assumption (forced fit through the origin, Fig 13b) resulted in a higher correlation coefficient ($r = 0.958$). This can be interpreted as meaning that the linear relation shown in Fig 13b represents a closer approximation to the "true" relation between quenching and transport as compared to Fig 13a.

The possibility that a small, but significant portion of chl a fluorescence quenching is due to CO_2 fixation cannot be completely excluded. The possibility that CO_2 fixation affects chl a fluorescence quenching, as well as the known effect of O_2 on chl a fluorescence (Miller et al., 1991), probably introduces an element of variability in the correlation between initial rates obtained using the two methods (Fig 13). These possibilities however do not detract from the overall conclusion that chl a fluorescence can provide a monitor for DIC transport rates, regardless of the DIC species utilized in transport (Fig 13; Miller et al., 1991; Espie et al., 1992). Further studies of the effects of photoreduction of O_2 and C_i fixation on chl a fluorescence quenching should yield insights into the mechanism underlying the basis between DIC transport and fluorescence quenching.

It should be noted that silicon fluid experiments and chl a fluorescence experiments were performed under different actinic light intensities (300 and 100 μmol photons.m^{-2}.s^{-1}, respectively). These conditions were chosen because; (1) at higher actinic light intensities, Q_A becomes more oxidized, thus decreasing the effective span of F^*_v (G.S. Espie, pers. comm.) (2) the nature of silicon fluid experiments precludes mixing of the tube contents after injection of $H^{14}CO_3^-$, thus the attenuation of the light intensity through the tube became a concern and it was decided to increase the light intensity so that DIC transport was not light limited. The differing light conditions did not adversely affect the correlation between DIC transport and fluorescence quenching since the effects of pH, Na^+, and EZA on chl a fluorescence as a reporter for DIC transport were essentially confirmed by silicon fluid experiments (Figs. 3 - 5, 7, 8, 11 - 13, 16 - 19).

EFFECT OF Na^+ ON HCO_3^- TRANSPORT IN AIR-GROWN CELLS

The initial rate of HCO_3^- transport in air-grown cells of Synechococcus UTEX 625 was found to increase with increasing Na^+ in an apparent Michaelis-Menten fashion (Figs 3 & 11). Similar results have been obtained with air-grown cells of Anabaena variabilis (Reinhold et al., 1984). Corresponding Na^+ dependent increases in the initial rates of chl a fluorescence quenching indicated that chl a fluorescence is a useful means of estimating the kinetic behaviour of Na^+ dependent HCO_3^- transport (Figs 4 & 12). The Na^+ requirement for photosynthesis, HCO_3^- transport, and chl a fluorescence quenching was found to decrease with increasing pH in the range from 8.0 - 9.5 (Figs 10 & 12). Previous results have indicated that at lower pH (6.5 - 7.0) and at higher DIC (> 100 μM), there is also a decrease in the Na^+ requirement for photosynthesis (Espie and

Canvin, 1987; Canvin et al., 1990). Low pH and high DIC tend to privilege CO_2 transport over HCO_3^- transport, resulting in a larger contribution of the Na^+ independent CO_2 transport mechanism to total DIC uptake (Espie et al., 1988). By contrast, at pH $\geq$ 8.0 and with 20 μM DIC, the observed DIC uptake can be largely considered to be due to HCO_3^- transport. Thus, the lower $K_{1/2}^{Na+}$ for HCO_3^- transport with increasing pH observed for air - grown cells is particular to the Na^+ dependent HCO_3^- transport mechanism.

The close correspondence between the pH dependence of $K_{1/2}^{Na+}$ for photosynthesis (Fig 10) and the pH dependence of the $K_{1/2}^{Na+}$ for measurements of either HCO_3^- transport or chl a fluorescence quenching (Fig 12) results from the fact that photosynthesis is limited by the rate of transport at low external DIC (Mayo et al., 1989). The possibility that the pH dependence of $K_{1/2}^{Na+}$ for photosynthesis was due to a combined effect of pH and Na^+ on the utilization of the internal DIC can be discounted based on the observation of a similar pH effect on the $K_{1/2}^{Na+}$ for HCO_3^- transport (Fig 12) and also based on evidence indicating that the relation between CO_2 fixation and internal DIC is unaffected by external Na^+ in both air-grown and standing culture cells (Espie and Kandasamy, 1992).

Recent work has shown that Synechococcus R2 (PCC7942) actively extrudes Na^+ and thereby generates a Na^+ motive force ($\Delta\mu_{Na+}$ = -150 mV, negative inside) with Na^+_o at 50 mM (Ritchie, 1992). The possibility that Na^+ dependent HCO_3^- transport is driven by a Na^+:HCO_3^- symport is thus consistent with this evidence for a substantial Na^+ motive force in cyanobacteria. The data of Ritchie (1992) was used to calculate the

theoretical stoichiometries for $Na^+:HCO_3^-$ symport (Fig 30). The accumulation ratios for HCO_3^- uptake in the range which has previously been observed corresponded to theoretical stoichiometries for $nNa^+:HCO_3^-$ of between 1.7 and 3.1. Even with the extreme accumulation ratio for DIC uptake of 10,000 fold, the stoichiometry did not greatly exceed 3. By contrast, the stoichiometry of $nH^+:HCO_3^-$ with under 1000 fold accumulation of DIC at pH_o of 9.5 was found to be 17 (Zenvirth et al., 1981). The substantial influx of Na^+ which would result from the postulated $Na^+:HCO_3^-$ symport would presumably have to be disposed of by an active efflux mechanism. The results of Ritchie (1992) favor a model where a Na^+ ATPase pump is the efflux mechanism rather than a $Na^+:H^+$ antiport. At pH_o of 9.5, the contribution of the measured membrane potential (-130 mV) to $\Delta\mu_{H+}$ was effectively cancelled by the effect of ΔpH, reducing the $\Delta\mu_{H+}$ to less than -10 mV, and thereby reducing the driving force for Na^+ efflux by $Na^+:H^+$ antiport (Ritchie, 1992).

The theoretical stoichiometries shown in Fig 30 also predict that depolarization of the membrane potential would occur under conditions of active HCO_3^- transport by $Na^+:HCO_3^-$ symport. This is contrary to the evidence for a transient hyperpolarization concomitant with DIC transport in Anabaena variabilis (Kaplan et al., 1982). However, DIC transport in their experiments was initiated with 1 mM DIC which results in considerable ambiguity as to the main DIC species being transported. The experiments of Kaplan et al (1982) need to be repeated with Na^+ dependent cells and lower DIC ($<100\ \mu M$) in order to determine whether any changes in membrane potential result from HCO_3^- transport.

FIGURE 30

Theoretical stoichiometries of putative $nNa^+:HCO_3^-$ symport mechanism for Na^+ dependent HCO_3^- transport as a function of Na^+_o. Thermodynamic parameters ($\Delta\psi$ and $\Delta\mu_{Na+}$) were obtained from Figure 4 of Ritchie (1992). $\Delta\mu_{HCO3-}$ was calculated for three different ratios of $[HCO_3^-]_i/[HCO_3^-]_o$ (10^2, 10^3, 10^4) using $\Delta\psi$ from Ritchie 1992.

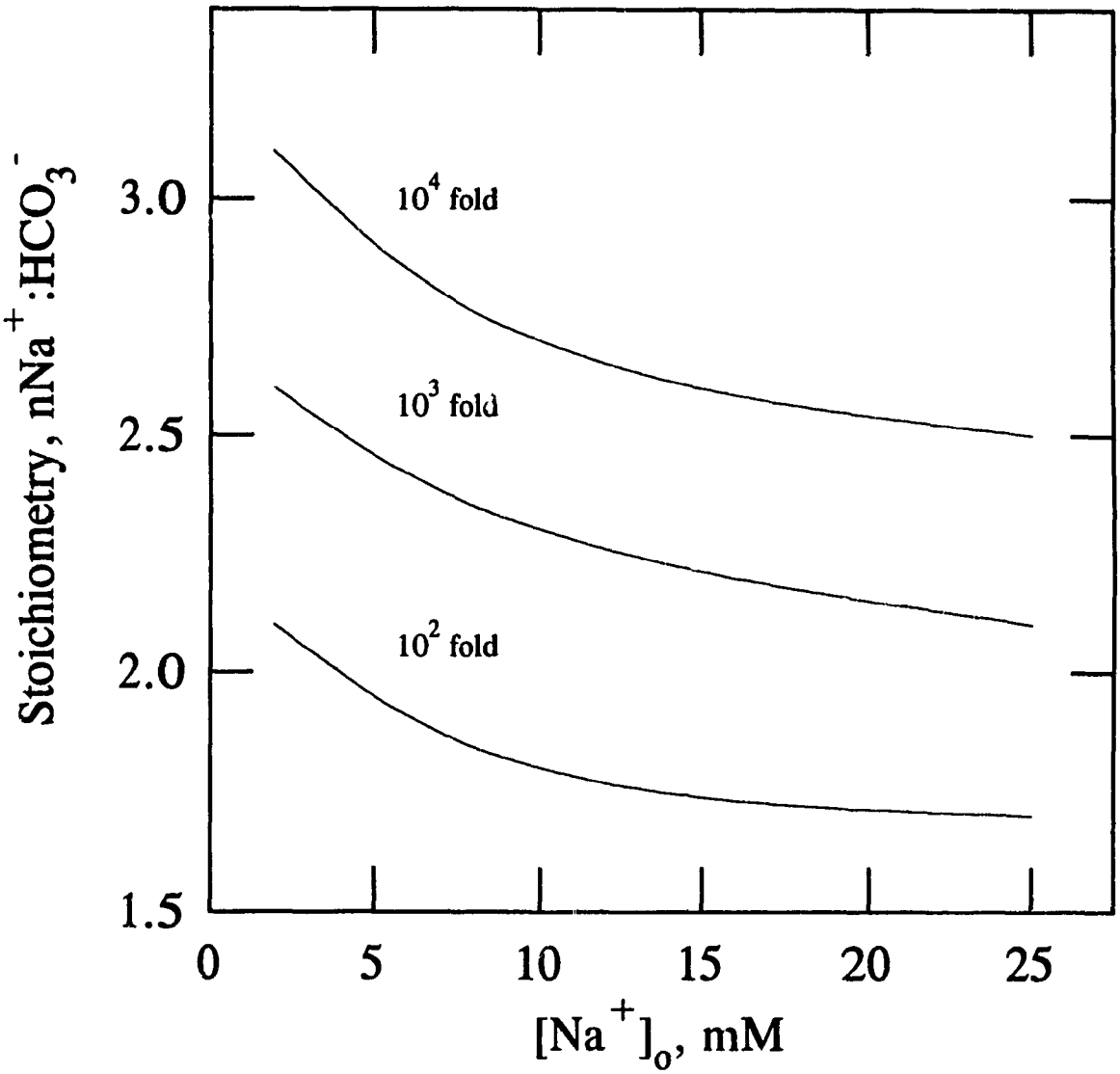
Stoichiometry, $nNa^+:HCO_3^-$
3.0
2.5
2.0
1.5
10^4 fold
10^3 fold
10^2 fold
0
5
10
15
20
25
$[Na^+]_o$, mM

Unfortunately, the experiments conducted by Ritchie (1992) were performed on Synechococcus grown on 5 % CO_2 (v/v), thus it is likely that these cells were incapable of HCO_3^- transport (Price and Badger, 1989b). Nonetheless, since the major component of $\Delta\mu_{Na+}$ in Ritchie's (1992) study was found to be $\Delta\psi$, and since $\Delta\psi$ has previously been shown to be in the range of -90 to -120 mV in air-grown cells (Zenvirth et al., 1981; Miller et al., 1984b), the possible stoichiometries for $nNa^+:HCO_3^-$ symport shown in Fig 30 are likely to be valid for air-grown cells of Synechococcus UTEX 625 if this is the mechanism for Na^+ dependent HCO_3^- transport in these cells.

The possibility that Na^+ is required for pH regulation in Synechococcus UTEX 625 cannot be completely discounted by the findings of Ritchie (1992). Alkalophilic, heterotrophic bacteria are known to require Na^+ for pH homeostasis at pH 10.5 and higher (Krulwich and Guffanti,1989). The active efflux of Na^+ is thought to be driven by localized H^+ gradients which are generated by high concentrations of respiratory chain components present in the plasma membrane of these bacteria (Krulwich and Guffanti, 1989). An increase in the intracellular pH in Synechococcus UTEX 625 has previously been observed upon incubation in Na^+ free medium at pH 9.6 and in the absence of DIC transport (Miller et al., 1984b). It is difficult, however, to reconcile the effect of bulk pH_o on the $K_{1/2}^{Na+}$ for HCO_3^- transport (Fig 12) if the Na^+ effect is due solely to a requirement for Na^+ in pH homeostasis requiring the use of localized H^+ gradients. Moreover, during steady-state photosynthesis the generation of intracellular OH^- from the dehydration of HCO_3^- to form CO_2 would exacerbate the pH regulatory problem confronted by a cell generating substantial localized H^+ gradients as a driving force for

active Na^+ efflux. The results of Figs 10 and 12 are therefore more consistent with a mechanism whereby Na^+ is bound to a titratable group on the extracellular face of the transport mechanism. A Na^+ binding site would presumably carry a negative charge to favour electrostatic interactions with Na^+. Increasing the pH in the range 8.0 to 9.5 would increase the proportion of negatively charged binding sites if this site contains an amino acid with a pK_A in this range. Na^+ could act to stimulate HCO_3^- uptake either by a conformational change in the transport protein which stimulates coupling of HCO_3^- uptake to the expenditure of an energy source such as ATP hydrolysis, or by being passively transported itself, with HCO_3^- transport being energized by the flow of Na^+ down its electrochemical gradient. Recent work, (R. Kandasamy, M.Sc. thesis, 1991) has shown that Na^+ dependent HCO_3^- transport was inhibited by the ionophore monensin. Monensin is a polyether carboxylic acid which catalyzes the electroneutral exchange of Na^+ for H^+, thereby collapsing the Na^+ gradient between the cells and the medium. Inhibition of Na^+ dependent HCO_3^- transport by monensin, therefore, strongly suggests a role for the Na^+ electrochemical gradient in HCO_3^- uptake. No evidence was found in this study for an allosteric effect of Na^+ on either photosynthesis or HCO_3^- transport.

The uptake of HCO_3^- by a primary active transport mechanism has been predicted to result in membrane hyperpolarizations of approximately 9 $mV.msec^{-1}$ (Miller, 1991). The opening of Na^+ channels in the plasma membrane of cyanobacteria could thus provide a mechanism for maintaining electrical homeostasis during DIC transport since the reversal potential for Na^+ has been found to be at least 100 mV positive of the resting potential in high DIC grown cells of Synechococcus PCC 7942 (Ritchie,1992).

Thus the depolarizing effect of an increase in membrane permeability to Na^+ could conceivably counteract the hyperpolarization induced by HCO_3^- uptake.

THE EFFECT OF EXOGENOUS DIC ON PHOTOSYNTHESIS AND HCO_3^- TRANSPORT

The requirement for mM levels of Na^+ for HCO_3^- transport is not a constitutive feature of DIC transport. Both 30 $\mu L.L^{-1}$ CO_2 grown and standing culture cells are capable of Na^+ independent HCO_3^- transport (Figs 22 & 25; Espie and Canvin,1987; Espie and Kandasamy,1992), and both of these cell types experience a low exogenous DIC concentration during the log phase of growth (Table 1). Standing culture cells would appear to possess a residual amount of Na^+ dependent HCO_3 transport since both DIC transport and photosynthesis initiated by the addition of HCO_3^- are stimulated by up to 60 % upon the addition of 25 mM Na^+ (Espie and Canvin, 1987; Espie and Kandasamy, 1992). By contrast, the Na^+ stimulation of HCO_3^- transport and photosynthesis by 25 mM Na^+ in 30 $\mu L.L^{-1}$ CO_2 grown cells did not exceed 30 % (Figs 14,15,and 22). The lower exogenous DIC experienced by 30 $\mu L.L^{-1}$ CO_2 grown cells during log phase as compared to standing culture corresponded to a decrease in the $K_{1/2}^{DIC}$ for photosynthesis and also corresponded with lower levels of Na^+ stimulation of photosynthesis (Table 1). The level of exogenous DIC experienced by the cells during growth would thus appear to be an environmental cue not only for regulating the affinity for DIC transport but also for the suppression or prominence of Na^+ dependent HCO_3^- transport.

THE DIFFERENTIAL EFFECT OF EZA ON Na^+ DEPENDENT AND INDEPENDENT HCO_3^- TRANSPORT MECHANISMS

Based on evidence that both CO_2 and HCO_3^- transport were equally inhibited by the carbonic anhydrase inhibitor, EZA, Price and Badger (1989a) proposed a transport mechanism for DIC uptake whereby CO_2 and HCO_3^- transport shared a common pathway. These investigators proposed an obligate dehydration-hydration cycle for HCO_3^- uptake (Fig 1a). In contrast to the model proposed by Price and Badger (1989a) where only one HCO_3^- transport pathway is described, two pathways for HCO_3^- transport are evident in Synechococcus UTEX 625 grown under different conditions. The Na^+ dependent HCO_3^- transport mechanism is strictly and specifically dependent on mM levels of Na^+ for activity (Espie et al., 1988b), inhibited by amiloride or monensin (Kandasamy, M.Sc. thesis, 1991), and relatively insensitive to treatment with low levels of EZA (<100 μM; Fig 19). The Na^+ independent mechanism is relatively insensitive to both amiloride and monensin (Kandasamy, M.Sc. thesis, 1991), however low levels of EZA (<100 μM) exert an inhibitory effect on HCO_3^- transport by this mechanism (Figs 17,22, and 25, Table 2; Tyrrell and Espie,unpublished data).

The inhibition of Na^+ independent HCO_3^- transport by EZA was evident in measurements of photosynthesis and chl a fluorescence quenching in both standing culture and 30 $\mu L.L^{-1}$ CO_2 grown cells (Fig 16). The inhibitory effect of EZA on HCO_3^- transport could be seen in direct measurements of HCO_3^- using the silicon fluid centrifugation technique (Figs 17, 22, and 25, Table 2). The possibility that photosynthetic electron transport was inhibited by EZA, possibly at the HCO_3^- binding

located on the reducing side of PQ can be discounted based on the observation that low concentrations of EZA (< 100 μM) were relatively innocuous in measurements of chl a fluorescence in air - grown cells (Fig 18). Furthermore, the direct measurement of electron transport through PS II revealed only 20 % inhibition with 600 μM EZA present (Price and Badger, 1989b). The ability of chl a fluorescence to to monitor the size of the internal DIC pool even when EZA was present was further confirmed by the observation that the inhibition of chl a fluorescence quenching by EZA could be reversed by the addition of 5 mM DIC (Tyrrell and Espie, unpublished data).

If EZA exerted an inhibitory effect on internal carbonic anhydrase, then the relation between internal DIC and carbon fixation would show reduced carbon fixation for similar internal DIC levels when EZA was present. Price and Badger (1989a) showed that the utilization of the internal DIC pool was not affected by 200 μM EZA. Measurements of carbon fixation in relation to internal DIC in standing culture cells led to the same conclusion (data not shown).

The differential effect of EZA on the two different HCO_3^- transport mechanisms was evident in cell types which manifested both types of HCO_3^- transport. Thus, the relief of EZA inhibition of photosynthesis and fluorescence quenching afforded by the presence of 25 mM Na^+ in standing culture and 30 $\mu L.L^{-1}$ CO_2 grown cells resulted in lower levels of inhibition by EZA as compared to when only 100 μM Na^+ was present (Fig 16). Direct measurements of pool formation and initial rates of HCO_3^- transport indicated that the protective effect of Na^+ on the inhibition of chl a fluorescence quenching and photosynthesis was exerted at the level of the HCO_3^- transport mechanism

(Figs 17 and 22, Table 2) and did not result from an effect of Na^+ on either photosynthetic electron transport or on the utilization of the DIC pool for use in photosynthesis.

The lower level of Na^+ protection against EZA inhibition in 30 $\mu L.L^{-1}$ CO_2 grown cells as compared to standing culture cells is not surprising considering that 30 $\mu L.L^{-1}$ CO_2 grown cells typically possess less residual Na^+ stimulation of photosynthesis and HCO_3^- transport as compared to standing culture cells (Figs 22 & 25, Table 1).

The difference between the results shown in this study and the results of Price and Badger (1989a) with regards to EZA inhibition of HCO_3^- transport can be reconciled by the fact that Price and Badger (1989a) conducted all of their experiments with 18 mM Na^+ present and did not conduct any experiments in the absence of Na^+. Furthermore, the cyanobacteria used in the study by Price and Badger (1989a) were grown at 30 $\mu L.L^{-1}$ CO_2 and thus more than likely possessed marginal levels of Na^+ dependent HCO_3^- transport. Initial rates of HCO_3^- transport reported by Price and Badger (1989a) were inhibited by 51 % in the presence of 400 μM EZA with 100 μM HCO_3^-, which compares favourably to the 40 % inhibition of the initial rate of HCO_3^- transport by 200 μM EZA with 100 μM HCO_3^- and 25 mM Na^+ present (Fig 25b). Thus, the different interpretations with regard to the HCO_3^- transport mechanisms based on the data presented in this study and the data presented by Price and Badger (1989a) are probably not due to quantitative differences in the inhibition of Na^+ independent HCO_3^- transport in the two systems, but are more likely based on the selective use of EZA on cells grown under varying growth DIC and in the absence and presence of mM levels of Na^+.

CO_2 AND HCO_3^- TRANSPORT: SEPARATE OR COMMON PATHWAYS ?

The model for DIC uptake proposed by Price and Badger (1989a) predicts that inhibition of the common step in the translocation of either HCO_3^- or CO_2 (hydration of CO_2 as/before it enters the cytosol as HCO_3^-) (Fig 1a) would result in the equal inhibition of CO_2 and HCO_3^- transport. The large amounts of both either CO_2 or HCO_3^- (100 μM) used by these investigators would lead to the presence of a large amount of the other DIC species in the external medium before the first sampling time (10 sec). The half-time for the hydration of CO_2 at pH 8.0 and 30°C is approximately 8 seconds (Miller et al., 1988a). "Active species" experiments conducted with the intention of comparing CO_2 and HCO_3^- uptake rates are thus less ambiguous when low levels of DIC are used. Uptake of DIC initiated by the addition of 10 μM CO_2 by cells possessing the high-affinity CO_2 transporter was rapid and essentially complete by the first sampling time (10 sec.;Fig 21; Miller et al., 1988b). Since CO_2 represents only 1.6% of the total DIC at equilibrium at pH 8.0 and 30°C, uptake initiated by the addition of 10 μM HCO_3^- results in a negligible amount of extracellular CO_2 and therefore does not confound the interpretation of possible effects regarding the inhibition of HCO_3^- transport by EZA. Accordingly, the substantial inhibition of Na^+ independent HCO_3^- transport by 75 μM EZA (Figs 17, 22, and 25, Table 2; Tyrrell and Espie, unpublished data) can unambiguously be compared to the negligible effect of 75 μM EZA on CO_2 transport in standing culture cells when CO_2 was present at 10 μM (Fig 21). The inhibition of the initial rate of fluorescence quenching by EZA was much more evident when HCO_3^- was added as compared to when CO_2 was added to 30 $\mu L.L^{-1}$ CO_2 grown cells when both CO_2 and HCO_3^- were added at

10 μM (Fig 20). Equal inhibition of HCO_3^- and CO_2 induced fluorescence quenching was evident only when 400 μM EZA was added (Fig 20). Similarly, Price and Badger (1989a) reported equal inhibition of both CO_2 and HCO_3^- transport in 30 $\mu L.L^{-1}$ CO_2 grown cells with 400 μM EZA present. Thus, the difference in the interpretation of the results obtained by Price and Badger (1988a) and the results reported here are probably due in large part to lower levels of DIC used in this study for the purpose of comparing the effects of EZA on CO_2 and HCO_3^- transport and due to the lower amounts of EZA used in this study.

There was a wide concentration range of EZA for which HCO_3^- transport was preferentially inhibited over CO_2 transport when both were present at 10 μM (Figs 20 & 21). These results by themselves do not discount the possibility that Na^+ independent HCO_3^- transport shares a common translocatory step with CO_2 transport however they are in direct contrast with the results of Price and Badger (1989a) which these investigators present as evidence in favor of a common pathway. Since the $K_{1/2}^{CO2}$ for the high - affinity CO_2 transport is on the order of 0.2 μM (Espie et al.,1991), and the $K_{1/2}^{DIC}$ for the Na^+ independent HCO_3^- transport mechanism is on the order of 10 - 20 μM (Figs 22 & 25), it could be argued that the differential inhibitory effect of EZA on CO_2 and HCO_3^- transport could be due to the fact that the CO_2 concentration used was 50 - 100 fold higher than the $K_{1/2}^{CO2}$ while HCO_3^- was added at a maximum of 5 - 10 fold higher than $K_{1/2}^{DIC}$ in transport experiments.

The K_I for EZA inhibition for EZA inhibition of the Na^+ independent HCO_3^- transport mechanism was found to be 58 $\pm$ 17 μM (SEM, n=4) in experiments similar

to the ones shown in Figs 24 & 26. This value agrees well with the EZA concentration required for 50 % inhibition (40 to 50 μM EZA, Fig 17) of HCO_3^- transport in standing culture cells at a DIC concentration (20 μM) close to the $K_{1/2}^{DIC}$ for transport in these cells (21.0 $\pm$ 9.0 μM, SEM n = 4). If the K_I of EZA inhibition of CO_2 transport is similar to the K_I for EZA inhibition of HCO_3^- transport, due to a common hydration step being EZA sensitive, then 50 % inhibition of EZA transport should be evident with approximately 50 μM EZA and 0.2 μM CO_2 . Alternatively, if CO_2 and Na^+ independent HCO_3^- transport share a common pathway, then there should be an effect of HCO_3^- on CO_2 transport. Competition experiments of this nature measuring CO_2 disappearance from the medium against an increasing background of HCO_3^- transport should show whether or not Na^+ independent HCO_3^- transport interferes with ongoing CO_2 transport.

H_2S has been shown to be inhibitory for the high affinity CO_2 transport mechanism, yet neither Na^+ dependent nor Na^+ independent HCO_3^- transport were inhibited by H_2S (Espie et al., 1989; Espie and Kandasamy, 1992). Carbon oxysulfide (COS) has been shown to selectively inhibit CO_2 transport, with no effect on Na^+ dependent HCO_3^- transport (Miller et al., 1989). However, a recent report indicates that Na^+ independent HCO_3^- transport may be inhibited by COS with 1/4 the effectiveness seen with CO_2 transport (Badger and Price, 1990).

The inhibition of CO_2 transport by COS or H_2S under conditions where HCO_3^- transport was occuring resulted in an increase in the extracellular levels of CO_2 (Miller et al., 1989; Espie et al., 1989). These results indicated that intracellular dehydration of recently transported HCO_3^- resulted in a massive efflux of internally generated CO_2. This

increase in extracellular CO_2 levels was not evident when the CO_2 transport inhibitors were not present (Miller et al.,1989; Espie et al.,1989). The CO_2 transport mechanism thus acts as a CO_2 "scavenging" mechanism and contributes to DIC transport under normal circumstances of DIC uptake. For this reason, the inhibition of CO_2 transport by high levels of EZA (>200 μM) (Figs 20 & 21) is probably responsible for the apparent inhibition of Na^+ dependent HCO_3^- transport by similar amounts of EZA (Figs 18 & 19). Both the initial rate of fluorescence quenching and DIC transport were less inhibited by 200 μM EZA for Na^+ dependent HCO_3^- transport as compared to CO_2 transport (Figs 18 - 21). This is the the pattern of inhibition one would expect to find if the Na^+ independent mechanism were less sensitive to EZA than the CO_2 transport mechanism, and if CO_2 transport contributed to HCO_3^- uptake by virtue of its "scavenging" capacity.

INHIBITORY SPECIES OF EZA

EZA is a sulfonamide inhibitor of carbonic anhydrase, a Zn^{2+} metalloenzyme. The deprotonated (anionic) form of the inhibitor is proposed to bind to the active site Zn^{2+} and displace the bound hydroxide ion, which is normally catalytically active in the hydration of CO_2 (Coleman, 1975). The inhibition of the initial rate of chl a fluorescence quenching (as a monitor for HCO_3^- transport) by either $EZAH_2$ (Fig 29a) or $EZAH^-$ (Fig 29b) revealed that the protonated form of the inhibitor was more likely to play a central role in the inhibition of transport than $EZAH^-$. Since it is the anionic form which inhibits CA from animal sources (Coleman, 1975), the results indicate that either the inhibited protein is dissimilar to CA in this regard, or perhaps that the site of inhibition is surrounded by lipid and/or hydrophobic protein moities. The former possibility is not

unanticipated since it has not been shown conclusively that DIC interconversion is an obligatory step in the translocation pathway, and since the active site of the HCO_3^- transport pathway could share some structural features with animal or plant carbonic anhydrase without necessarily carrying out the same function. In the latter case, the protonated species ($EZAH_2$) has greater access to the site of inhibition than $EZAH^-$ and might explain the prominence of this species in the inhibition of chl fluorescence quenching. The equilibrium between $EZAH^-$ and $EZAH_2$ in the membrane environment allows the possibility that $EZAH^-$ is the inhibitory species in this hydrophobic environment, however the K_I for $EZAH^-$ would have to be orders of magnitude lower than the measured K_I for EZA inhibition of HCO_3^- transport (58 μM). Values of K_I for inhibition of human CAII by acetazolamide, another sulfonamide inhibitor similar to EZA have been found to be as low as 10 nM (Silverman, 1991). It is likely however that the site of inhibition by EZA is in a more hydrophobic environment than would be expected for a peripheral membrane protein.

SUMMARY AND CONCLUSION

The rapid response of chl a fluorescence to changes in the internal DIC, as opposed to changes in the rate of photosynthesis, allows for its use as a convenient and non-invasive method for measuring DIC transport. The initial rate of chl a fluorescence quenching was used to estimate the initial rate of Na^+ dependent HCO_3^- transport. The $K_{1/2}^{Na+}$ for this transport process was found to be sensitive to changes in external pH, decreasing as external pH was increased. The pH effect on HCO_3^- transport was also evident in measurements of chl a fluorescence quenching and photosynthesis.

The results presented in this thesis are consistent with the view that HCO_3^- transport in Synechococcus UTEX 625 proceeds through two separate and distinct pathways, one being dependent on mM levels of Na^+, and one being independent of the Na^+ ion. In support of this view, the Na^+ independent mechanism was found to be very sensitive to low amounts of EZA ($< 100\ \mu M$) while the Na^+ independent mechanism was found to be largely insensitive to this amount of EZA. The prominence or suppresion of the Na^+ dependent HCO_3 transport mechanism corresponded to changes in the exogenous DIC experienced during the log phase of growth.

The differential effect of EZA on CO_2 and HCO_3^- transport argue in favour of separate transport pathways for the Na^+ independent HCO_3^- transport pathway and the high-affinity CO_2 transport mechanism, however the possibility exists that the differential effect is due to the different substrate affinities for these two transport mechanisms.

REFERENCES

Andrew, T. J., Abel, K. M., 1981. Kinetics and subunit interaction of ribulose bisphosphate carboxylase - oxygenase from the cyanobacterium Synechococcus sp. J. Biol. Chem. 256: 8445 - 8451

Badger, M. R. 1987. The $C0_2$ concentrating mechanism in aquatic phototrophs. In The Biochemistry of Plants. eds. M. D., Hatch, N. K., Boardman, 10: 219 - 276 Toronto: Academic Press 429 pp.

Badger, M. R., Andrews, T. J., 1982. Photosynthesis and inorganic carbon usage by the marine cyanobacterium, Synechococcus sp. Plant Physiol. 70: 517 - 523

Badger, M. R., Bassett, M., Comin, H. N. 1985. A model for HCO_3^- accumulation and photosynthesis in the cyanobacterium Synechococcus sp. Plant Physiol. 77: 465 -471

Badger, M. R., Gallagher, A. 1987. Adaptation of Photosynthetic $C0_2$ and HCO_3^- accumulation by the cyanobacterium Synechococcus PCC 6301 to growth at different inorganic carbon concentrations. Aust. J. Plant Physiol. 14: 189 - 201

Birmingham, B. C., Colman, B. 1979. Measurement of carbon dioxide compensation points of freshwater algae. Plant Physiol. 64: 892 - 95

Blubaugh, D. J. & Govindjee 1988. The molecular mechanism of the bicarbonate effect at the plastoquinone reductase site of photosynthesis. Photosynthesis Research 19: 85 - 128

Blumwald, E., Wolosyn, J. M., Packer, L. 1984. Na^+/H^+ exchange in the cyanobacterium Synechococcus 6311. Biochem. Biophys. Res. Commun. 122: 452 - 59

Canvin, D. T. 1990, Photorespiration and CO_2 concentrating mechanisms. In Plant Physiology, Biochemistry, and Molecular Biology, eds. D. T. Dennis, D. H. Turpin, Longman Scientific and Technical, Essex, England

Canvin, D. T., Miller, A. G., Espie, G. S. 1987. C_3 photosynthesis in algae: The importance of inorganic carbon concentrating mechanisms. In Carbon Dioxide As a Source of Carbon, eds. M. Aresta, G. Forti, pp 199 - 212 D. Reidel

Canvin, D. T., Miller, A. G., Espie, G. S. 1990. Inorganic carbon concentrating processes in cyanobacteria. In Proceedings of the International Congress of Plant Physiology, Vol 1, eds. S. K. Sinha, P. V. Sane, S. C. Bhargava, P. K. Agrawal, pp 569 - 580 , Indian Agricultural Research Institute, New Delhi, India

Cao J. & Govindjee 1988. Bicarbonate effect on electron flow in a cyanobacterium Synechocystis PCC 6803. Photosynthesis Research 19: 277 - 285

Coleman, J. E. 1975. Chemical reactions of sulfonamides with carbonic anhydrase. Ann. Rev. Pharmacology 15: 221 - 242

Coleman, J. R., Colman, B. 1981. Inorganic carbon accumulation and photosynthesis in a blue - green alga as a function of external pH. Plant Physiol. 67: 917 - 921

Espie, G. S., Canvin, D. T. 1987. Evidence for Na^+ - independent HCO_3^- uptake by the cyanobacterium Synechococcus leopoliensis. Plant Physiol. 84: 125 - 130

Espie, G. S., Kandasamy, R. A. 1992. Na^+ - independent HCO_3^- transport and accumulation in the cyanobacterium Synechococcus UTEX 625. Plant Physiol. 98: 560 - 568

Espie, G. S., Miller, A. G., Birch, D. G., Canvin, D. T. 1988a. Simultaneous transport of CO_2 and HCO_3^- by the cyanobacterium Synechococcus UTEX 625. Plant Physiol. 87: 551 - 554

Espie, G. S., Miller, A. G., Canvin, D. T. 1988b. Characterization of the Na^+ - requirement in cyanobacterial photosynthesis. Plant Physiol. 88: 757 - 763

Espie, G. S., Miller, A. G., Canvin, D. T. 1989. Selective and reversible inhibition of active CO_2 transport by hydrogen sulfide in a cyanobacterium. Plant Physiol. 91: 387 - 394

Espie, G. S., Miller, A. G., Canvin, D. T. 1991. High affinity transport of CO_2 in the cyanobacterium Synechococcus UTEX 625. Plant Physiol. 97: 943 - 953

Genty, B., Briantais, J-M., Baker, N. R. 1989. The relationship between the quantum yield of photosynthetic electron transport and quenching of chl a fluorescence. Biochim. et Biophys. Acta 990: 87 - 92

Holmes, J. J., Weger, H.G., Turpin, D.H. 1989. Chlorophyll a fluorescence predicts total photosynthetic electron flow to CO_2 or NO_3^-/NO_2^- under transient conditions. Plant Physiol. 91: 331 - 337

Ingle, R. K., Colman, B. 1976. The relationship between carbonic anhydrase activity and glycolate excretion in the blue-green alga Coccochloris peniocystis. Planta 128: 217 - 223

Kandasamy, R.A. 1991. HCO_3^- transport in the cyanobacterium Synechococcus leopoliensis UTEX 625. M.Sc. Thesis, Concordia University

Kaplan, A., Badger, M. R., Berry, J. A. 1980. Photosynthesis and the intracellular inorganic carbon pool in the bluegreen alga Anabaena variabilis: Response to external CO_2 concentration. Planta 149: 219 - 226

Kaplan, A., Scherer, S., Lerner, M. 1989. Nature of the light - induced H^+ efflux and Na^+ uptake in cyanobacteria. Plant Physiol. 89: 1220 - 1225

Kaplan, A., Zenvirth, D., Reinhold, L., Berry, J. A. 1982. Involvement of a primary electrogenic pump in the mechanism for HCO_3^- uptake by the cyanobacterium Anabaena variabilis. Plant Physiol. 69: 978 - 982

Krulwich, T. A., Guffanti, A. A. 1989. The Na^+ Cycle of Extreme Alkalophiles: A Secondary Na^+/H^+ Antiporter and Na^+/Solute Symporters. J. Bioenergetics Biomembr. 21: 663 - 679

Lanaras, T., Hawthornthwaite, A. M., Codd, G. A. 1985. Localization of carbonic anhydrase in the cyanobacterium Chlorogleopsis fritschii. FEMS Microbiol.Lett. 26: 285 - 288

Mackinney, G. 1941. Absorption of light by chlorophyll solutions. J. Biol. Chem. 140: 435 - 463

Maren, T. H. 1967. Carbonic anhydrase: chemistry, physiology and inhibition. Physiol. Rev. 47: 591 - 781

Mayo, W. P., Williams, T. G., Birch, D. G., Turpin, D. H. 1986. Photosynthetic adaptation by Synechococcus leopoliensis in response to exogenous dissolved inorganic carbon. Plant Physiol. 80: 1038 - 1040

Mayo, W. P., Elrifi, I. R., Turpin, D. H. 1989. The relationship between ribulose bisphosphate concentration, dissolved inorganic carbon (DIC) transport and DIC - limited photosynthesis in the cyanobacterium Synechococcus leopoliensis grown at different concentrations of inorganic carbon. Plant Physiol. 90: 720 - 727

Mckay, R. M. L., Gibbs, S. P., Espie, G. S. 1992. Effect of dissolved inorganic carbon on mode of carbon transport, expression of carboxysomes and localization of RUBISCO in cells of the cyanobacterium Synechococcus UTEX 625. Archiv. Microbiol. (in press)

Miller, A.G. 1990 Inorganic carbon transport and assimilation in cyanobacteria. In Autotrophic Microbiology and One - Carbon Metabolism, ed. G.A. Codd, pp. 25 - 33, Kluwer Academic Publishers, Netherlands

Miller, A. G., Canvin, D. T. 1985. Distinction between $HCO^-_3$and CO_2 dependent photosynthesis in the cyanobacterium Synechococcus leopoliensis based on the selective response of the HCO_3^- transport to Na^+. FEBS. 187:29 - 32

Miller, A. G., Canvin, D. T. 1987. The quenching of chlorophyll a fluorescence as a consequence of the transport of inorganic carbon by the cyanobacterium Synechococcus UTEX 625. Biochim Biophys. Acta. 894: 407 - 413

Miller, A. G., Canvin, D. T. 1987. Na^+ - stimulation of photosynthesis in the cyanobacterium Synechococcus UTEX 625 grown on high levels of inorganic carbon. Plant Physiol. 84: 118 - 124

Miller, A. G., Canvin, D. T. 1989. Glycolaldehyde inhibits CO_2 fixation in the cyanobacterium Synechococcus UTEX 625 without inhibiting the accumulation of inorganic carbon or the associated quenching of Chlorophyll a fluorescence. Plant Physiol. 91: 1044 - 1049

Miller, A. G., Colman, B. 1980. Active transport and accumulation of bicarbonate by a unicellular cyanobacterium. J. Bacteriol. 143: 1253 - 1259

Miller, A. G., Espie, G. S., Canvin, D. T. 1988a. Chl a fluorescence yield as a monitor of both active CO_2 and HCO_3^- transport by the cyanobacterium Synechococcus UTEX 625. Plant Physiol. 86: 655 - 658

Miller, A. G., Espie, G. S., Canvin, D. T. 1988b. Active transport of CO_2 by the cyanobacterium Synechococcus UTEX 625. Plant Physiol. 86: 677 - 683

Miller, A. G., Espie, G. S., Canvin, D. T. 1988c. Active transport of inorganic carbon increases the rate of O_2 photoreduction by the cyanobacterium Synechococcus UTEX 625. Plant Physiol. 88: 6 - 9

Miller, A. G., Espie, G. S., Canvin, D. T. 1989. Use of carbon oxysulfide, a structural analog of CO_2, to study active CO_2 transport in the cyanobacterium Synechococcus UTEX 625. Plant Physiol. 90: 1221 - 1231

Miller, A. G., Espie, G. S., Canvin, D. T. 1991. The effects of inorganic carbon and oxygen upon fluorescence in the cyanobacterium Synechococcus UTEX 625. Can. J. Bot.: 69: 1151 - 1160

Miller, A. G., Turpin, D. H., Canvin, D. T. 1984a. Growth and photosynthesis of the cyanobacterium Synechococcus leopoliensis in HCO_3^- - limited chemostats. Plant Physiol. 75: 1064 - 1070

Miller, A. G., Turpin, D. H., Canvin, D. T. 1984b. Na^+ requirement for growth, photosynthesis and pH regulation in the alkalotolerant cyanobacterium Synechococcus leopoliensis. J. Bacteriol. 159: 100 - 106

Mullineaux, C.W., Allen, J.F. 1990. State 1 - State 2 transitions in the cyanobacterium Synechococcus 6301 are controlled by the redox state of electron carriers between Photosystems 1 and 2. Photosynthesis Research 23: 297 - 311

Ogren, W. L. 1984. Photorespiration: pathways, regulation, and modification. Ann.Rev. Plant Physiol. 35: 415 - 442

Price, G. D., Badger, M. R. 1989a. Ethoxyzolamide inhibition of CO_2 uptake in the cyanobacterium Synechococcus PCC 7942 without apparent inhibition of internal carbonic anhydrase activity. Plant Physiol. 89: 37 - 43

Price, G. D., Badger, M. R. 1989b. Ethoxyzolamide inhibition of CO_2 - dependent photosynthesis in the cyanobacterium Synechococcus PCC 7942. Plant Physiol. 89: 44 - 50

Reinhold, L., Kosloff, R., Kaplan, A. 1991. A model for inorganic carbon fluxes and photosynthesis in cyanobacterial carboxysomes. Can. J. Bot. 69: 984 - 988

Reinhold, L., Volokita, M., Zenvirth, D., Kaplan, A. 1984. Is HCO_3^- transport in Anabaena a Na^+ symport? Plant Physiol. 76: 1090 - 1092

Reinhold, L., Zviman, M., Kaplan, A. 1987. Inorganic carbon fluxes and photosynthesis in cyanobacteria - a quantitative model. In Progress in Photosynthesis Research ed. J. Biggens, pp. 289 - 296. Dordrecht: Martinus Nijhoff

Ritchie, R.J. 1992. Sodium transport and the origin of the membrane potential in the Cyanobacterium Synechococcus R - 2 (Anacystis nidulans) PCC 7942. J. Plant Physiol. 139: 320 - 330

Schreiber, U., Schliwa, U., Bilger, W. 1986. Continuous recording of photochemical and non - photochemical fluorescence quenching with a new type of modulation fluorometer. Photosynth. Res. 10: 51 - 62

Shelp, B. J., Canvin, D. T. 1984. Evidence for bicarbonate accumulation by Anacystis nidulans. Can. J. Bot. 62:1398 - 1403

Shively, J.M., Bryant, D.A., Fuller, R.C., Konopka, A.E., Stevens, S.E.Jr., Strohl, W.R. 1988. Functional inclusions in prokaryotic cells. Int. Rev. Cytol. 113: 35 - 100

Segel, I. H. 1988. Biochemical Calculations, 3rd Edition, J. Wiley and Sons, New York

Sivak, M.N., Walker, D.A. 1985. Chlorophyll a fluorescence: can it shed light on fundamental questions in photosynthetic carbon fixation? Plant, Cell and Environment 8: 439 - 448

Silverman, D. N. 1991. The Catalytic Mechanism of Carbonic Anhydrase. Can.J. Bot. 69: 1070 - 1078

Truesdale, A., Downing, B. 1955 The solubility of Oxygen in pure water and sea - water. J. Appl. Chem. (London) 5: 53 - 63

Tu, C., Spiller, H., Wynns, G. C., Silverman, D. N. 1987. Carbonic anhydrase and the uptake of inorganic carbon by Synechococcus sp. (UTEX 2380) Plant Physiol. 85: 72 - 77

Turpin, D. H., Miller, A. G. 1985. Predicting the kinetics of dissolved inorganic carbon limited growth from the short-term kinetics of photosynthesis in Synechococcus leopoliensis (Cyanophyta). J. Phycol. 21: 409 - 418

Yagawa, Y., Shiraiwa, Y., Miyachi, S. 1984. Carbonic anhydrase from the blue - green alga (Cyanobacterium) Anabaena variabilis. Plant and Cell Physiol. 25: 755 - 783

Zenvirth, D., Volokita, M., Kaplan, A. 1984. Evidence against H^+ - HCO_3^- symport as the mechanism for HCO_3^- transport in the cyanobacterium Anabaena variabilis. J. Membrane Biol. 79: 271 - 274